Manufacturing Methods for a Solid Rocket Motor Propelling a Small, Fast Flight Vehicle

by

Kelly J. Mathesius

B.S. in Aerospace Engineering
Massachusetts Institute of Technology (2017)

Submitted to the Department of Aeronautics and Astronautics
in partial fulfillment of the requirements for the degree of

Master of Science in Aeronautics and Astronautics

at the

MASSACHUSETTS INSTITUTE OF TECHNOLOGY

June 2019

Author .....
Department of Aeronautics and Astronautics
May 23, 2019

Certified by .....
R. John Hansman
T. Wilson Professor in Aeronautics
Thesis Supervisor

Accepted by .....
Sertac Karaman
Associate Professor of Aeronautics and Astronautics
Chair, Graduate Program Committee

Manufacturing Methods for a Solid Rocket Motor Propelling a Small, Fast Flight Vehicle

by

Kelly J. Mathesius

Submitted to the Department of Aeronautics and Astronautics
on May 23, 2019, in partial fulfillment of the
requirements for the degree of
Master of Science in Aeronautics and Astronautics

Abstract

A gap exists in the design space for aircraft mass and speed: no flight vehicles with a mass of less than 10 kg and speed greater than 100 m/s are available. The small, fast "Firefly" flight vehicle is being developed to explore the capabilities and challenges for aircraft in this gap. The compact Firefly aircraft is configured around a long-endurance, end-burning solid rocket motor that provides 2-3 minutes of powered flight.

Challenges exist for manufacturing solid rocket motors for small, fast aircraft such as Firefly. Achieving desired motor performance requires a void-free propellant grain and thermal liner and a strong propellant-to-liner bond. However, observations and tests following several motor manufacturing attempts have revealed voids in the propellant and liner and delamination at the propellant-to-liner interface. Manufacturing defects such as these have led to large increases in chamber pressure and thrust during a static fire test of a motor.

This thesis describes the development and implementation of manufacturing methods for slow-burning, long-endurance motors used in small, fast aircraft. Innovative tooling and rigorous procedures have been developed to help ensure the consistent production of a long-endurance solid rocket motor. Successful static firings of a test motor validate the effectiveness of many of the developed manufacturing methods.

Thesis Supervisor: R. John Hansman
Title: T. Wilson Professor in Aeronautics

Acknowledgments

I thank my wonderful parents, Pam and Merlin Mathesius, for their unfailing love and encouragement. Thank you for always supporting my curiosity and giving me the opportunities while growing up to pursue my passions in space exploration and rocketry. I am so grateful that you are my Mom and Dad. I thank my brother, Ross Mathesius, for his companionship – thanks for being a nerd with me when we're home.

I thank my labmate, Matt Vernacchia, for his camaraderie, support, and wisdom. Working and building Firefly with you is an honor. I am truly privileged to share life with you every day.

I thank my friend and former labmate, Dr.[1] Tony Tao. I am sincerely grateful to call you my friend and have you in my life. It was an honor to work and learn with you last year.

I am grateful to the rest of the Firefly team: 2LT Jon Spirnak, and undergraduates Jakob Coray, Jovan Zhang, Phil Phan, Herbie Turner, and Katya Bezugla. I would particularly like to acknowledge the work of Jakob Coray in the development of our liner manufacturing procedures.

I am grateful for AeroAstro's technical instructors: Dave Robertson and Todd Billings. You have showed me how to manufacture and test my ideas.

I appreciate the contributions of our sponsors and advocates at Lincoln Laboratory and BAE Systems. Their support makes what we do possible.

I thank my advisor, Prof. John Hansman, for his wisdom, guidance, and loyalty. I have learned much.

[1] finally

Contents

Chapter 1

Introduction

1.1 Small, fast aircraft design-space gap

A gap exists in the design-space for aircraft mass and speed. As shown in Figure 1-1, no small, fast flight vehicles with a mass of less than 10 kg and a speed greater than 100 m/s are available. Consequently, the capabilities and challenges for small, fast vehicles of this size and speed are vastly unexplored.

In order to develop a vehicle in this gap, a propulsion technology must be determined. Slow-burning solid rocket motors are a promising choice due in part to their scalability, simplicity, and high energy density.

1.2 Aircraft concept: Firefly

The "Firefly" aircraft is being used as a development vehicle to explore and demonstrate the capabilities of a small, fast aircraft.[1] Firefly is a solid rocket-propelled flight vehicle with an approximate loaded mass of 2 kg and speed of Mach 0.8. It folds into a canister with bounding dimensions of 70 mm $\times$ 70 mm $\times$ 480 mm.

[1]The Firefly aircraft was initially conceived and designed by Dr. Tony Tao and Matthew Vernacchia of the MIT Department of Aeronautics and Astronautics. A detailed discussion of the development of Firefly and its propulsion system can be found in Vernacchia's thesis [6].

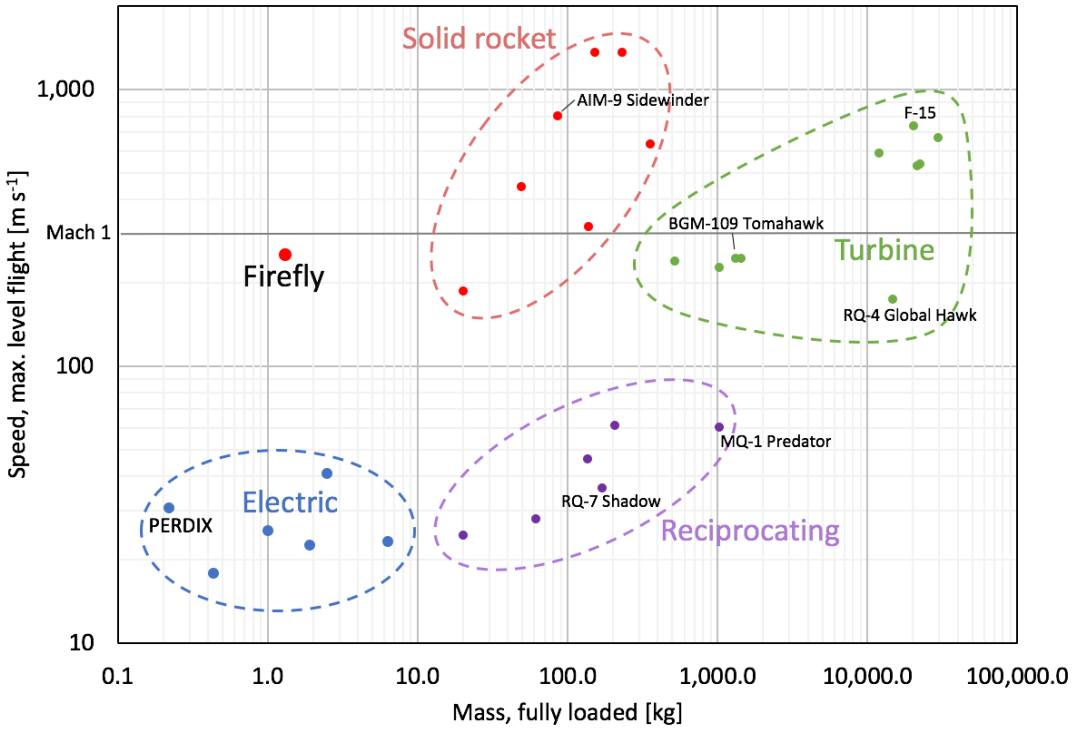

Figure 1-1: Speed, mass, and propulsion technology of selected available U.S. military aircraft. The Firefly vehicle exists in a relatively unexplored small, fast flight regime. Data from [1] [2] [3] [4] [5].

1.2.1 Concept of operations

The Firefly vehicle is deployed from a host aircraft as a mid-air drop. An aft stabilizer helps to stabilize the vehicle immediately after deployment, and also contains the igniter for the rocket motor. A folding wing, tail, and control surfaces unfold after deployment to help stabilize the aircraft as well. After the vehicle is stabilized and the motor is ignited, the aft stabilizer is discarded, and the aircraft begins its 2-3 minutes of powered flight. Once the motor burns out, the vehicle continues in gliding flight for an additional 4-6 minutes before the mission is concluded. This concept of operations is illustrated in Figure 1-2.

1.2.2 Aircraft design

The vehicle is built around a 3D-printed titanium motor case, as shown in Figure 1-3. The motor case serves as pressure vessel for the solid rocket motor used to propel

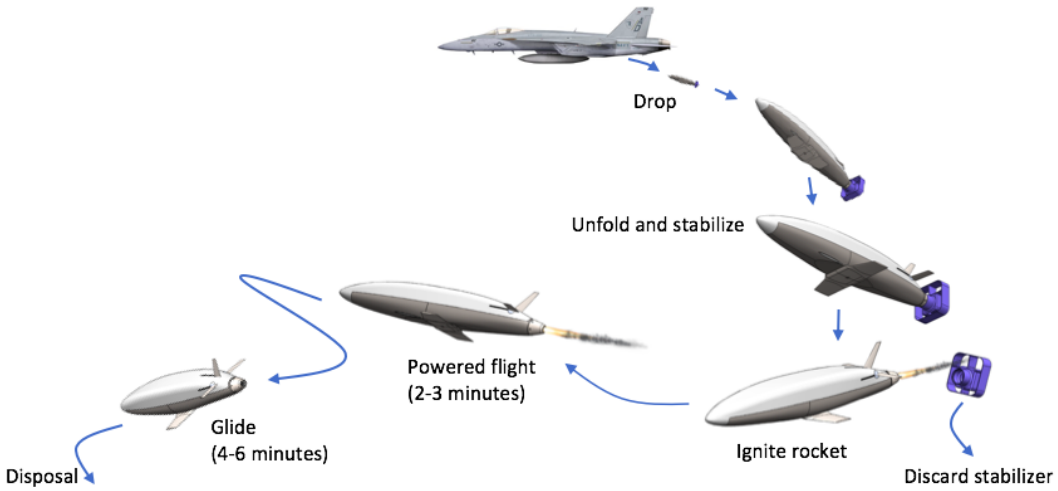

Figure 1-2: The deployable Firefly vehicle has several mission phases.

the vehicle. The bottom half of the motor case also forms part of the outer structure of the entire Firefly aircraft. A fairing is attached to the top of the motor case to complete the rest of the outer geometry, and contains the top and forward payloads of the vehicle. A wing on the bottom of the vehicle serves as a lifting surface. A vertical tail and servo-actuated horizontal tails help to stabilize and actively control the vehicle during the flight. On the aft end of the vehicle is a rocket nozzle assembly consisting of a nozzle carrier, nozzle insulator, and nozzle insert.

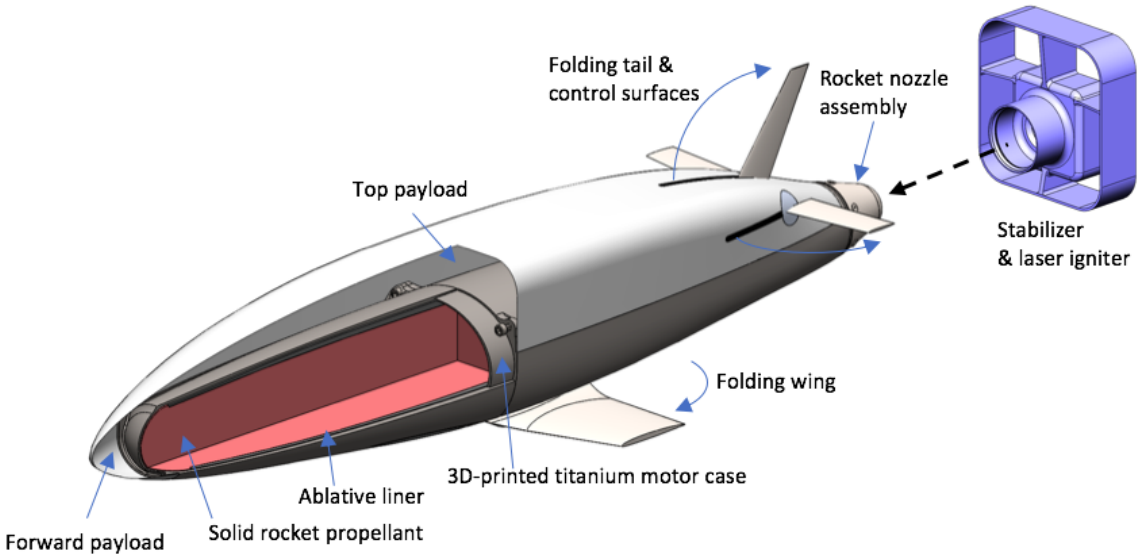

Figure 1-3: The Firefly vehicle is built around a solid rocket motor.

The solid rocket motor consists of several components, including the propellant and liner. The motor uses an end-burning configuration which is ignited at the aft end of the vehicle. The flame front proceeds forward along the vehicle length until all the propellant is consumed, as shown in Figure 1-4.

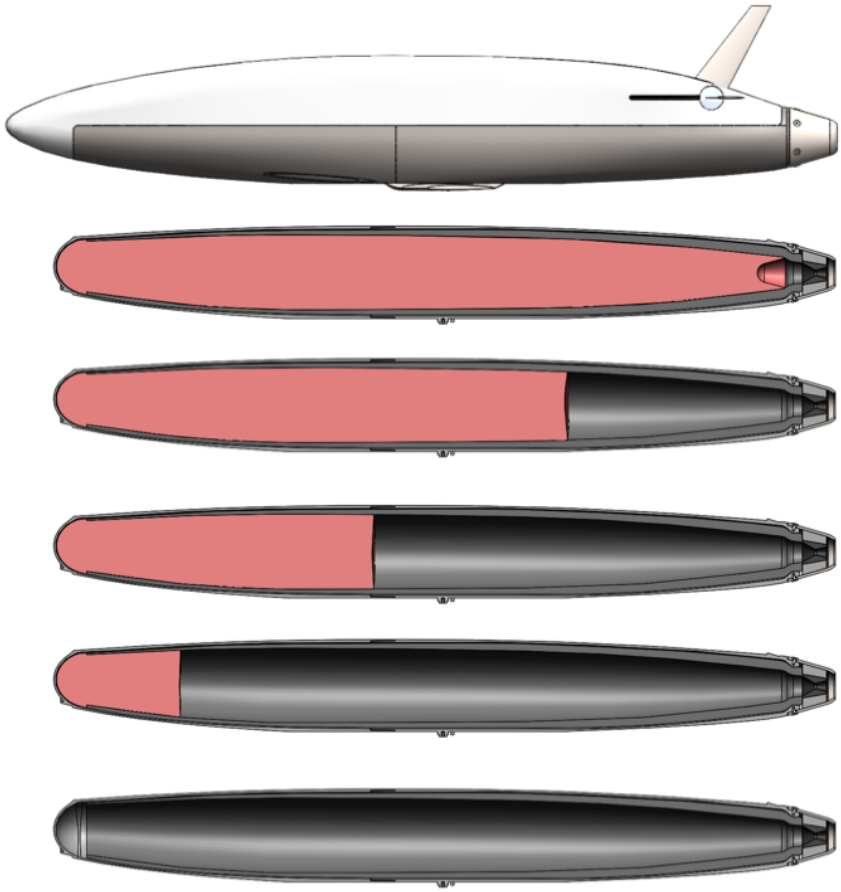

Figure 1-4: Firefly uses a contoured motor in an end-burning configuration.

The propellant is an ammonium perchlorate composite propellant which burns to propel the aircraft. It is doped with a chemical burn rate suppressant which helps to reduce the propellant's burn rate. The burn rate suppressant is added in different proportions to different segments of the motor which allows acceptable chamber pressure and thrust to be maintained despite a changing propellant burning area. The liner encases the propellant in order to provide thermal protection for the motor case and the rest of the vehicle. The two-part titanium motor case is joined around the motor before integration with the rest of the vehicle.

1.3 Test motor: Titanium Candle

The "Titanium Candle" motor is a test motor with a similar aspect ratio, mass, and size as the Firefly motor, but with a simpler cylindrical geometry, as depicted in Figure 1-5.[2] The simplified geometry allows for faster and more reliable motor production, testing, modeling, and analysis than is currently possible for the Firefly "flight-like" motor. The Titanium Candle motor therefore enables the propellant, liner, and manufacturing techniques to be developed and iterated on while many of the details of the flight-like motor are still being determined.

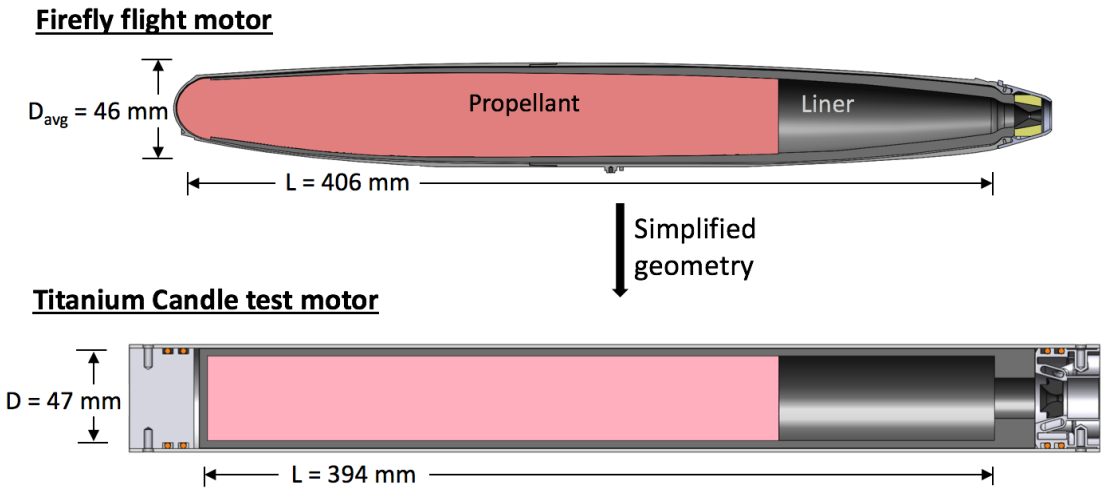

Figure 1-5: The Titanium Candle test motor has a simplified geometry to enable faster development of the propellant and liner.

1.3.1 Test motor design

Titanium Candle utilizes a simple cylindrical geometry for the propellant, liner, and motor case. A titanium tube serves as the motor case for this configuration, and is sealed using custom forward and aft closures. The aft closure contains the nozzle and has channels for flowing water to cool the nozzle during static firings of the motor. There are additional ports on the aft closure for attaching a pressure transducer and thermocouple for data collection during firings of the motor.

[2]The Titanium Candle test motor was conceived and designed by Jon Spirnak of the MIT Department of Aeronautics and Astronautics in order to characterize the ablation of the thermal liner for Firefly. More details on his work can be found in his thesis [7].

The propellant has a constant cross-sectional area and the liner has a constant thickness for the entire motor. This allows measurements of thrust, chamber pressure, and liner ablation to be made without having to account for changes in propellant burn area or liner thickness.

1.4 Manufacturing challenges for small, fast flight vehicles

The small scale and end-burning motor configuration of the Firefly vehicle create a need for precise manufacturing methods for the motor's propellant and liner. A small defect in the propellant or liner – such as a void in the propellant or a region of poor adherence between the propellant and liner – can cause a corresponding increase in propellant burning area. For a small end-burning motor, this increase in burning area can lead to large fluctuations in vehicle chamber pressure and thrust, while being insignificant in a vehicle of larger scale. Consequently, rigorous manufacturing methods are required for the successful production of the Firefly motor. However, many challenges have been encountered while developing these motor manufacturing methods.

1.4.1 Propellant

The Firefly vehicle requires a low thrust, long endurance motor in order to meet its mission requirements. Solid rocket motors with these characteristics require high-density propellant in order to maximize endurance and precise burning areas in order to have the desired chamber pressure and vehicle thrust.[3] However, voids in the propellant can change the burning area of the regressing propellant surface, as shown in Figure 1-6.

For a small-scale end-burning motor, seemingly small voids can result in a significant change in chamber pressure and thrust once exposed. As an example of

[3] A discussion of the effect of burning area on chamber pressure and thrust is given in Section 2.5.

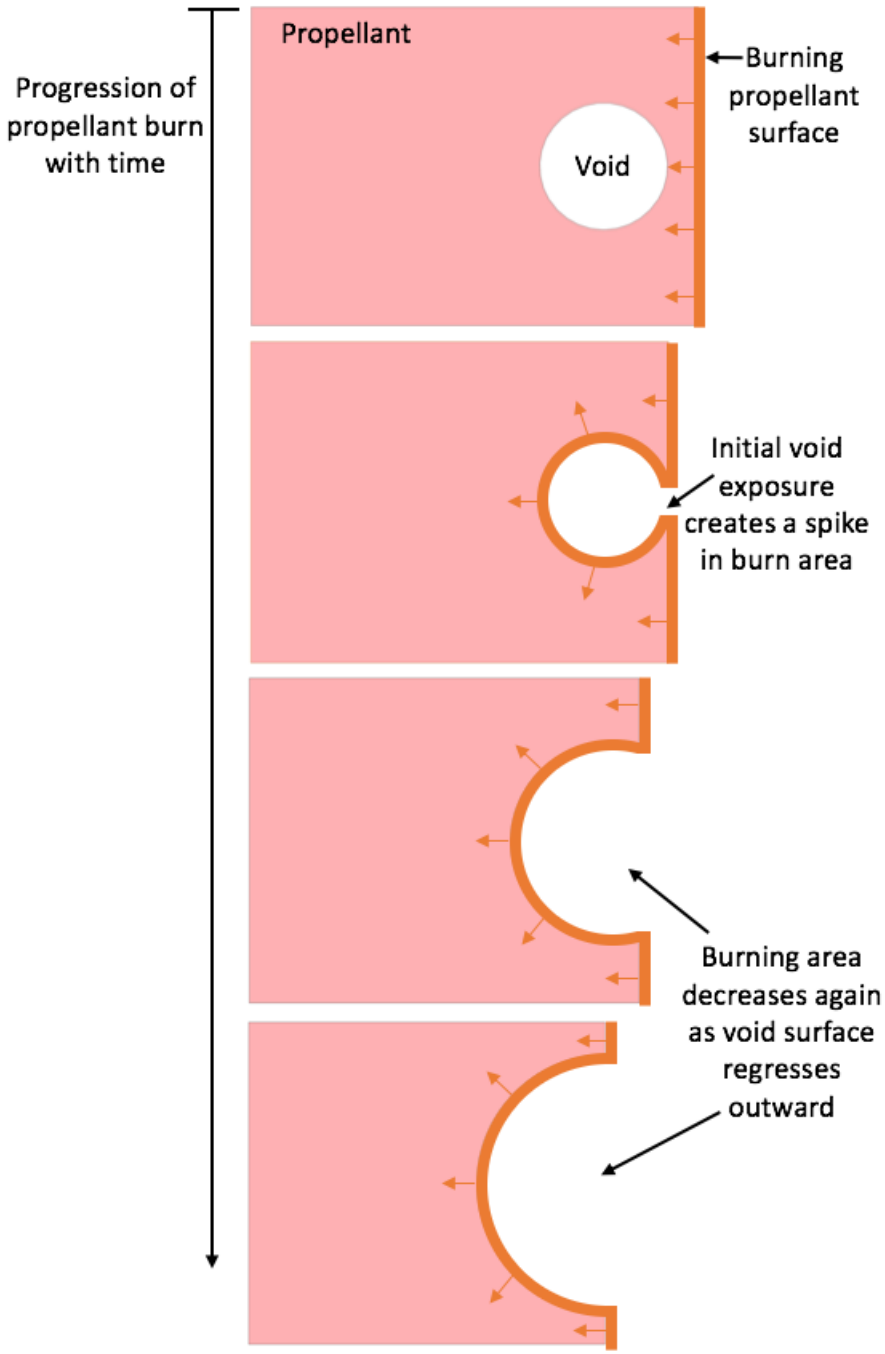

Figure 1-6: The exposure of a void as propellant burns results in an increased propellant burning area.

the relative effects of void exposure on chamber pressure for flight vehicles of different scales, consider two solid rocket-propelled vehicles: Firefly and the AIM-9M Sidewinder missile. Selected specifications for each are given in Table 1.1.

Table 1.1: Selected vehicle specifications for Firefly and AIM-9M Sidewinder missile.

	Firefly	**AIM-9M Sidewinder**
Motor mass [kg]	~1.5	44.9 [8]
Motor length [mm]	406	1803 [8]
Motor diameter [mm]	~46	127 [8]
Burning area [mm^2]	~1700	$\mathcal{O}(10^5)$

For each vehicle, the peak increase in chamber pressure due to the exposure of a 10 mm diameter spherical void is modeled.[4] A depiction of the resulting spikes in vehicle chamber pressure are shown in Figure 1-7. The results of this brief example are illustrative of an important point: the effects of manufacturing flaws in propellant can be substantial for a small vehicle such as Firefly, while being insignificant for vehicles of larger scale. Precise manufacturing strategies for small, fast vehicles are therefore especially important due to the relative impact on vehicle performance.

Early in the propellant development program, flaws in the manufacturing processes for Titanium Candle propellant grains led to the existence of voids. In the case of the Titanium Candle propellant grain cross-section shown in Figure 1-8, volatiles in the propellant precursors caused many small 1-3 mm voids to form in the cured propellant. These voids reduced the density of the propellant grain, and additionally could have impacted the motor performance. To avoid the risk of damaging motor hardware and instrumentation, the grain was never burned. These manufacturing flaws, and their potential for causing substantial increases in vehicle chamber pressure and thrust, motivate the development of improved procedures and tooling for propellant manufacturing.

1.4.2 Liner

Processes for manufacturing the liner are also challenging. Due to Firefly's end-burning motor configuration, the liner serves not only to thermally protect the ti-

[4]Appendix A shows a method for calculating pressure fluctuations resulting from increases in burning area.

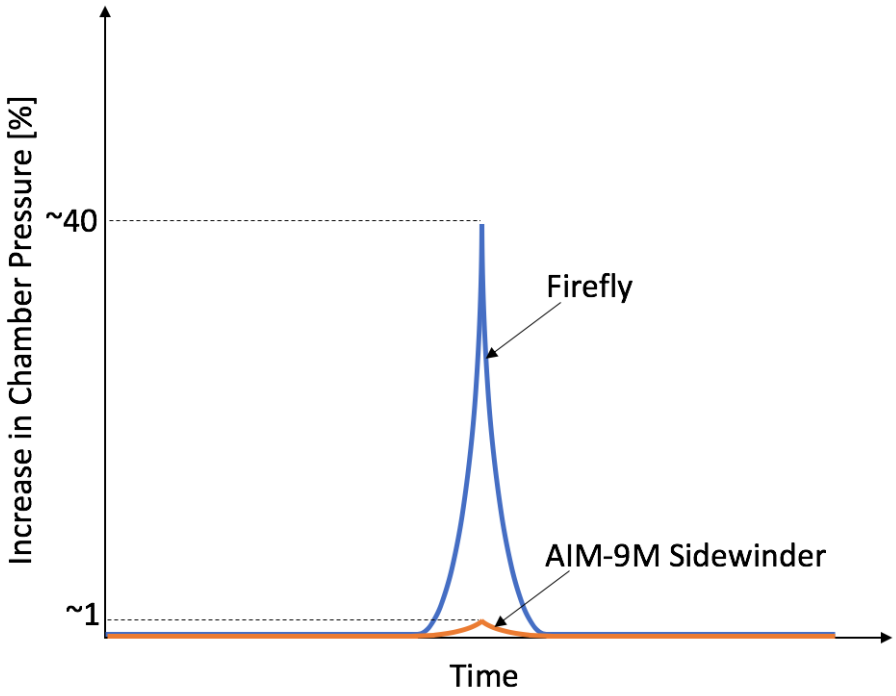

Figure 1-7: The relative increase in chamber pressure due to the exposure of a 10 mm void is substantially greater for Firefly than the larger AIM-9M Sidewinder missile.

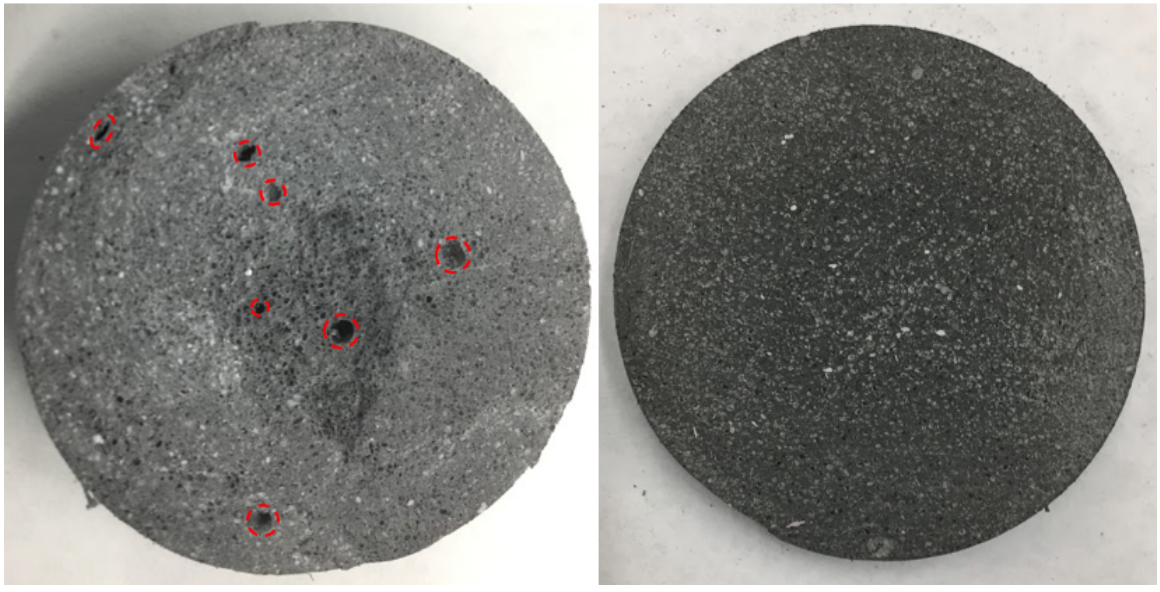

Figure 1-8: Volatiles in the propellant mixture led to the formation of many small 1-3 mm voids (left) in a test motor propellant grain. Development of improved manufacturing methods has helped to create denser, void-free propellant (right).

tanium motor case from the hot combustion products of the propellant, but it also inhibits the edges of the propellant grain to prevent edge-burning. As shown in Figure 1-9, if an end-burning motor is not inhibited at its edges, the burning area increases as the edges of the propellant burn.

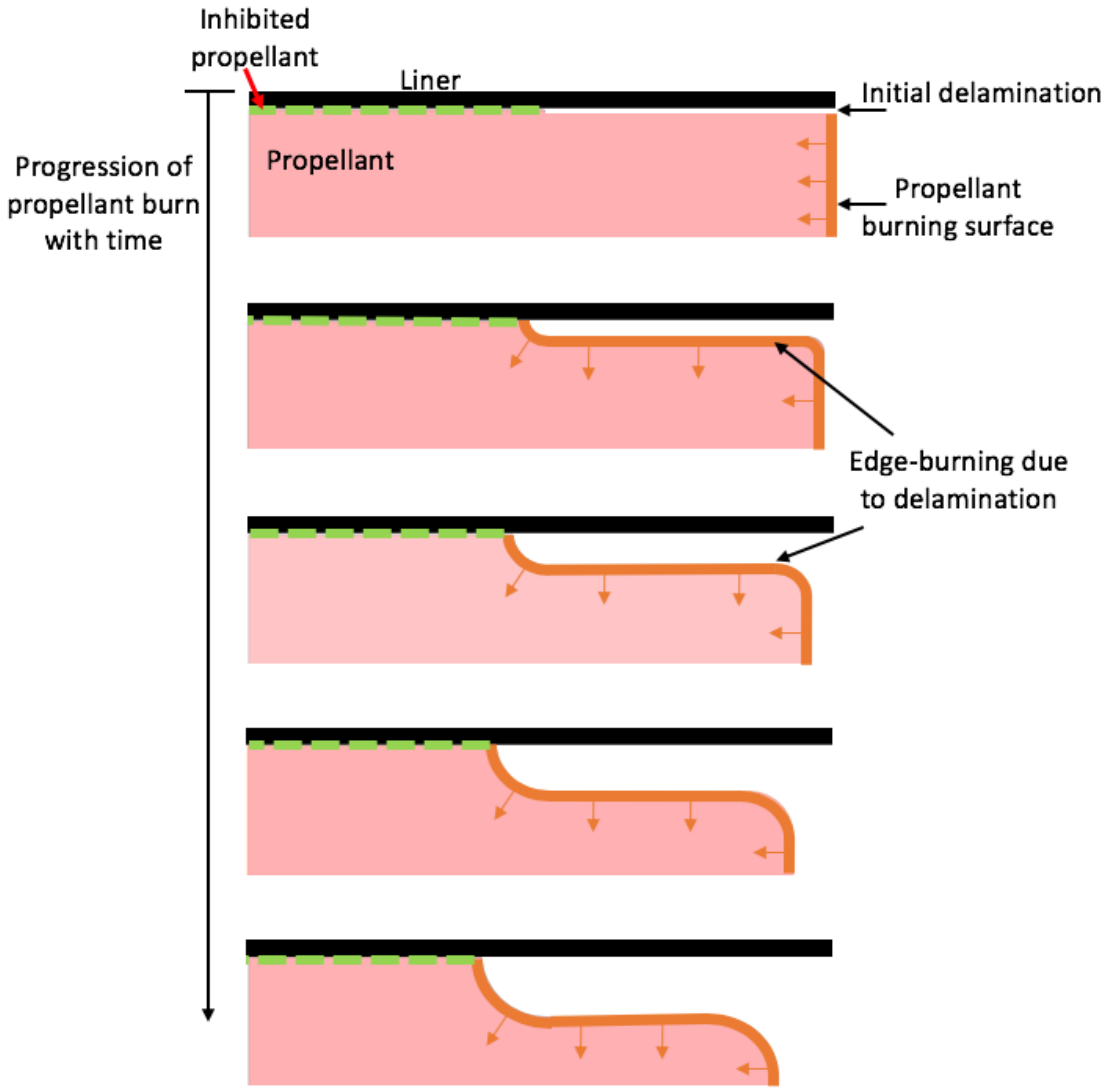

Figure 1-9: Failed inhibition at the edges of an end-burning motor leads to substantial increase in burning area through edge-burning.

Improper preparation of the propellant grain surface has led to delamination between the propellant grain and the liner in previous Titanium Candle motor castings, as shown in Figure 1-10. In the event of delamination between the propellant and liner, edge-burning ensues as a large area on the outer surface of the propellant grain

is exposed. An illustration of liner delamination and propellant edge-burning for the Titanium Candle motor is shown in Figure 1-11. Inherent material properties of the propellant and liner make maintaining a strong propellant-to-liner bond difficult: the polar nature of polyurethane rubber in the propellant is incompatible with the nonpolar silicone rubber of the liner [9].

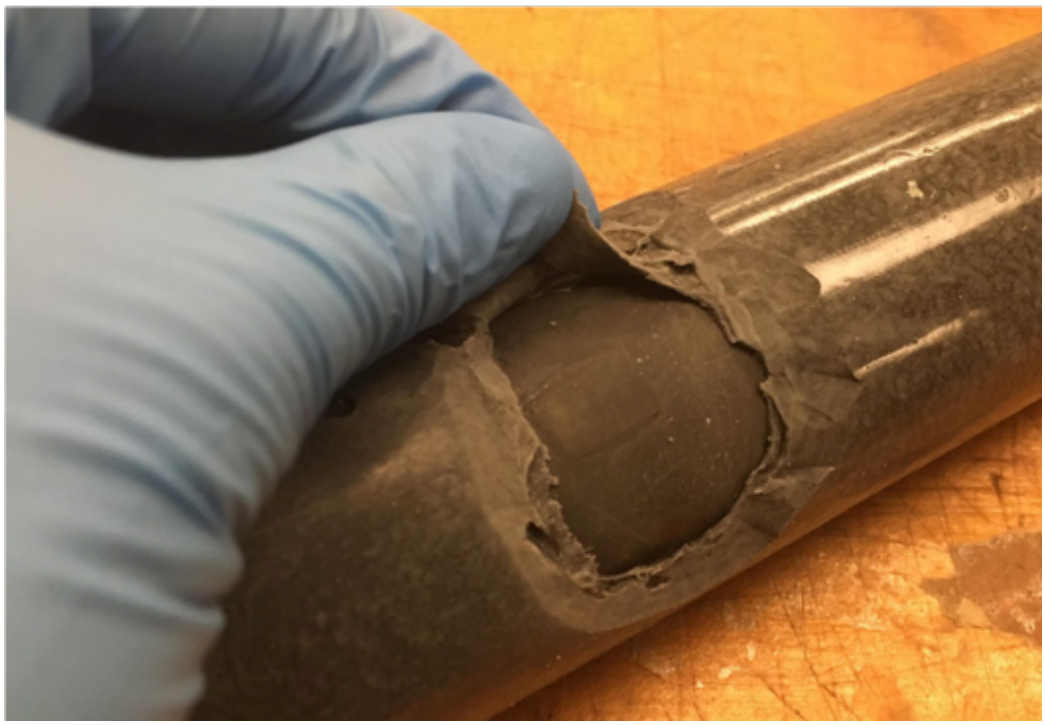

Figure 1-10: Poor surface preparation has led to delamination between the propellant grain and liner for a Titanium Candle motor.

The bonding of silicone rubbers to polyurethane materials is regularly done in the field of facial prosthetics. Numerous clinical studies in this field report the regular delamination of these two components in use [10] [11] [12]. Other studies directly looking at the bonding of silicone thermal insulating materials to solid propellant grains also report difficulty for adhering the two materials [13]. Despite these challenges, researchers from these studies report that careful substrate preparation and application of an appropriate primer can help with the bonding of these two materials. Liner manufacturing methods involving these strategies can be explored to prevent delamination and edge-burning for Firefly as well.

The bond between the liner and propellant has failed before in a static fire of the

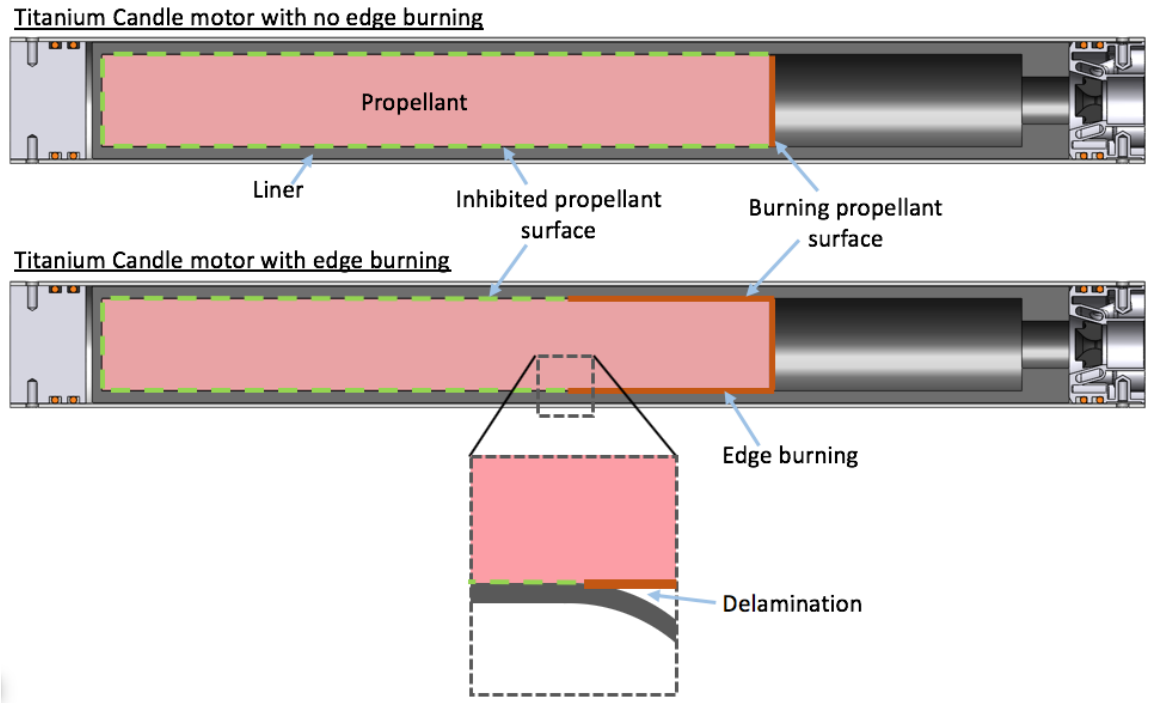

Figure 1-11: Delamination between the propellant and liner for the Titanium Candle motor leads to edge-burning.

Titanium Candle motor, leading to edge-burning and severe over-pressurization of the motor case. Measured values for chamber pressure and thrust were nearly an order of magnitude greater than expected, as shown by the static fire data in Figure 1-12. These results are unacceptable for producing a low-thrust, long-endurance motor. In order to address this edge-burning problem, careful manufacturing methods are developed to create a consistent and robust propellant-to-liner bond.

1.5 Document structure

The production of the Firefly vehicle and Titanium Candle motor has required the implementation of quality-driven manufacturing methods. These methods enable the manufacture of dense, void-free propellant grains with strong propellant-to-liner bonds, and are critical for achieving proper motor performance. This thesis documents the development of these methods, their implementation, and their impact on motor performance as measured in motor static fire tests.

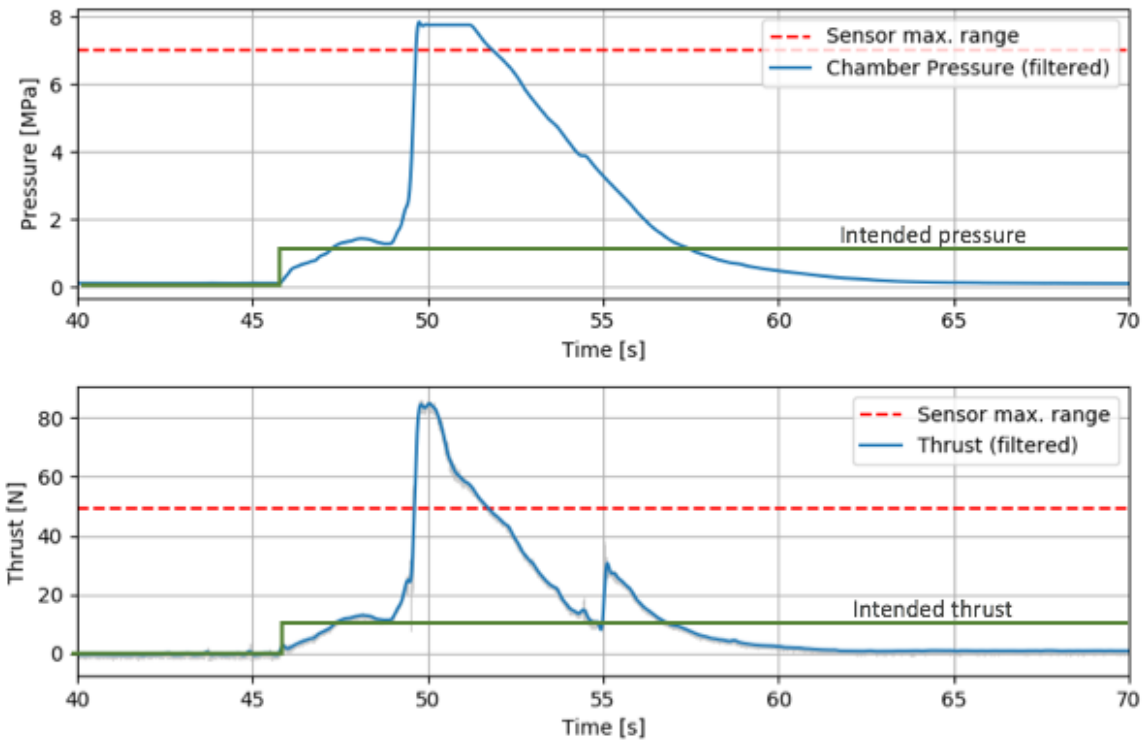

Figure 1-12: Edge-burning during a Titanium Candle static fire led to unintentionally large pressure and thrust levels.

A background review on relevant topics related to solid rocket motors is presented in Chapter 2. Current developed manufacturing methods and tooling for Titanium Candle and extensions of these methods for multi-segment propellant grains and flight-like motor geometries are describe in Chapter 3. Theory and tests for the manufacturing of high-quality propellant and liner are given in Chapter 4. Motor static fire test setups and data are presented in Chapter 5. Concluding remarks are lastly provided in Chapter 6.

Chapter 2

Solid rocket motors for small, fast flight vehicles

In order to motivate requirements and develop manufacturing methods for solid rocket motors used in small, fast aircraft, an understanding of motor components, configurations, and internal ballistics is necessary. This chapter provides a discussion of relevant topics for solid rocket motors in the context of the design and manufacturing of the Firefly motor.

2.1 Motor components

Solid rocket motors are mechanically simple propulsion devices with only a few key components [14]:

- The *propellant* is a solid grain containing both fuel and oxidizer. It burns to produce hot combustion products which give rise to the motor's chamber pressure and thrust.
- The *motor case* contains the propellant grain and acts as a pressure vessel for the combustion products during motor operation.
- The *thermal insulation* protects the motor case from the hot gasses produced from the burning propellant.

- The *igniter* delivers energy to the propellant surface and pressurizes the motor case in order to initiate stable combustion of the propellant.

- The *nozzle* expands and accelerates the high pressure gas in the motor case in order to produce thrust.

These basic components are depicted for a general solid rocket motor in Figure 2-1. All of these components are considered for the design and manufacturing of the Firefly flight motor.

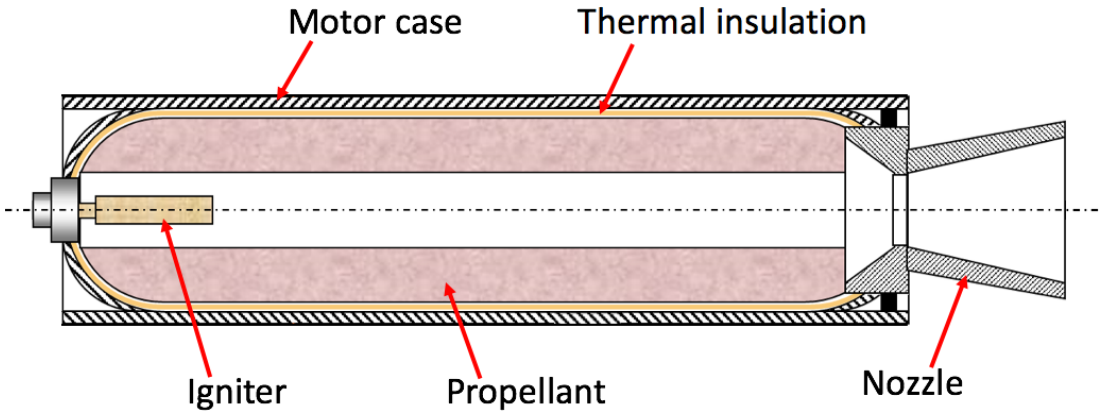

Figure 2-1: Solid rocket motors are mechanically simple propulsion devices with only a few key components. Modified from [15].

2.2 Motor configurations

The components in solid rocket motors can be configured in a number of ways in order to achieve mission objectives. In the design of small, fast flight vehicles, the configuration choice for the propellant is especially important, since it can significantly impact the thrust and powered flight time for the vehicle.

Some of the most common propellant configurations include end-burners, core-burners, and core-burners with slots. These configurations are illustrated in Figure 2-2. A brief description of these configurations is given below:

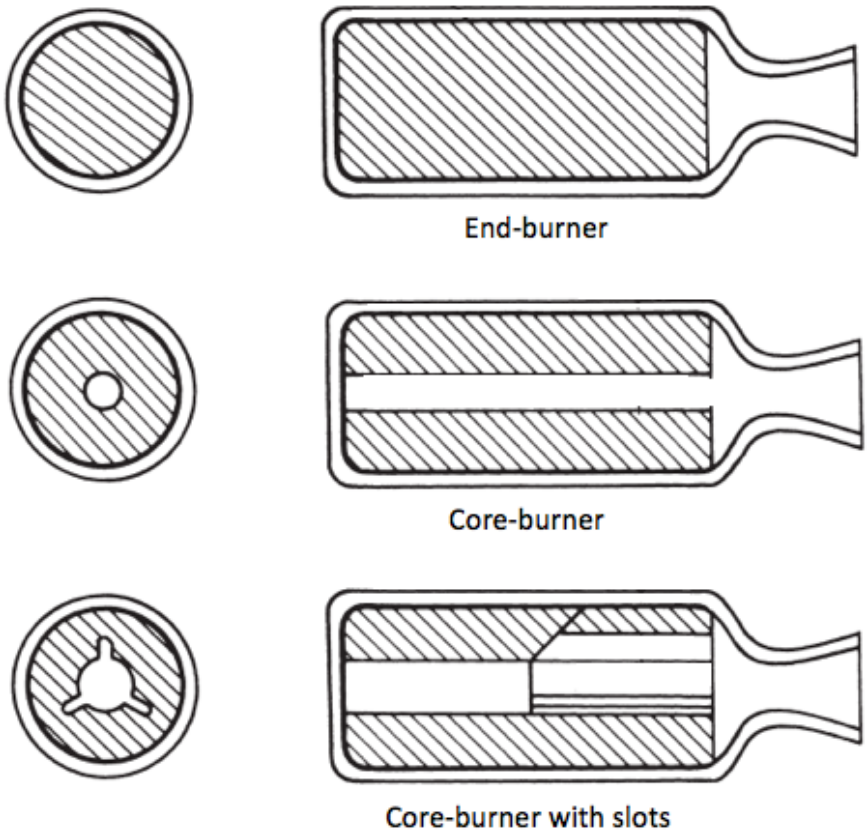

Figure 2-2: Different motor configurations have different burning surface areas and thrust profiles. Modified from [16].

- *End-burners* have a single exposed propellant face while the edges are inhibited. The propellant regresses axially along the length of the motor as the propellant burns. These motors have a typically neutral thrust profile, since the burning area of propellant remains constant for the duration of the burn.

- *Core-burners* have a typically cylindrical propellant grain with a hollow circular core. The entire interior surface of the core burns, and the surface of the core regresses radially outward as the propellant burns. Core-burning motors display a progressive thrust profile, since the burning area of the propellant increases as the propellant surfaces regresses outwards.

- *Core-burners with slots* are similar to simple core-burners as they both have hollow cores with interior burning surfaces. In addition to the simple cylindrical core, these motors have slots that add additional surface area to the core. The

core regresses generally radially outward as the propellant burns, although the slots create tangential regression as well. The exact design of the core slots is usually chosen to achieve a desired thrust profile, which is typically neutral or progressive.

The objectives of the Firefly vehicle require a motor with a relatively low thrust and long endurance. These objectives can best be achieved using an end-burning motor configuration. In this configuration, the burning area for the entire burn is relatively small, which aids in creating a low-thrust motor. Additionally, in an end-burner, the flame front proceeds axially along the entire length of the motor, instead of in the generally smaller radial direction for the other configurations. This axial progression leads to a relatively long propellant burn time, which is best for maximizing vehicle endurance. However, end-burning motors create additional challenges for thermal protection of the motor case, which will be discussed further in Section 2.8.

2.3 Ammonium perchlorate composite propellants

The Firefly flight motor uses an ammonium perchlorate composite propellant (APCP) to power the vehicle during flight. These propellants have a number of desirable properties for small, fast, long-endurance flight vehicles, including a high energy density, wide range of stable ambient temperatures, and good handling and storage qualities [16]. Many sources provide descriptions of the properties and composition of APCPs, and information from these sources is summarized in this section [14] [16] [17] [18].

2.3.1 Composition

Composite propellants are a heterogenous mixture of fuel, oxidizer, and other components. The common components in APCPs are given below:

- The *oxidizer* for this specific type of propellant is ammonium perchlorate (NH_4ClO_4). It has good compatibility with other propellant materials and a high oxidizing

potential, and is the most commonly used oxidizer in solid propellant manufacturing.

- The *binder* is a polymer which provides a structural matrix for the rest of the propellant components. They are typically organic rubbers which also serve as a fuel.
- The *curative* is an agent that cross-links the prepolymers in the binder to form the solid rubber matrix for the propellant.
- The *plasticizer* is a low viscosity liquid which helps to improve the rheological properties and extend the pot life of the uncured propellant.
- An *opacifier* is an additive used to make propellant opaque, which prevents heat from the flame from being radiatively transferred deep into the solid propellant.
- *Metal fuels* are powdered metals added into the solid propellant mixture in order to increase its density and combustion temperature, which can improve performance.
- *Burn rate modifiers* are additives that can catalyze or suppress the burn rate, allowing the propellant burn rate, and consequently thrust, to be tailored for some objective.

No metal fuel is used in the Firefly propellant due to the low-thrust, long duration requirements for the motor. Additionally, the motor uses a burn rate suppressant to further reduce the motor's chamber pressure and thrust, which is discussed further in Section 2.6.

2.4 Performance parameters

Many parameters are important for evaluating the performance of solid rocket motors. These parameters allow motors with different propellants, configurations, and nozzle geometries to be compared and provide metrics for design and manufacturing improvements. Several of these parameters will be described in this section.

2.4.1 Thrust

The momentum flux of combustion products from a solid propellant exiting a motor imparts a thrust force on its containing vehicle. The thrust imparted on a vehicle is

$$F = \dot{m}v_e + (p_e - p_a)A_e \tag{2.1}$$

where $\dot{m}$ is the mass flow rate of combustion products, v_e is the exit velocity, p_e is the nozzle exit pressure, p_a is atmospheric pressure, and A_e is the nozzle exit area. The $\dot{m}v_e$ term is the thrust contribution due to the exiting momentum of the combustion products, and the $(p_e - p_a)A_e$ term is the thrust due to the pressure difference between the nozzle exit pressure and atmospheric pressure. If the nozzle exit expansion area ratio is matched such that the nozzle exit pressure equals the atmospheric pressure, then Equation 2.1 simplifies to

$$F = \dot{m}v_e \tag{2.2}$$

2.4.2 Total impulse

The total impulse, I, for a rocket motor can be found by simply integrating the motor's thrust over time:

$$I = \int F \mathrm{d}t \tag{2.3}$$

The total impulse is related to the energy stored and subsequently released in a rocket motor. For a motor with constant thrust and short startup and ending transients, the total impulse is simply

$$I = Ft_{burn} \tag{2.4}$$

where t_{burn} is the motor burn time.

2.4.3 Specific impulse

The specific impulse, I_{sp}, for a motor is a measure of efficiency which quantifies the impulse delivered per unit weight of propellant. The average specific impulse is therefore equal to a motor's total impulse divided by the total weight of propellant expelled. This can be expressed as

$$I_{sp} = \frac{\int F \mathrm{d}t}{g \int \dot{m} \mathrm{d}t} = \frac{I}{m_p g} \tag{2.5}$$

where g is the standard gravitational acceleration, $\dot{m}$ is the propellant mass flow rate, and m_p is the total mass of propellant.

The instantaneous specific impulse can be written as

$$I_{sp} = \frac{F}{g\dot{m}} = \frac{c}{g} \tag{2.6}$$

where c is the effective exhaust velocity of the motor, such that $F = \dot{m}c$. When the nozzle is matched such that $p_e = p_a$, the effective exhaust velocity is equal to the actual average exhaust velocity, or $c = v_e$.

2.4.4 Coefficient of thrust

By definition, the coefficient of thrust is

$$C_F \equiv \frac{F}{A_t p_c} \tag{2.7}$$

where F is the thrust force, A_t is the nozzle throat area, and p_c is the chamber pressure. Since the coefficient of thrust is not dependent on chamber temperature, it is roughly independent of the propellant choice. This makes it a useful performance parameter for comparing nozzle geometries and evaluating the effect of gas expansion in the nozzle on thrust.

Using the coefficient of thrust permits a simplified equation for vehicle thrust. By simply rearranging Equation 2.7, vehicle thrust can be calculated using

$$F = C_F A_t p_c \tag{2.8}$$

For a matched nozzle, where $p_e = p_a$, the coefficient of thrust can be found using [16]

$$C_F\left(p_c, p_e, \gamma\right) = \sqrt{\frac{2\gamma^2}{\gamma - 1}\left(\frac{2}{\gamma + 1}\right)^{\frac{\gamma+1}{\gamma-1}}\left[1 - \left(\frac{p_c}{p_e}\right)^{\frac{1-\gamma}{\gamma}}\right]} \tag{2.9}$$

where γ is the ratio of specific heats for the combustion products, p_c is the chamber pressure, and p_e is the nozzle exit pressure.

2.4.5 Characteristic velocity

The characteristic velocity, c^*, for a motor is a performance parameter that is useful for comparing the quality of different propellants. It is defined as

$$c^* \equiv \frac{p_c A_t}{\dot{m}} \tag{2.10}$$

where p_c is the chamber pressure, A_t is the nozzle throat area, and $\dot{m}$ is the mass flow rate through the nozzle. By making proper substitutions for terms in Equation 2.10, the characteristic velocity can be written as [16]

$$c^*\left(R, \gamma, T_c\right) = \sqrt{\frac{RT_c}{\gamma\left(\frac{2}{\gamma+1}\right)^{\frac{\gamma+1}{\gamma-1}}}} \tag{2.11}$$

where R is the specific gas constant for the combustion products, γ is the ratio of specific heats for the combustion products, and T_c is the combustion chamber temperature. Because the characteristic velocity is only dependent on properties of the combustion products, it is roughly constant for a particular propellant choice.

With the characteristic velocity also defined, vehicle thrust can be expressed in another way:

$$F = C_F \dot{m} c^* \tag{2.12}$$

This expression is interesting since the effects of the propellant formulation – through the characteristic velocity, c^* – and the nozzle geometry – through the coefficient of thrust, C_F – can roughly be separated from each other when expressing the vehicle thrust.

2.5 Internal ballistics

An understanding of internal ballistics for solid rocket motors – the mechanisms by which solid rocket propellants burn and how these mechanisms influence chamber pressure, thrust, and other performance parameters – is necessary for designing small, fast aircraft and motivating their manufacturing methods. A review of several key aspects of internal ballistics for solid rocket motors is described in this section.

2.5.1 Mass flow

The rate of change of mass inside the combustion chamber for a solid rocket motor can be expressed as

$$\frac{dm_c}{dt} = \dot{m}_{in} - \dot{m}_{out} \tag{2.13}$$

where m_c is the mass of gas in the combustion chamber, $\dot{m}_{in}$ is the mass flow rate of gas entering the combustion chamber due to the burning propellant, and $\dot{m}_{out}$ is the mass flow rate of gas exiting the combustion chamber through the nozzle.

The mass flow rate of gas exiting through the nozzle can be expressed by rearranging the definition for the characteristic velocity given in Equation 2.10. This yields the expression

$$\dot{m}_{out} = \frac{p_c A_t}{c^*}. \tag{2.14}$$

The mass flow rate of gas entering the chamber due to the burning propellant can be found using

$$\dot{m}_{in} = r A_b \rho_p \tag{2.15}$$

where r is the propellant burn rate with units of velocity, A_b is the burning area, and ρ_p is the density of the solid propellant. In steady-state propellant combustion, the rate of change of mass inside the combustion chamber is zero, or

$$\left.\frac{dm_c}{dt}\right|_{steady} = \dot{m}_{in} - \dot{m}_{out} = 0. \tag{2.16}$$

2.5.2 Equilibrium chamber pressure and thrust

For a reasonable range of chamber pressures, the burn rate of a propellant can be related to the chamber pressure using an empirical burn rate law,

$$r = a {p_c}^n \tag{2.17}$$

where r is the propellant burn rate, p_c is the chamber pressure, a is the burn rate coefficient, and n is the burn rate exponent. The values for a and n are determined experimentally for a particular propellant.

With this relation between the burn rate r and the chamber pressure p_c, an expression for the equilibrium chamber pressure can be found. If the expressions for $\dot{m}_{out}$ and $\dot{m}_{in}$, given in Equations 2.14 and 2.15 respectively, are substituted into the steady-state mass flow expression given in Equation 2.16, the resulting equilibrium chamber pressure is

$$p_{c,eq.} = \left(K_n \rho_p c^* a\right)^{\frac{1}{1-n}} \tag{2.18}$$

where

$$K_n \equiv \frac{A_b}{A_t}. \tag{2.19}$$

Equilibrium thrust can be determined by substituting the equilibrium pressure expression in Equation 2.18 into the thrust expression in Equation 2.8 to get

$$F_{eq.} = C_F \left(p_{c,eq.}, p_e, \gamma \right) A_t p_{c,eq.} \tag{2.20}$$

The expressions for equilibrium in Equations 2.18 and 2.20 can be used to see how chamber pressure and thrust change with an increase in burning area. Figure 2-3 shows theoretical trends for the Titanium Candle test motor calculated using the equilibrium equations. Similar increasing trends would be expected for any stable propellant formulation.

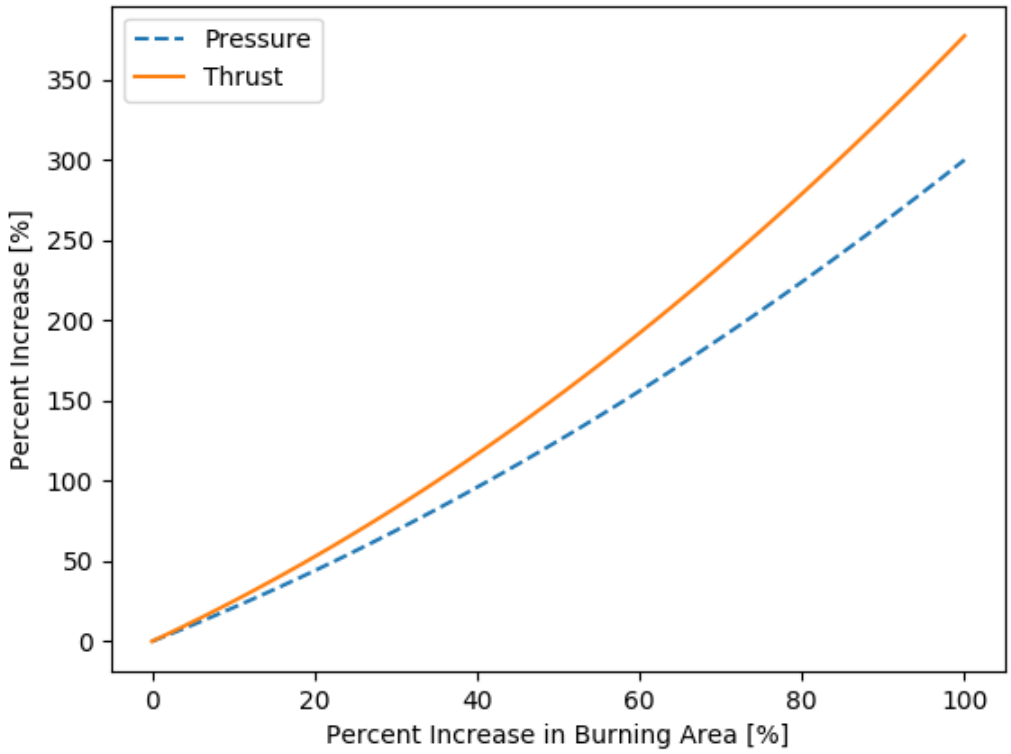

Figure 2-3: Small increases in burning area can have a significant effect on the chamber pressure and thrust for the Titanium Candle motor.

2.6 Burn rate suppression with oxamide

Propellant burn rate suppressants can be used to help produce low-thrust, long-endurance motors needed for small, fast flight vehicles. In the case of the Firefly flight motor, the burn rate suppressant oxamide is used. This section provides background information on oxamide, its effects on burn rate, and applications for small, fast aircraft.

2.6.1 Oxamide as a coolant

Oxamide $(CONH_2)_2$ is a chemical which can be added to composite propellants in order to reduce their burn rate. It does so by functioning as a coolant for the propellant's surface. Since oxamide decomposes endothermically and at a temperature that is lower than the propellant surface temperature, it absorbs a significant amount of energy at the propellant's surface [19] [20]. This slows down both the condensed- and gas-phase reactions at the surface, effectively reducing the burn rate [21].

2.6.2 Predictive model of oxamide's effect

Vernacchia derived a predictive model for the effect of oxamide on a propellant's burn rate [6].[1] The model assumes a baseline propellant with a known burn rate r^* is doped with some mass fraction w_{om} of oxamide. The model predicts the burn rate for the oxamide-doped propellant $r(w_{om})$ as a function of the oxamide mass fraction w_{om}, such that

$$r(w_{om}) = \phi_{om}(w_{om})\, r^* \tag{2.21}$$

where

$$\phi_{om}(w_{om}) = \frac{1 - w_{om}}{1 + \lambda w_{om}}. \tag{2.22}$$

[1] A detailed discussion of the model's derivation and its comparison to experimental data can be found in Sections 2.6 and 3.4 of Vernacchia's thesis [6].

The dimensionless model parameter λ is a function of gassification enthalpies for oxamide and the undoped propellant and is defined as

$$\lambda \equiv \frac{\Delta h_{gas}^{om} - \Delta h_{gas}^{*}}{\Delta h_{gas}^{*}} \tag{2.23}$$

where Δh_{gas}^{om} is the gassificaiton enthalpy of oxamide and Δh_{gas}^{*} is the gassification enthalpy of the undoped propellant. Thermochemical data suggests that λ is between 4 and 15 for most APCPs.

2.6.3 Applications for small, fast flight vehicles

The Firefly flight vehicle needs a low-thrust motor that provides a relatively constant thrust. However, the contoured shape of the end-burning motor means the propellant burning area changes throughout the burn, which can have significant effects on the chamber pressure and thrust, as shown in Figure 2-3. More specifically, the Firefly propellant burn area varies by approximately a factor of 5 throughout the burn. If the same propellant formulation was used for the entire motor, values for chamber pressure and thrust could fluctuate more than an order of magnitude throughout the burn.[2]

A motor containing multiple segments of oxamide-doped propellants can be used to achieve a more constant thrust and chamber pressure in a motor with varying burn area. Vernacchia's model can be used to predictively determine appropriate fractions of oxamide for each propellant segment. For a target thrust of 8 N, the Firefly propellant grain can be cast in 5 segments with different oxamide fractions to produce acceptable thrust and pressure profiles, as shown in Figure 2-4. This need for multi-segment motors motivates the development of multi-segment propellant mixing and casting methods.

[2]See Appendix A for a sample calculation of these fluctuations.

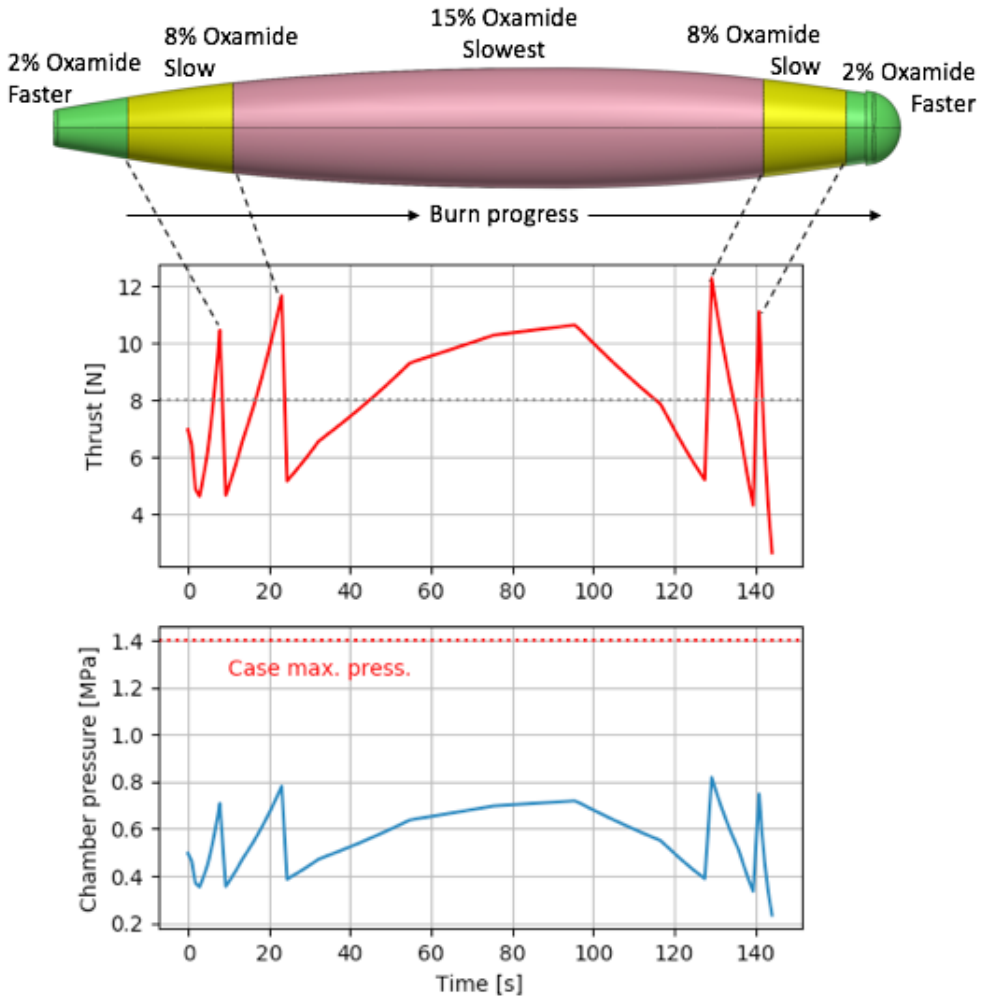

Figure 2-4: Oxamide can be added in different proportions throughout Firefly's propellant grain in order to control chamber pressure and thrust.

2.7 Propellant ignition

Considerations for reliable propellant ignition must also be made in the design and manufacture of solid rocket motors. For slow-burning motors doped with burn rate suppressants, such as the Firefly motor, ignition can be especially challenging for several reasons:

- Slow-burning propellants typically exhibit a minimum required pressure in order to ignite and achieve stable combustion, which is dependent on the burn rate suppressant concentration.

- Due to the addition of a burn rate suppressant which decomposes endothermically when heated, a relatively large amount of energy must be transferred to the propellant's surface to sufficiently raise its temperature and initiate propellant combustion, as compared to faster burning propellants.

To ignite the Firefly motor, a laser is shone through the nozzle and used to ignite a starter propellant grain, which is a small piece of faster burning propellant that ignites more readily than the oxamide-doped propellant in the vehicle's motor. When this starter grain burns, it pressurizes the chamber with its combustion products and also transfers energy to the surface of the vehicle's propellant grain. Both of these functions help to ignite the motor.

To aid in reliable propellant ignition, test motors have been designed with a six-pointed star-shaped starter pocket in the aft end of the propellant grain, as shown in Figure 2-5. This pocket increases the propellants burning area at ignition, which helps the chamber to pressurize quickly and achieve stable combustion. The starter pocket also serves as a place to insert the starter propellant grain.

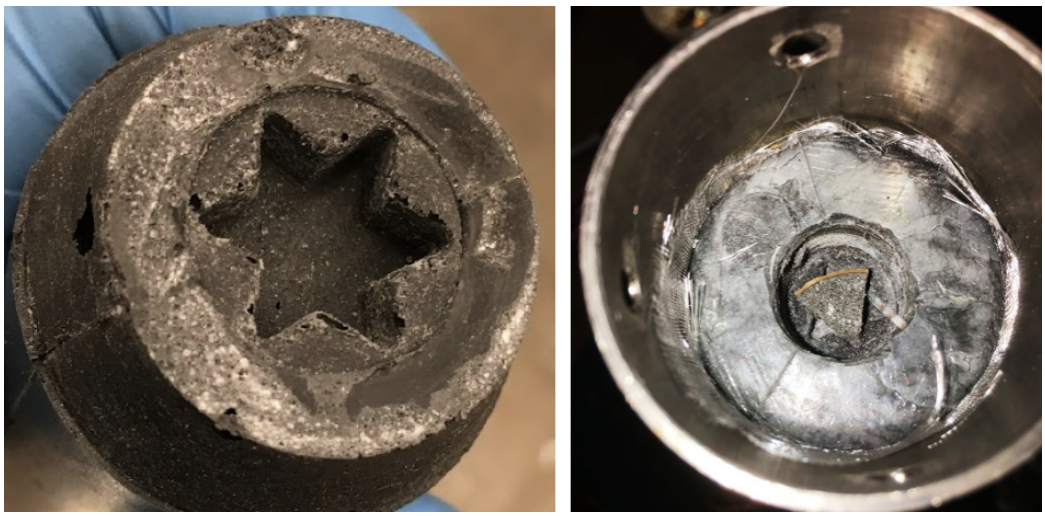

Figure 2-5: The star-shaped propellant starter pocket (left) creates more surface area for propellant ignition. A starter grain is inserted into the starter pocket (right) in order to ignite the propellant.

2.8 Thermal management

All solid rocket motors require some method for managing heat transferred to the motor case and vehicle hardware form the intensely hot combustion products in the motor. This section discusses several thermal management methods for solid rocket motors, as well as challenges and solutions for thermal management in long-burning motors for small, fast flight vehicles such as Firefly.[3]

2.8.1 Methods of thermal management for solid rocket motors

Several methods of thermal management for solid rocket motors are possible:

- *Heat sink* methods rely on a thick, conductive motor case which simply acts as a heat sink during the motor burn. The case must have sufficient heat capacity such that the total heat transferred to the case does not increase the temperature above some safe limit.

- *Inert insulator* methods use layers of low thermal conductivity materials to reduce the thermal conduction between the combustion products and the motor case.

- *Ablative insulator* methods use materials which endothermically decompose during the motor burn to remove heat from the insulator's surface.

For fast burning motors, the temperature of the case never achieves a steady-state value: the propellant is fully consumed only a fraction of the way into the thermal transient. These motors are able to use heat sink, inert insulator, or very thin ablative insulator methods to manage the relatively small amount of total energy transferred to the motor case. However, long-endurance solid rocket motors, such as the Firefly flight motor, require methods for thermal management that can protect the motor case for several minutes. A layer of ablative insulation is effective for these requirements.

[3]Spirnak's thesis discusses thermal management for Firefly in more detail [7].

2.8.2 Thermal management for long-endurance motors

The Firefly motor uses a composite ablative material consisting of silicone rubber and chopped carbon and silica fibers to protect the motor case from the hot combustion products in the motor. Since the volume occupied by the liner directly subtracts from the volume of propellant that can be stored inside the motor case, it is desirable for the liner to be as thin as possible. The Firefly motor therefore requires a thin layer of insulation around the entire motor, as shown in Figure 2-6. This thin layer also needs to inhibit the edges of the propellant to prevent edge-burning, as discussed in Section 1.4.2. This need for a thin, consistent, well-adhered layer of thermal liner motivates the development of careful manufacturing methods for its production.

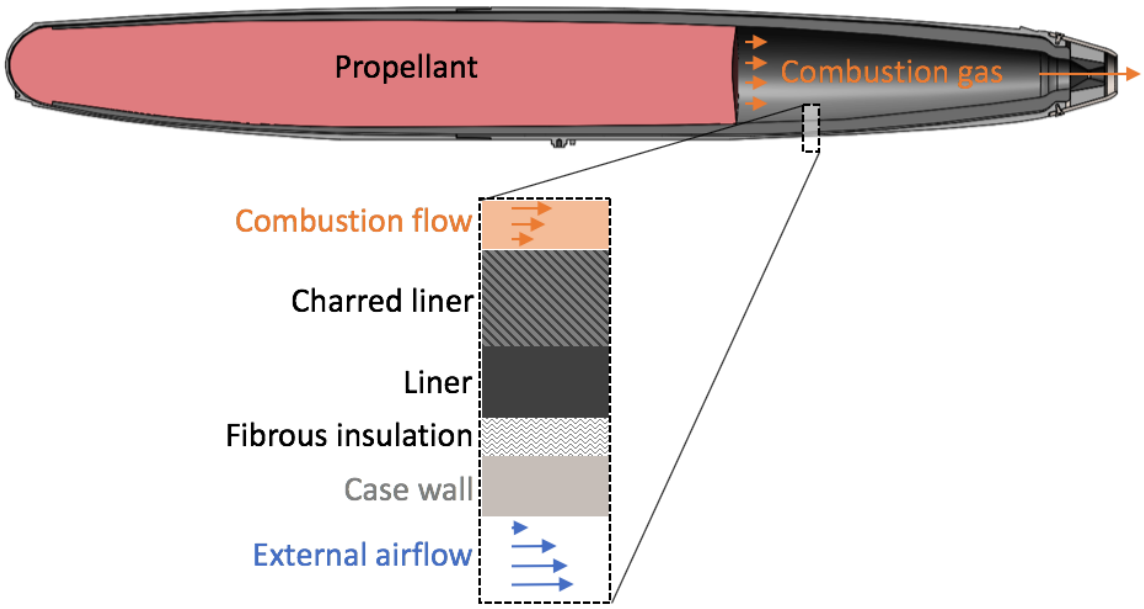

Figure 2-6: Firefly uses a thin layer of an ablative insulating liner to protect the motor case from the hot combustion gasses in the motor.

Chapter 3

Motor manufacturing methods

Manufacturing methods for solid rocket motors used in small, fast flight vehicles were developed using the Titanium Candle test motor detailed in Section 1.3. This chapter will describe the methods used for manufacturing the propellant and liner for this configuration. Additional considerations for extending the motor manufacturing process to cast multi-segment propellant grains and flight-like motor geometries are then described.

3.1 Manufacturing process

An innovative manufacturing process is required for manufacturing motors to enable small, fast aircraft. The manufacturing procedures and hardware were developed with the goal of producing consistently dense propellant grains and liners with a robust propellant-to-liner bond to prevent edge-burning. The propellant grain is mixed and cast first, and then the liner is subsequently injected and cured around the propellant. A high-level overview of this process is shown below in Figure 3-1.The details of the casting hardware and propellant formulation will be discussed first, followed by the procedures.

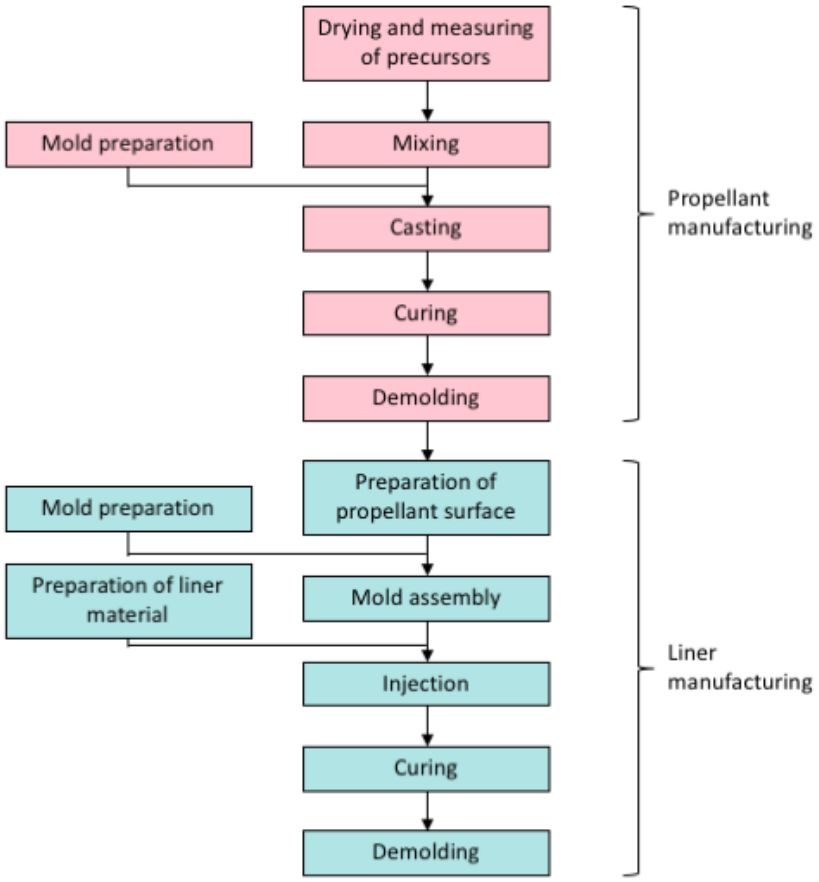

Figure 3-1: The manufacturing process for the propellant and liner consists of many steps.

3.1.1 Manufacturing hardware

Molds

The propellant and liner each have a unique exterior geometry, and so different molds are required for casting each. For manufacturing the liner, a set of custom CNC-machined aluminum molds are fabricated to match the exterior geometry of the liner, as shown in Figures 3-2 and 3-3.

These molds have many features to enable and simplify the casting process:

- *Ports* allow for a vacuum pump to be connected to pull vacuum on the molds. The ports additionally serve as sprues for vacuum injection of the liner material during the casting process.

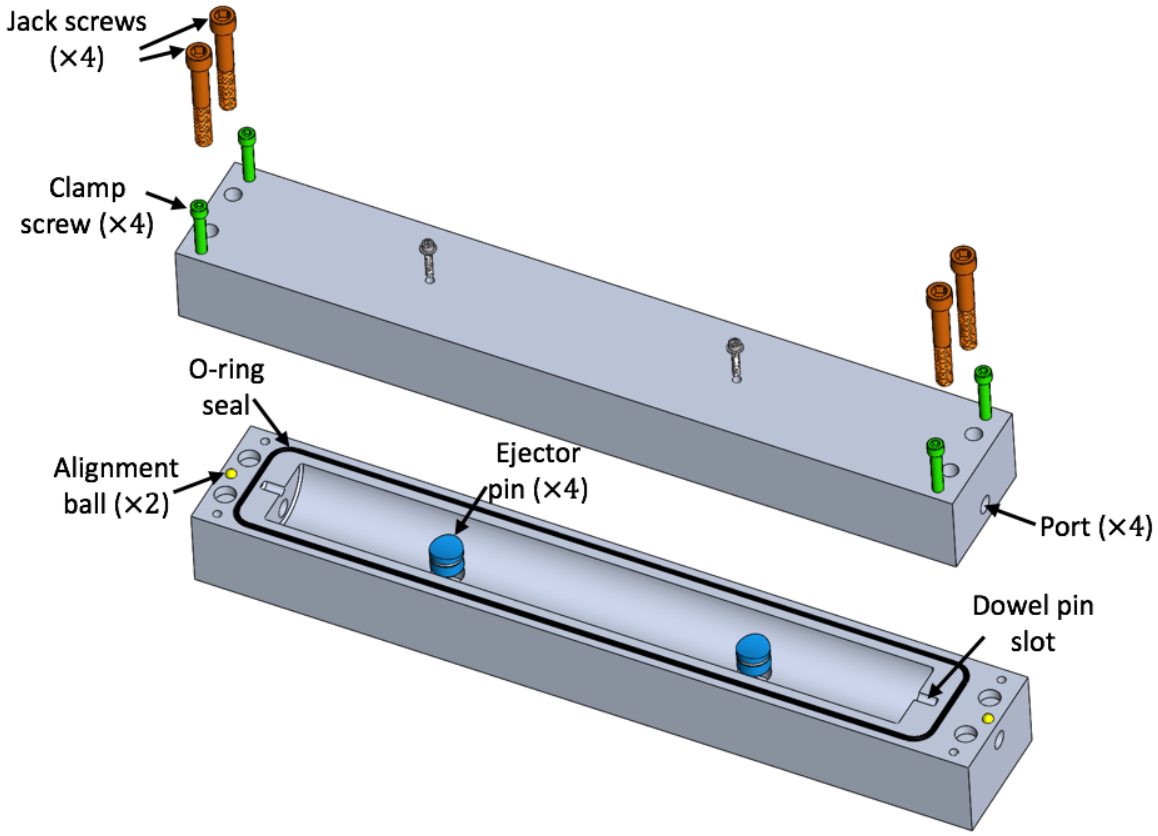

Figure 3-2: The Titanium candle mold assembly has many features to enable propellant casting.

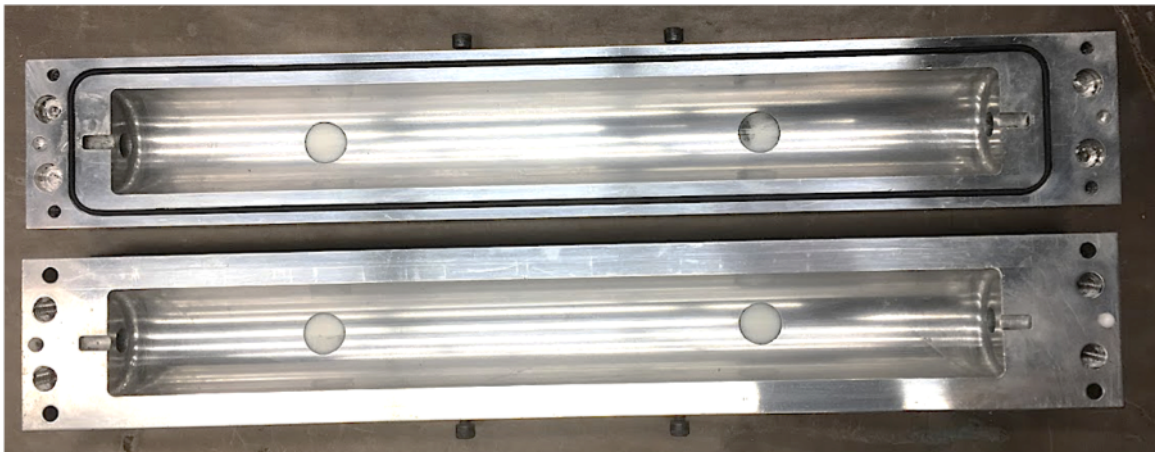

Figure 3-3: The CNC-machined mold halves create the correct outer geometry for casting the liner.

- *Clamp screws* around the perimeter of the molds clamp the two mold halves together during the casting process.
- An *o-ring seal* enables mold sealing once the clamp screws are tightened.
- *Alignment balls* serve as an interface between the mold halves to ensure precise alignment during clamping.
- *Dowel pin slots* serve as mounting points for a starter pocket insert and other tools.
- *Jack screws* allow the mold halves to be jacked open following cure. This greatly simplifies the demolding process in the case that the liner adheres to the mold.
- *Ejector pins* on either mold half allow the motor to be separated from the mold should it adhere during cure. O-rings seal the pins to the molds during casting. Ejector screws can be threaded into holes on the outside of the mold to press on the ejector pins and force the cured motor out of the molds.

A space for the insulating liner must be reserved when casting the propellant in aluminum molds. To do this, a set of silicone "space-savers" in the geometry of the liner are inserted into the liner molds during propellant casting. These space-savers, shown in Figure 3-4, create the proper outer geometry for the propellant grain and retain a gap which will subsequently be filled by the liner.

The following process is used to fabricate the space-savers:

1. A positive replica of the cylindrical propellant grain is turned using aluminum rod stock.
2. A 3D-printed spacer is attached to one end of the positive replica using a dowel pin. Additional dowel pins are inserted into the remaining exposed ends of the positive replica and 3D printed spacer. This assembly is shown in Figure 3-5.
3. The positive replica assembly is mounted inside the aluminum mold halves using the dowel pin slots. The dowel pins and dowel pin slots align the positive replica assembly such that there is a surrounding gap in the desired shape of the liner.

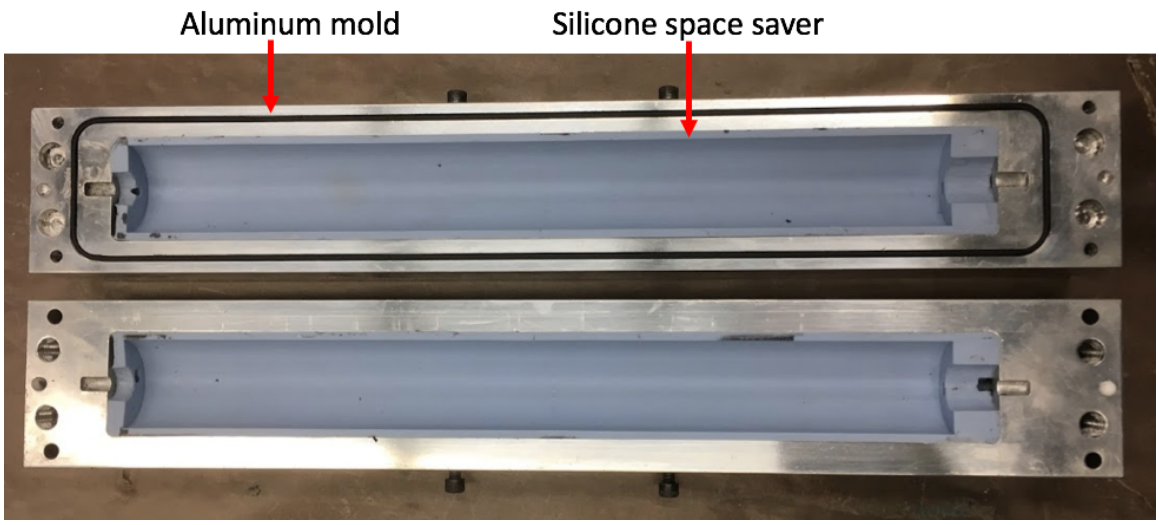

Figure 3-4: Silicone space-saver inserts are inserted into the aluminum liner molds for propellant casting. The space-saver reserves a gap for the subsequent liner casting and creates the proper geometry for casting the propellant grain.

Figure 3-5: A positive replica of a propellant grain and a 3D-printed spacer are used to make the silicone space savers.

4. Mold-making Silpak R2374 two-part RTV silicone is injected into the gap surrounding the replica propellant grain and 3D-printed spacer. The silicone is allowed to cure at room temperature for 24 hours.

5. The silicone and trapped positive replica are removed from the aluminum molds.

6. The silicone is cut length-wise into two pieces, releasing the trapped positive replica and producing the final silicone space-saver halves.

This tooling was designed to enable rapid design changes during development. With this combination of machined aluminum liner molds and silicone space-savers, the liner thickness and propellant geometry can be changed with relative ease. New CNC-machined aluminum molds are not required – only a new silicone space-saver is required.

Lastly, an insert is needed to mold the star-shaped starter-pocket described in Section 2.7 into the propellant grain during casting. A starter-pocket insert of the correct geometry, shown in Figure 3-6, is 3D-printed out of chopped carbon fiber reinforced nylon filament and can be inserted into the propellant molds during propellant casting. A dowel pin can be inserted into the end of the starter-pocket insert which fits into the dowel pin slots in the aluminum molds.

Figure 3-6: The starter pocket tool molds a star-shaped pocket into the aft end of the propellant grain. This creates more propellant surface area for ignition and provides a mounting location for the starter propellant grain.

Propellant mixer

In order to facilitate propellant mixing, a custom vacuum mixer is used. Mixing propellant under vacuum[1] helps to remove water and other volatiles from the propellant precursors and prevent air from being mixed into the propellant during mixing. A Bosch Universal Plus MUM6N10 kitchen mixer with a stainless steel bowl was modified in order to enable propellant mixing under vacuum, as shown in Figure 3-7.

The mixer has a single rotating shaft that passes up through the center of the

[1]The vacuum must be sufficient such that the pressure is less than the vapor pressure of water, ~ 3 kPa at room temperature.

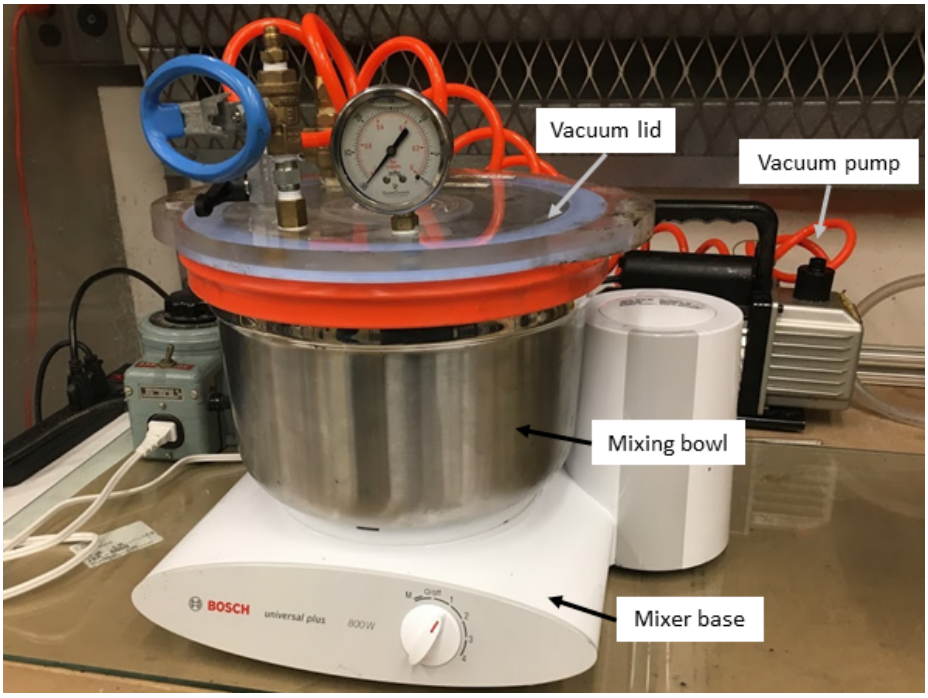

Figure 3-7: A custom vacuum mixer removes volatiles from the propellant precursors during mixing.

bowl, with an attachment for two geared paddles for mixing in the bowl. The relative simplicity of this mixer design – as opposed to the design of planetary mixers – means only a single rotating shaft needs to be sealed in order to pull vacuum. A 3D-printed insert with o-rings seals the rotating shaft to the rest of the mixing bowl. Images of the shaft seal insert and its installation into the mixing bowl are shown in Figures 3-8 and 3-9 respectively.

A vacuum lid with a silicone seal is fit to the top of the mixing bowl. The lid has a fitting for connecting a vacuum pump, a valve for releasing vacuum, and other attachments for operations during propellant mixing.

Propellant holder

A propellant holder is used for aiding in propellant surface preparation during liner casting, and is shown in Figure 3-10. A rotating propellant holder allows the propellant grain to be held and rotated without having to touch or contaminate its surface. The propellant grain is secured between two posts mounted to a piece of

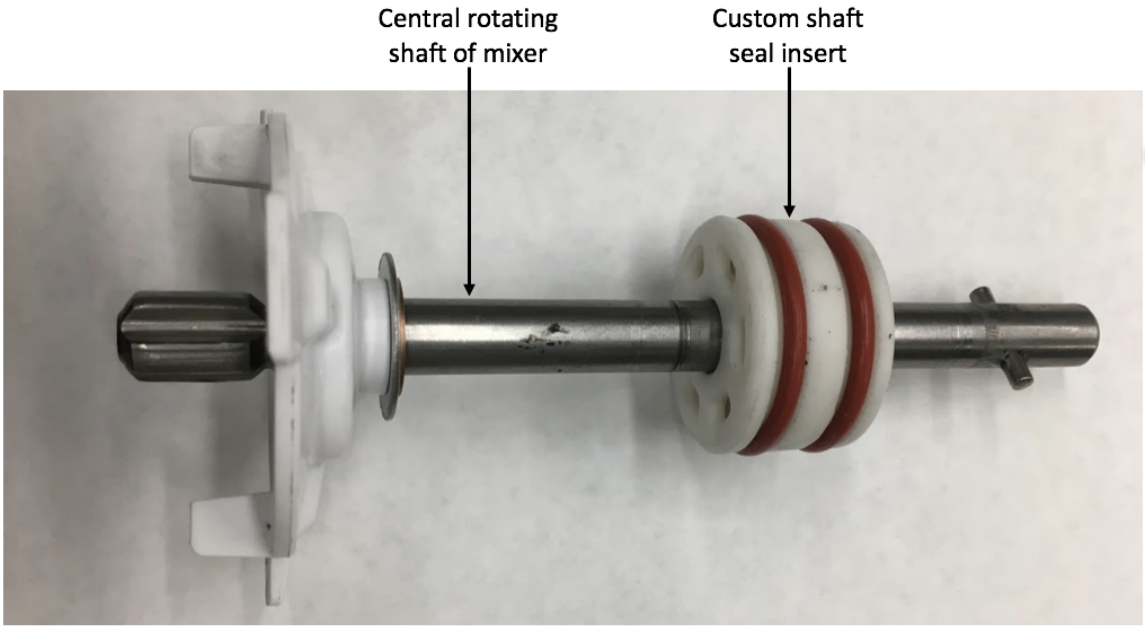

Figure 3-8: A 3D-printed shaft seal insert seals the central shaft of the mixer to the rest of the mixing bowl.

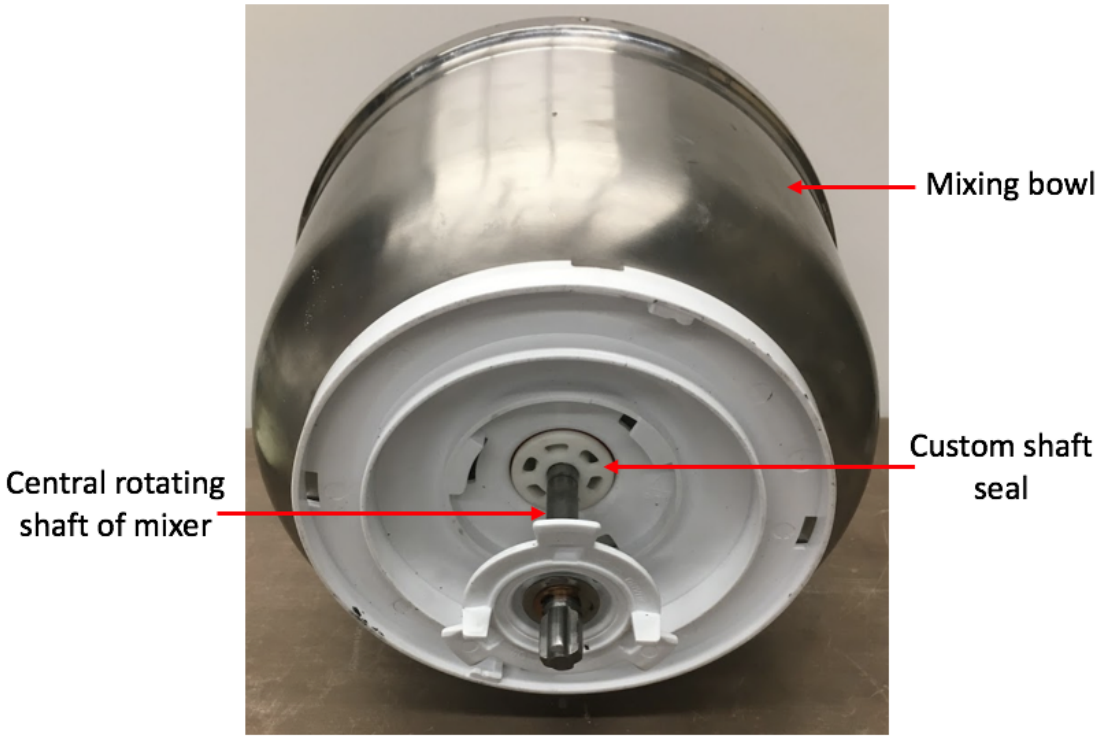

Figure 3-9: The central shaft with sealing insert is inserted into the central column of the bowl. This shaft seal allows vacuum to be pulled on the mixing bowl.

80/20 aluminum extrusion framing. A notched, 3D-printed grain mount holds the forward end of the propellant grain and serves as a knob for rotating the propellant. The starter-pocket insert tool interfaces with the posts to hold the aft end of the propellant grain.

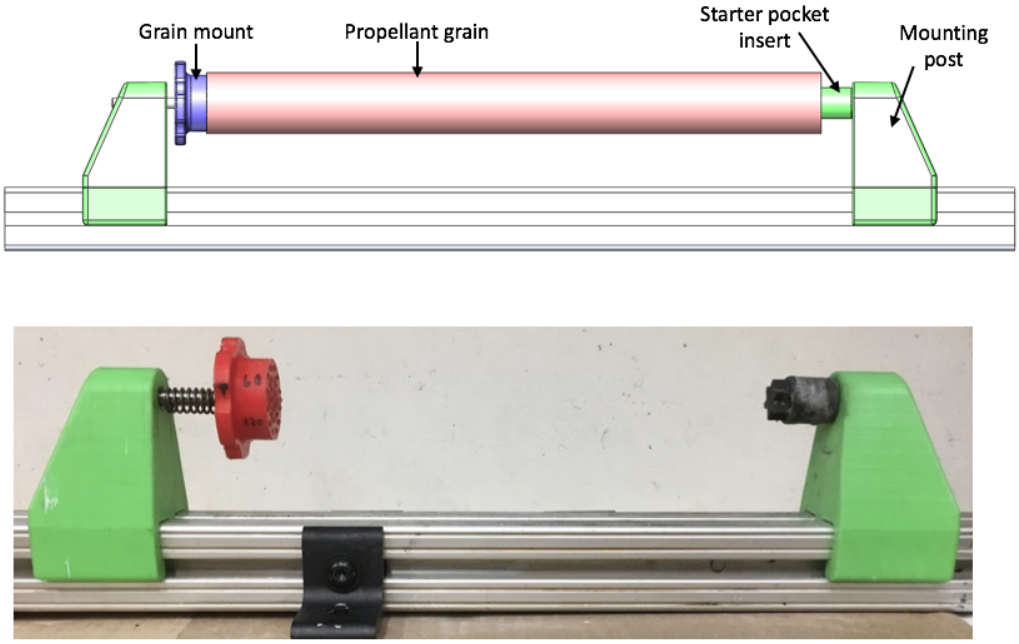

Figure 3-10: A propellant holder helps to hold and rotate the propellant grain for preparation of the propellant surface for liner casting.

Liner injection tooling

Additional hardware components are required for liner injection beyond the aluminum molds described above. After the liner material is prepared, it is placed into an aluminum cartridge assembly for injection around the propellant. This cartridge assembly is shown in Figure 3-11. A complete rendering of all molds and injection tooling is given in Figure 3-12.

The cartridge assembly has the following components:

- The *cartridge* consists of an aluminum tube with a volume of $\sim$ 650 cm^3 for containing the liner material. It is epoxied to a flat plate that can be clamped onto the aluminum molds.

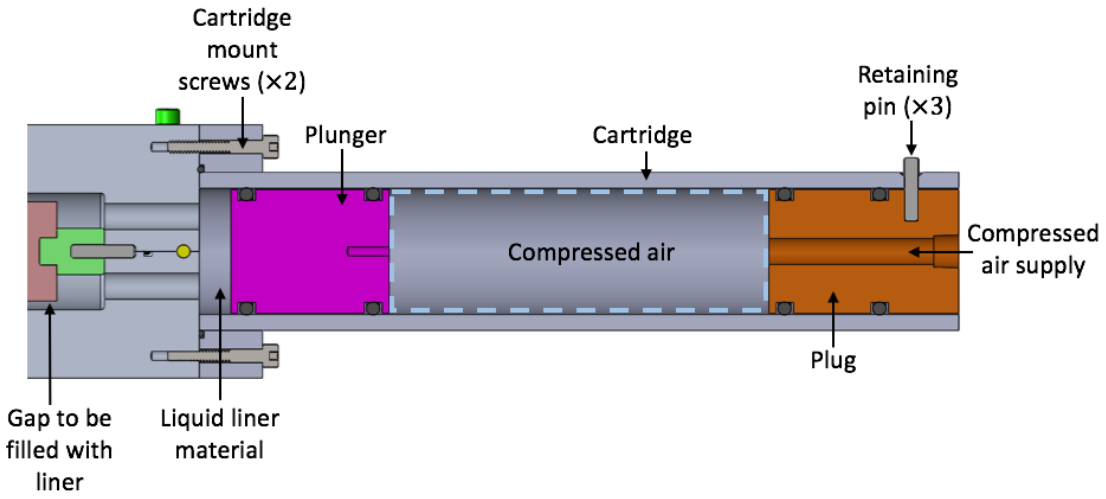

Figure 3-11: The cartridge assembly is used for injecting the liner around the propellant grain.

- The *plunger* is a cylindrical piece with o-rings that seals to the cartridge tube. It is drawn up the cartridge tube when vacuum is pulled on the molds, which injects the liner material into the liner molds.

- The *plug* is inserted into the bottom of the cartridge after plunger and liner material have been drawn upwards. Once fixed to the cartridge tube, the gap between the plug and plunger can be pressurized to aid in injection of the liner material.

- *Retaining pins* insert through the cartridge tube and into the plug in order to retain it during cartridge pressurization.

- *Clamp screws* attach the entire cartridge assembly to the aluminum liner molds.

3.1.2 Propellant formulation

A propellant formulation must be chosen before motor manufacturing procedures can be implemented. A typical propellant formulation for a single segment Titanium Candle motor uses a propellant that is doped with a 13% mass fraction of oxamide in order to achieve desired motor performance. This propellant formulation is given in

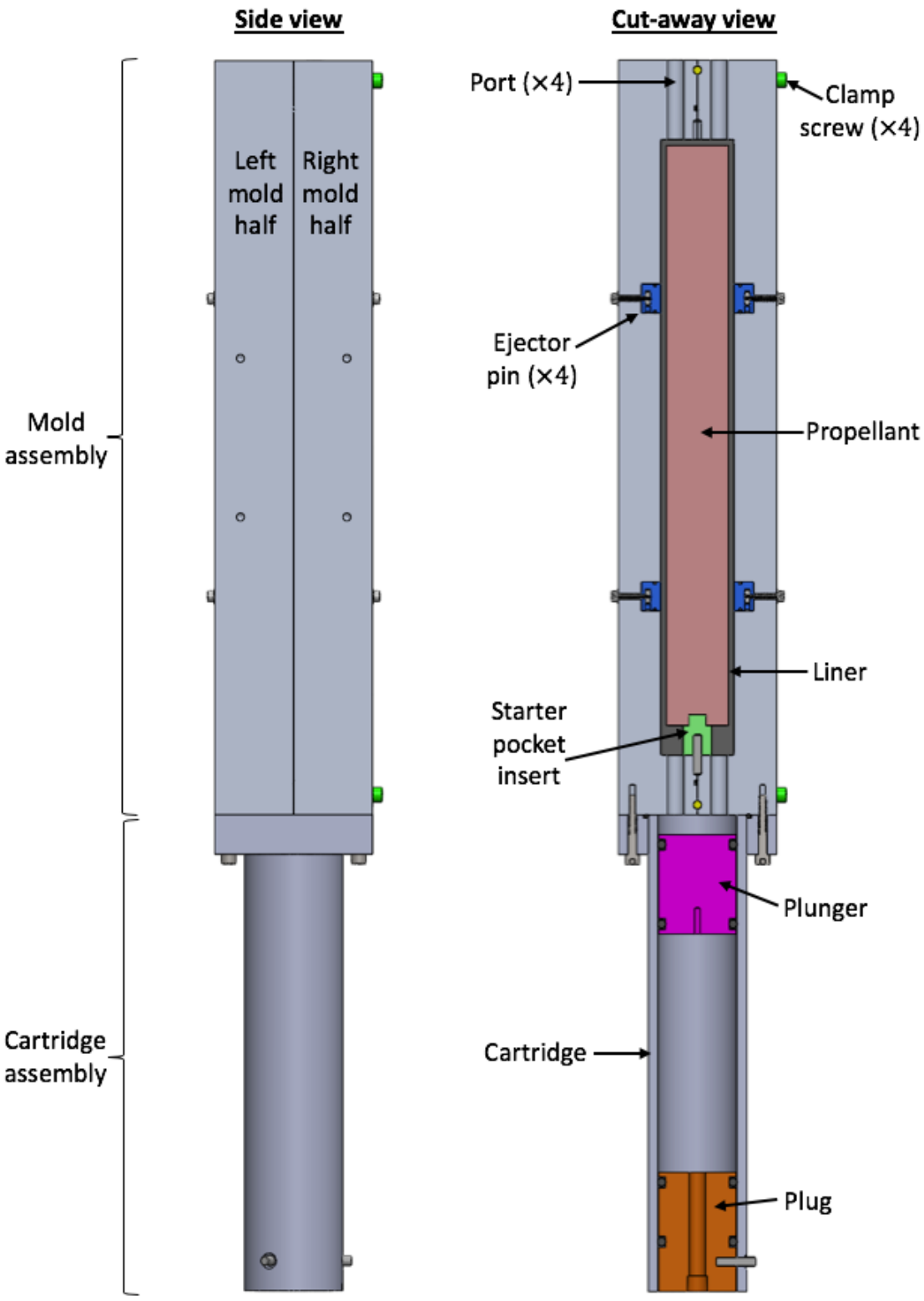

Figure 3-12: Molds, injection tooling, and many other pieces of custom hardware are needed to manufacture a Titanium Candle motor.

Table 3.1. A discussion of the process for creating formulations with different mass fractions of oxamide is given in Appendix B.

Table 3.1: Propellant formulation for typical Titanium Candle motor.

Component	**Chemical name**	**Manufacturer**	**Mass fraction**	**Nominal mass [g]**
Binder	Hydroxyl Terminated Polybutadiene (HTPB) Resin with HX-752 and CAO-5	RCS Rocket Motor Components	0.099	86.48
Plasticizer	Isodecyl Pelargonate (IDP)	RCS Rocket Motor Components	0.041	35.93
Opacifier	Graphite powder	Cretacolor	0.019	16.75
Oxidizer	Ammonium Perchlorate 200/400 Micron Blend	RCS Rocket Motor Components	0.696	609.00
Curative	Modified MDI Isocyanate	RCS Rocket Motor Components	0.015	13.09
Burn rate suppressant	Oxamide	Sigma-Aldrich	0.130	113.75

3.1.3 Procedures

Detailed propellant and liner casting procedures help to ensure consistent production of motors. The procedures are regularly updated to incorporate improvements determined through experiments and active process control.

After the production of the required casting hardware and selection of the desired propellant formulation, the propellant and liner casting procedures can be implemented. An illustrative overview of the manufacturing procedures is shown in Figure 3-13. These procedures will be described in detail in the following sections.

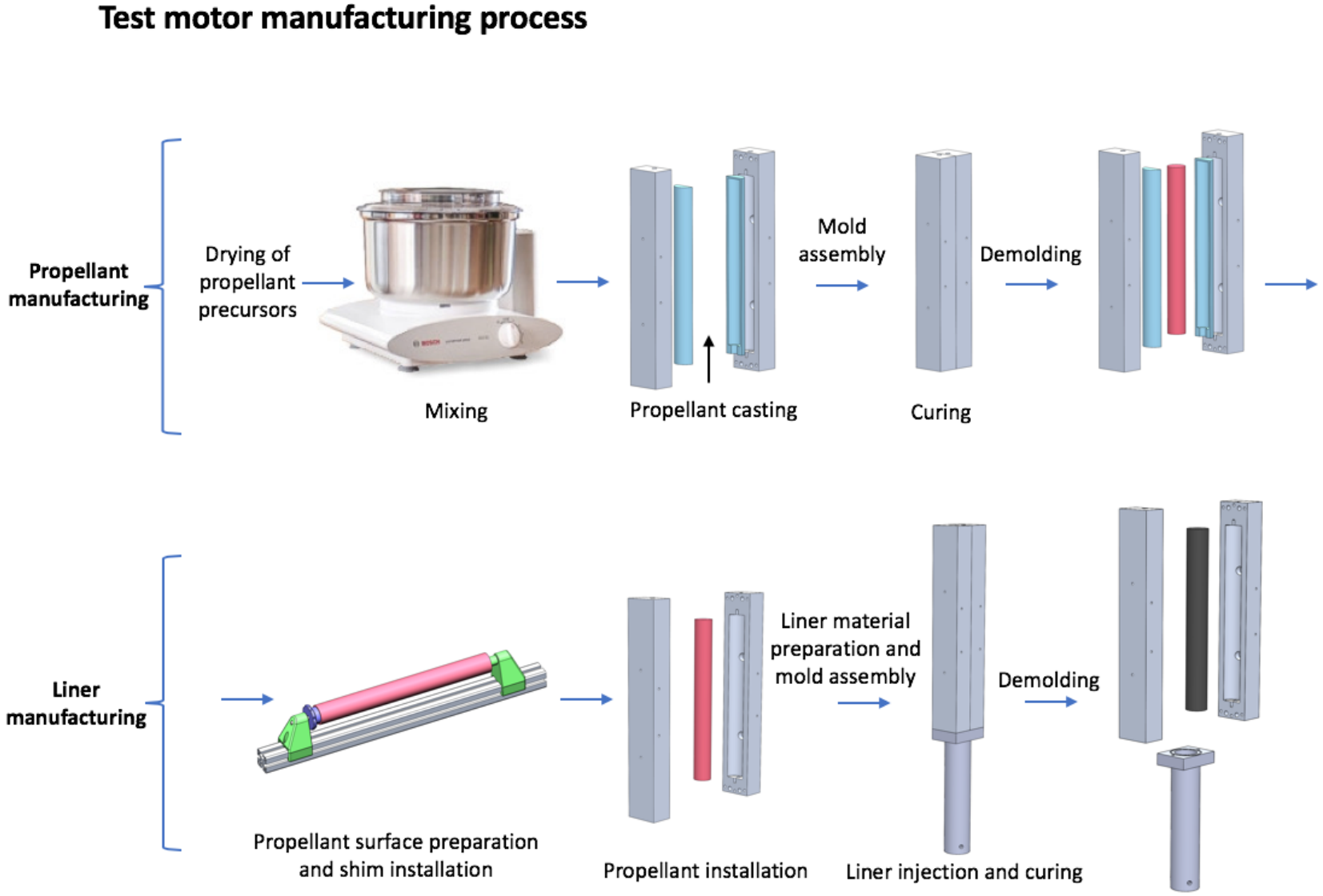

Figure 3-13: Manufacturing the propellant and liner is a multi-step process. Mixer image from [22].

Propellant casting

1. *Mold preparation* - The aluminum mold halves are cleaned with water and isopropanol. The silicone space-savers are inserted into the molds and cleaned with isopropanol to prevent any contamination of the propellant grain. The cured propellant releases easily from the surface of the silicone space-savers, so no mold releasing agent is required.

2. *Pre-measuring of precursors* - The required amounts of all solid propellant precursors – opacifier, oxidizer, and burn rate suppressant – are measured into bowls prior to the start of mixing. The burn rate suppressant tends to clump during storage, and so it is ground and sifted before being measured.

3. *Mixing* - The propellant precursors are mixed in several steps.

   (a) All liquids, except the curative[2], are added to the mixing bowl and then mixed for three minutes.

   (b) The opacifier and burn rate suppressant are pre-mixed by hand to reduce burn rate suppressant clumping. The components are added to the mixing bowl and then mixed for three minutes to incorporate.

   (c) With the mixer running, the oxidizer is added slowly to the mixing bowl. Once the oxidizer is incorporated, the vacuum lid is fit to the top of the bowl and vacuum is pulled on the bowl and the propellant mixture. The propellant is mixed under vacuum for one hour.[3]

4. *Curative injection* - After the propellant has been fully mixed, the curative is then finally added. The curative is injected with a syringe through a fitting with a valve in the vacuum lid, as shown in Figure 3-14. Injecting the curative in this way allows vacuum to be maintained on the propellant mixture during

[2]The manufacturer reports a 2 - 3 hour pot life once the curative has been added [23]. The curative is not added until the end of the mixing procedures in order to extend the working time for the propellant. See [14] for more information.

[3]Mixing time should be chosen to achieve optimal rheological properties for casting. See Section 4.2.2.

this step. The curative is mixed into the propellant for an additional 10 minutes in order to incorporate it.

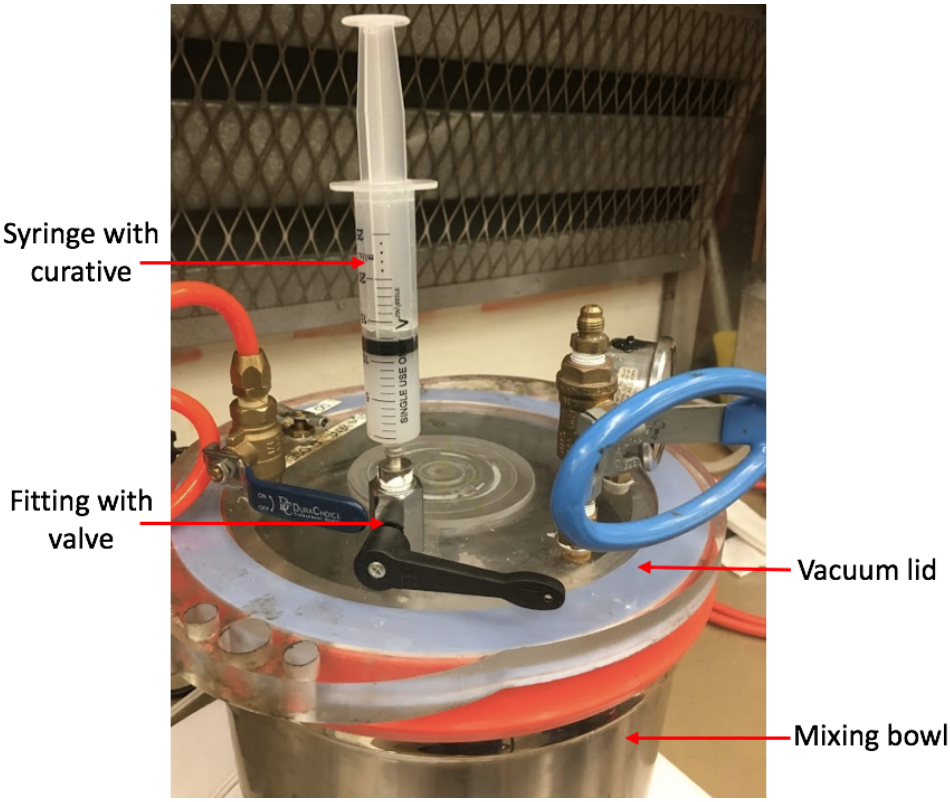

Figure 3-14: The curative is injected through a fitting in the vacuum lid.

5. *Casting* - The propellant is packed into the prepared molds. Small amounts of propellant are scooped from the mixing bowl into the molds and tamped using a rod or gloved hands to collapse any voids. This process of adding small amounts of propellant and tamping is continued until each mold half is slightly over-filled. An image of a mold filled with propellant is shown in Figure 3-15.

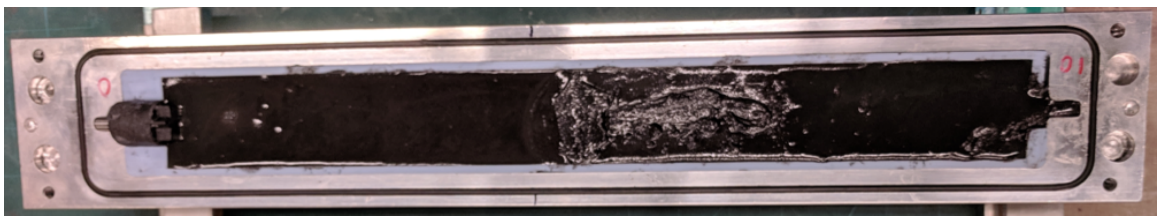

Figure 3-15: Propellant is added to the molds and tamped to collapse voids.

6. *Mold assembly* - The two mold halves are aligned using the alignment balls and clamped together using the clamp screws. Since the molds are slightly overpacked in the casting step, excess propellant will extrude out of the forward and aft ports. The molds are additionally clamped using C-clamps to ensure the molds do not bow apart.[4]

7. *Curing* - The propellant is allowed to cure for three days.[5] During the cure, the propellant molds are stored in an air-tight container with desiccant.

8. *Demolding* - The C-clamps and clamp screws are removed from the molds. Jack screws are threaded into one of the mold halves to jack the two mold halves apart. Once the molds are separated, the propellant grain is peeled away from the silicone space-saver. The propellant is stored in an air-tight container with desiccant until liner casting.

Liner casting

9. *Mold and cartridge preparation* - The mold halves, cartridge, and plunger are cleaned with isopropanol to remove any contaminants. Three coats of Fibre Glast 13 PVA mold release are applied to the interior surfaces of the mold halves and the top of the plunger.

10. *Propellant grain surface preparation* - The surface of the propellant grain is prepared to ensure a robust propellant-to-liner bond.[6] The propellant grain is mounted onto the propellant holder. The propellant grain is cleaned using a two-cloth method:

    (a) Acetone is applied to a clean lint-free cloth.

    (b) The grain is vigorously wiped with the acetone-soaked cloth.

    (c) The grain is immediately wiped again with a clean, dry lint-free cloth.

[4] In subsequent mold design, extra clamp screws are added to remove the need for C-clamps. See Section 3.3.

[5] The curative manufacturer reports a 3 - 5 day curing time at room temperature [23].

[6] Recommendations from the liner manufacturer for substrate preparation are reflected in this procedural step [24] [25].

These steps are repeated until all contaminants are removed from the surface, and the cloths are visibly clean after wiping the propellant grain.

The propellant grain is then primed using the Dow Corning 1200 OS primer. Three coats of the primer are applied to the propellant surface using the following steps:

(a) Approximately 15 ml of primer is poured into a clean container.

(b) A clean lint-free cloth is soaked in the poured primer.

(c) The soaked cloth is used to coat the surface of the grain in strokes along the length of the grain. The propellant holder is used to rotate the grain so the entire surface can be covered.

(d) The primer coat is allowed five minutes to dry.

This process is repeated for each coat. After the final coat, the primer is allowed an additional 30 minutes to fully dry.

11. *Shim installation* - Shims are installed onto the side of the propellant grain while it is still being held in the propellant holder. These shims help to center the propellant grain in the molds during liner injection. 12 diamond-shaped shims roughly 8 mm $\times$ 8 mm in size and with the desired liner thickness are cut from cured liner stock using a razor blade. The shims are cleaned with isopropanol to remove contaminants from their surfaces. A small amount of Permatex Ultra Black Gasket Maker silicone adhesive is applied to the surface of each shim which is then pressed onto the surface of the propellant grain in the desired location. 4 shims are adhered at 90°intervals at forward, aft, and central locations on the edge of the propellant grain. After all the side shims are installed onto the propellant surface, the propellant grain is placed into a motor mold half. An additional shim is then cut and adhered onto the forward end of the propellant grain as well to prevent forward movement. An image of installed shims on a propellant grain is shown in Figure 3-16.

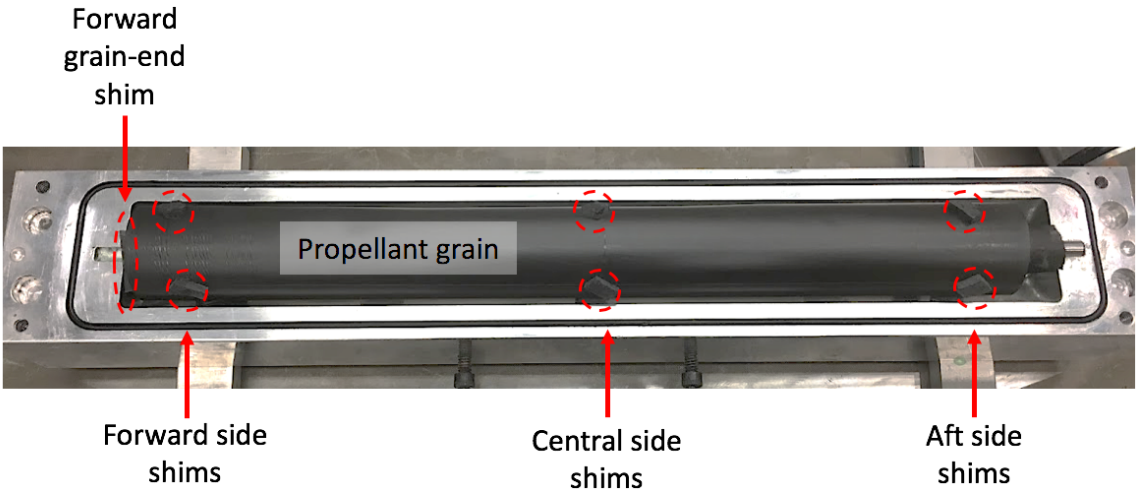

Figure 3-16: Shims are adhered to the surface of the propellant grain to center it in the molds during liner injection.

12. *Mold assembly* - The mold halves are aligned and carefully fit together such that the adhered shims are not disrupted. The mold haves are clamped together using the clamping screws.

13. *Liner material preparation* - The liner consists of a two-part Dow Corning 93-104 ablative material kit that is prepared according to Dow Corning's recommended methods [26]. The proper mass of the DC-93-104 base is added to a small bowl, and then degassed in a vacuum chamber for 30 minutes. After degassing, the proper mass of the DC-93-104 catalyst is added to the bowl. The two components are mixed thoroughly with a stirring rod for five minutes.

14. *Liner injection preparation* - The plunger is inserted into the bottom of the cartridge, and the prepared liner material is transferred into the cartridge on top of the plunger. The cartridge with plunger and liner are placed on a shake table for 10 minutes to settle the surface and collapse voids in the liner material. The cartridge is then mounted to the end of the propellant molds using a pair of mating screws.

15. *Liner injection* - Vacuum is pulled on the molds and attached cartridge using one of the available ports on the molds. A long pin is inserted into an eyebolt on

the bottom of the plunger to prevent the plunger from immediately rising due to the vacuum. The liner is allowed to degas for 10 minutes in this configuration. The pin is then removed from the plunger, so that the plunger can rise in the cartridge and the liner is injected into the gap surrounding the propellant. Once the gap is filled with liner and liner is extruding from the vacuum port, a valve is closed on the mold to seal it, and the vacuum pump is removed. The plug is inserted into the bottom of the cartridge and fixed in place with three radial pins. The gap between the plunger and plug is pressurized to ∼100 psig to further raise the plunger and compress the resin inside the mold.

16. *Curing* - While the cartridge is pressurized, the liner is cured. A flat heated sheet is placed on the surface of the mold and held in place with C-clamps. The mold is heated to a temperature of 65 C and the liner is cured at that temperature for 45 minutes. The heated sheet is then removed and the pressurized cartridge is vented.

17. *Demolding* - The liner is allowed 24 hours to cool and complete the curing reactions. After this time, the completed motor can be removed from the molds. The cartridge is unscrewed from the molds, and the jack screws are used to part the mold halves. Once the mold halves are separated, the cured liner will still be stuck in one of the mold halves. Ejector screws can then be threaded into the molds behind the ejector pins to push the cured liner out of the mold.

18. *Inspection* - The cured liner is carefully inspected for any voids. If no voids exist, the completed motor is stored in a sealed container with desiccant. If voids are present, the following void repair step is completed.

19. *Possible void repair* - Voids are occasionally present in the cured liner. If this is the case, the following modified procedure is followed:

    (a) Loose material surrounding the voids is cut away using a clean razor blade.

    (b) The molds are prepared according to Step 9.

    (c) The exposed void surface is prepared according to Step 10.

(d) The prepared propellant grain is placed directly into a prepared mold half.

(e) The required amount of liner material is prepared according to Step 13.

(f) The prepared liner is applied directly to the exposed and prepared void surface using a wooden craft stick. The molds are then aligned and clamped together with the clamping screws.

(g) The liner is cured according to Step 16.

(h) The repaired motor is demolded according to Step 17.

3.2 Extension to multi-segment propellant manufacturing

The processes described previously in Section 3.1 can be extended in order to cast multi-segment propellant grains. In a multi-segment motor, multiple propellants with different formulations are mixed and then cast together to cure into a single, seamless grain.

3.2.1 Hardware for multi-segment propellant manufacturing

Casting a multi-segment grain requires additional hardware beyond what is required for a single-segment grain. In order to have a precise boundary between two propellant segments at a desired location, a positionable and removable divider jig is used. This divider jig, shown in Figure 3-17, has several features that enable the casting of multi-segment grains:

- The divider jig *base* is a 3D-printed piece made from a polyethylene terephthalate glycol (PETG) filament that wraps around the propellant mold. It serves as a mounting fixture for many other pieces in the divider jig assembly.
- The *propellant divider* is a thin polyvinyl chloride acetate (PVCA) plastic piece that separates the propellant segments during casting, and can be removed for subsequent propellant curing.

- The divider jig *clamps* and *clamp screws* are used to clamp the propellant divider to the base during propellant casting.

- *Set screws* on the sides of the base piece allow the base and divider to be fixed to the propellant mold during casting, but can be easily loosened for removal of the divider jig.

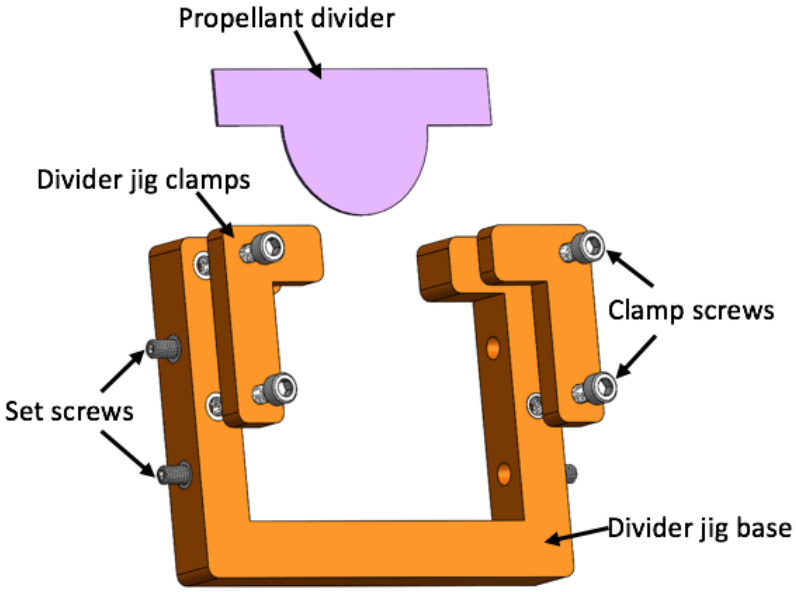

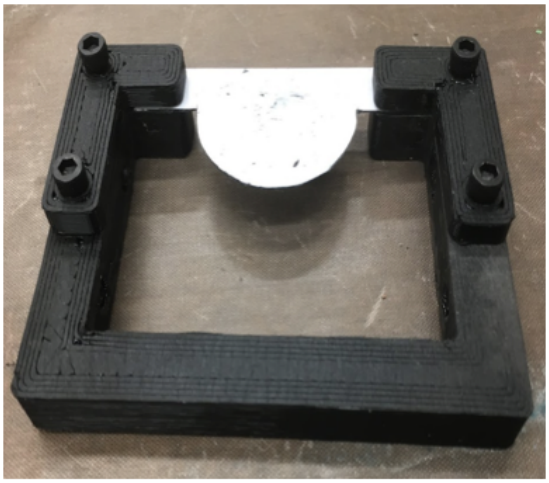

Figure 3-17: A divider jig seperates the uncured propellants in their molds for multi-segment propellant casting.

3.2.2 Procedures for multi-segment propellant manufacturing

The casting procedures must also be modified for the production of multi-segment propellant grains. The pot life of the curative presents a particular challenge for manufacturing a multi-segment grain. In order for each propellant segment to properly adhere and cure to its neighboring segments, all the propellant formulations must be mixed and cast within the limited timeframe prescribed by the pot life of the curative. The procedures for mixing a multi-segment grain must account for this timing limitation.

The following modified procedures are used for casting a multi-segment propellant grain:

1. The molds are prepared according to Step 1 from Section 3.1.3, with the addition that the propellant divider jigs are also installed at the desired locations on each mold half. Figure 3-18 shows the divider jig installed on a mold half.

2. Each propellant formulation is individually mixed in series, without the curative, according Steps 2 - 3 from Section 3.1.3. Mixed propellant is stored under vacuum while subsequent formulations are being mixed.

3. After each formulation has been mixed, the curative is added to each propellant formulation individually in series, according to Step 4 from Section 3.1.3.

4. Each propellant formulation is immediately cast according to Step 5 from Section 3.1.3 into the desired segment of the propellant mold after the addition of the curative.

5. After all segments are cast, the divider jigs are removed from the molds. The molds are then assembled, and the propellant is cured and demolded according to Steps 6 - 8 from Section 3.1.3.

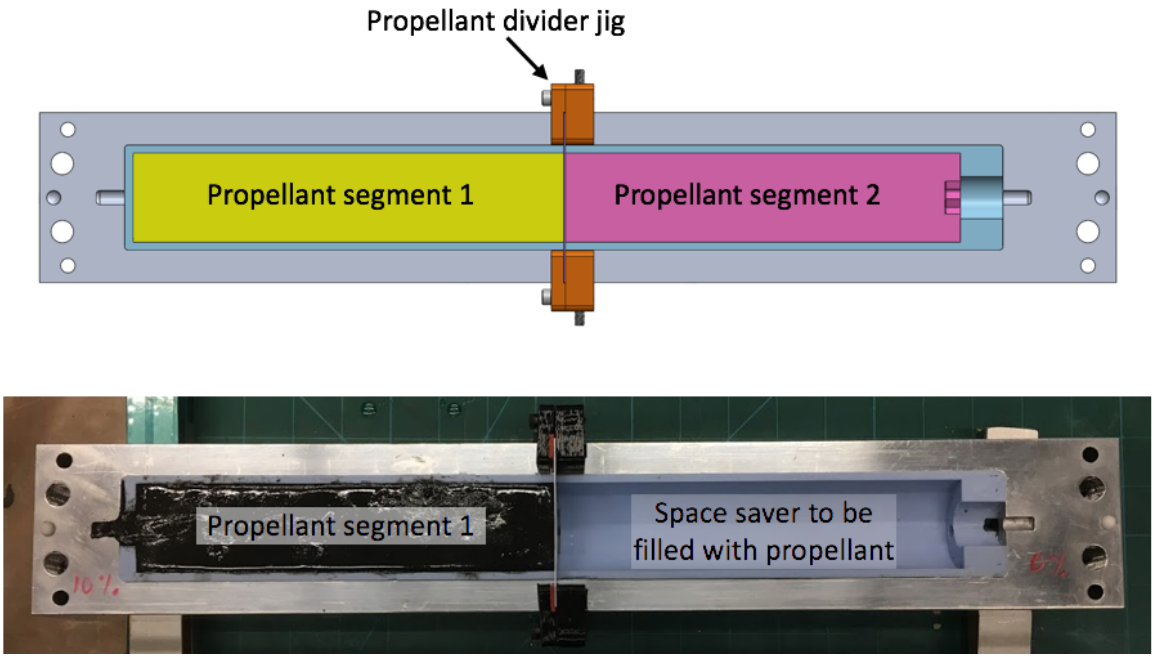

Figure 3-18: The propellant divider jig is installed on the molds to separate the different propellant segments during propellant casting.

3.3 Extension to flight-like motor manufacturing

The manufacturing process outlined in Section 3.1 for the test motor can be extended for casting a flight-like motor. For a flight-like motor, the propellant and liner are manufactured with the more complicated geometry of the actual Firefly vehicle. New casting hardware reflecting this geometry is required for manufacturing these motors.

3.3.1 Hardware for flight-like motor manufacturing

Motor mold halves defining the outer boundary of the motor are used for manufacturing the propellant and liner. These molds, shown in Figures 3-19 and 3-20, retain many of the same features as the Titanium Candle molds shown in Section 3.1.1.

The flight-like molds assemble similarly to the Titanium Candle molds. The flight-like molds also utilize many of the same features: alignment balls, an o-ring seal, clamp screws, and ejector pins. However there are several new or updated features:

- Additional *clamp screws* enable better and more repeatable sealing of the mold halves during propellant and liner casting.

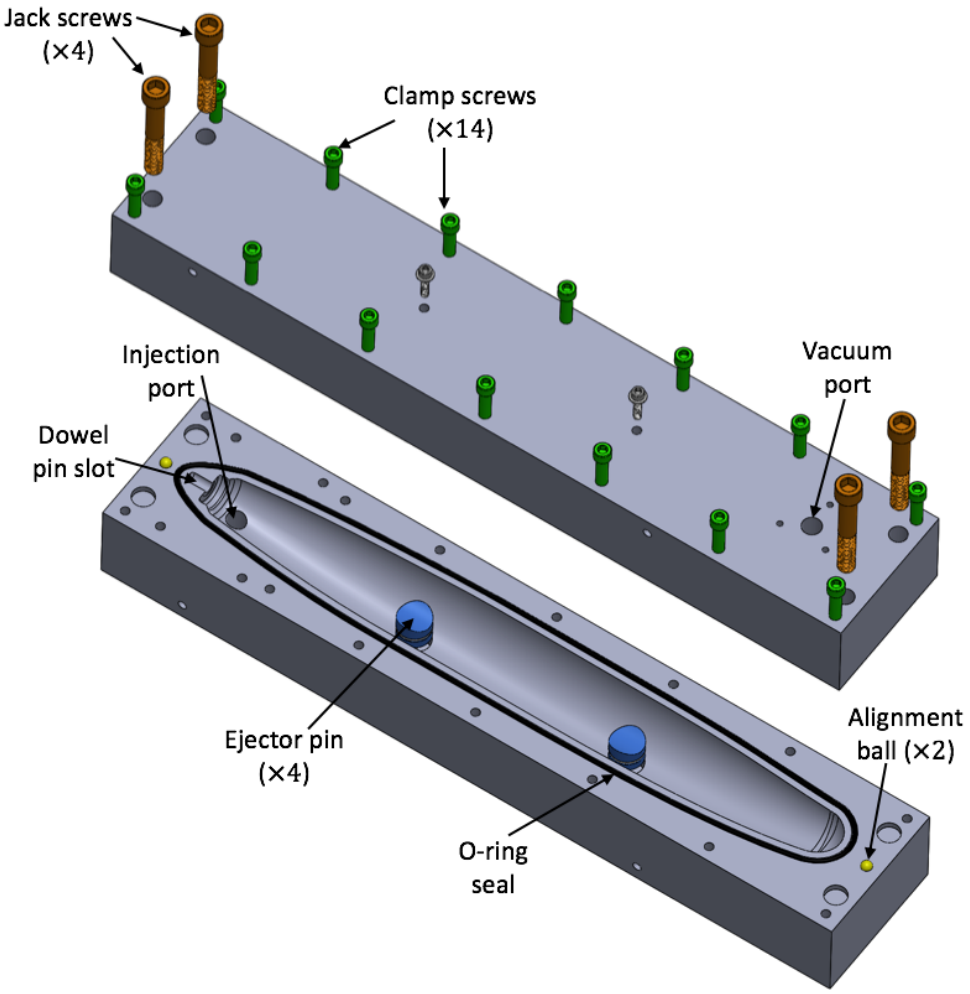

Figure 3-19: The flight-like molds have many new features to enable the production of flight-like motors.

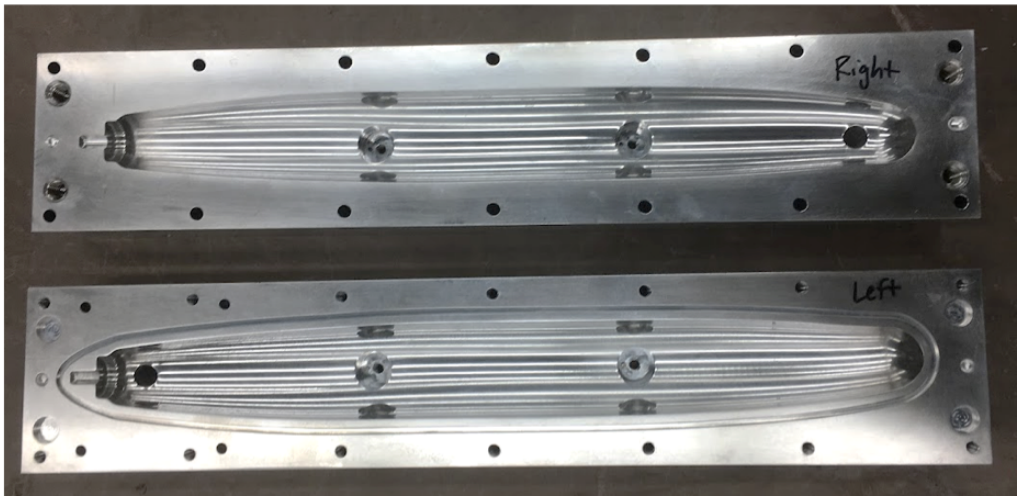

Figure 3-20: The flight-like propellant molds are used for casting motors in the actual Firefly geometry.

- The *ports* for pulling vacuum and injecting liner are moved from the ends of the mold halves to the sides. This is eliminates a gas leak path that exists on the Titanium Candle molds when injecting liner.

- *Heating sheet mounting points* allow two heating sheets for liner curing to be clamped to the molds using screws and a custom heating sheet mounting plate.

Additional hardware is used with the molds for liner casting, which is described below. A full rendering of the flight-like motor manufacturing hardware is shown in Figure 3-21.

- The *cartridge assembly* is clamped to the side of a motor mold half using four clamp screws.

- A threaded *vacuum flange* is attached to the other mold half using three clamp screws. The flange seals to the molds with an o-ring, and has a threaded port for attaching fittings to pull vacuum.

- *Heating sheet mounting plates* mount on both sides of the assembled molds and hold the heating sheets in place during liner cure.

- A *mold spacer* is fit underneath of the molds to make clearance for the ejector pin retaining screws, allowing the mold to rest flat on a horizontal surface.

3.3.2 Procedures for flight-like motor manufacturing

The procedures for casting a flight-like motor are nearly identical to those presented for the Titanium Candle configuration in Section 3.1.3. Very few modifications are required:

1. The molds are prepared, and the propellant is mixed, cast, cured, and demolded according to Steps 1 - 8 from Section 3.1.3.

2. The molds and the propellant grain surface are prepared for liner casting according to Steps 9 - 10 from Section 3.1.3.

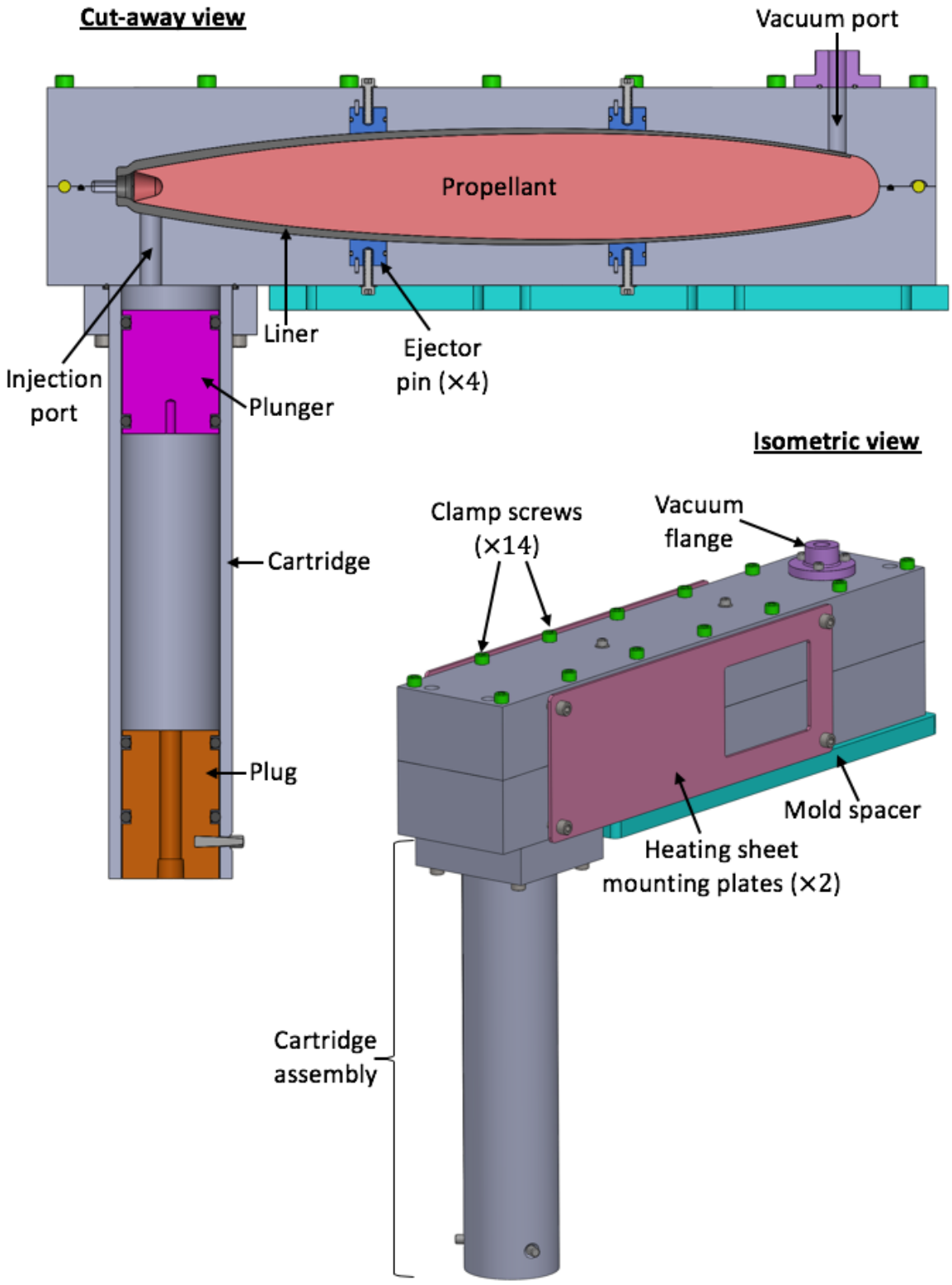

Figure 3-21: New manufacturing hardware enables the production of motors in the complex Firefly flight-like geometry.

3. Shims are applied to the propellant grain surface similarly to Step 11 from Section 3.1.3. The shims need to be cut to the appropriate thickness for each shim location. Additionally, no forward shim is required for mounting the propellant grain since the forward end of the propellant will already be in direct contact with the interior of molds.

4. The molds are assembled according to Step 12 from Section 3.1.3.

5. The liner material is prepared and injected into the molds according to Steps 13 - 15 from Section 3.1.3.

6. The liner is cured according to Step 16 from Section 3.1.3, with the exception that two heating sheets are affixed to the molds using the heating sheet mounting plates instead of C-clamps.

7. The completed motor is demolded according to Step 17 from Section 3.1.3.

In addition, the multi-segment casting hardware described in Section 3.2 is compatible with the flight-like molds with a simple modification to the geometry of the propellant divider.

Chapter 4

Development of quality-driven motor manufacturing techniques

The development of quality-driven manufacturing strategies for low-thrust, long endurance motors involves a combination of aspects stemming from manufacturing process control, component tests, and findings in literature. This chapter discusses these aspects in the development of techniques for manufacturing a robust propellant-to-liner bond and void-free propellant and liner.

4.1 Propellant-to-liner bond

A strong propellant-to-liner bond is critical for achieving intended motor performance for small, fast vehicles. However, as noted in Section 1.4.2, bonding the propellant to the liner is challenging due to an inherent incompatibility of the materials. Careful strategies are required for bonding these two motor components, and the development of these strategies is described here.

4.1.1 Surface preparation

Through the development of the manufacturing process for casting the liner, the importance of proper surface preparation of the propellant grain has become apparent.

Early methods for preparing the surface of the propellant grain for liner casting involved applying a thin layer of fast-curing epoxy to act as an inhibitor. It was this surface preparation technique that led to severe edge-burning of a Titanium Candle motor during the static fire attempt described in Section 1.4.2. In response to this, a series of peel tests between the liner and propellant using different surface preparations and inhibitor layers were used to evaluate the propellant-to-liner bond.[1]

In these tests, the surfaces of flat propellant samples were prepared with different inhibitors and primers, including no preparation, fast-curing epoxy, and a manufacturer recommended primer.[2] Liner material was applied to each prepared sample and heated in an oven until cured. A mylar tag was adhered to a starter portion of liner on each sample. A fish-hook scale was attached to each mylar tag, and the liner samples were pulled on until failure. Depictions of this test setup are shown in Figure 4-1.

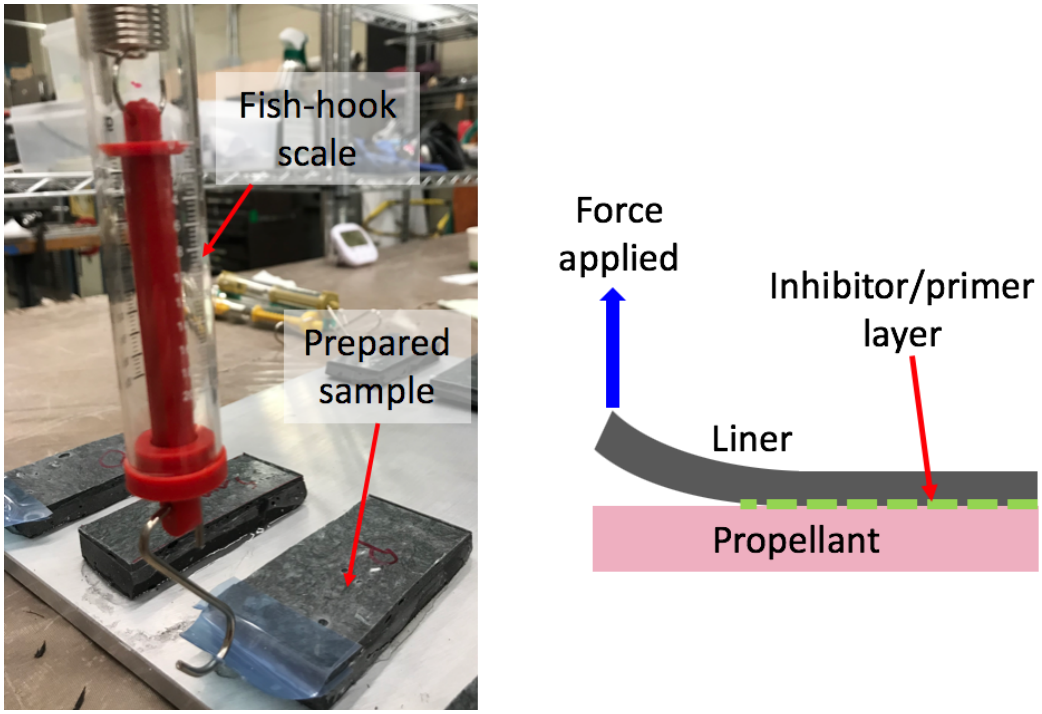

Figure 4-1: Peel tests were used to determine which inhibitor or primer method yielded the best propellant-to-liner bond.

[1]The author would like to acknowledge Jon Spirnak and Matthew Vernacchia of the MIT Department of Aeronautics and Astronautics for their contributions in designing and running these experiments.

[2]The product information for the Dow Corning 93-104 ablative material used for the liner recommends the use of the Dow Corning 1200 OS primer [26].

Of the samples tested, the samples with no preparation and with fast-curing epoxy showed the worst performance, with each having a peel strength of ∼0.1 N/mm. The sample prepared with the manufacturer recommended primer showed the best results, with a peel strength of ∼0.4 N/mm.

Application of the primer still requires rigorous processing techniques, or delamination between the propellant and liner can still occur, as shown previously in Figure 1-10. Many of these techniques are provided in the product information for the primer, including considerations for solvent choices for surface cleaning, surface cleaning methods, and handling recommendations [25] [24]. The product information guide for the liner is less specific on the amount of primer that should be applied and simply suggests that the layer should be "thin" [25]. However, the thickness of the primer layer has a substantial effect on the adhesion strength, and must be chosen carefully [27].

There are two key mechanisms which govern how adhesion interfaces fracture [28]:

- *cohesive fracture*, where the fracture between the two adherents occurs within the adhesive layer itself, and

- *interfacial fracture*, where the fracture occurs between one of the adherents and the adhesive layer.

Adhesion interfaces typically display cohesive strengths which are much larger than their interfacial strengths, and so ensuring a cohesive failure mode between two adherents is best for achieving high adhesion strength [28]. A qualitative illustration of the relationship between adhesion strength, applied primer, and fracture mechanisms is shown in Figure 4-2.

Through observations and process improvements made during Titanium Candle motor manufacturing iterations, three coats of the primer has been found sufficient to provide reliable coverage of the propellant grain surface and good adhesion between the propellant and liner materials.

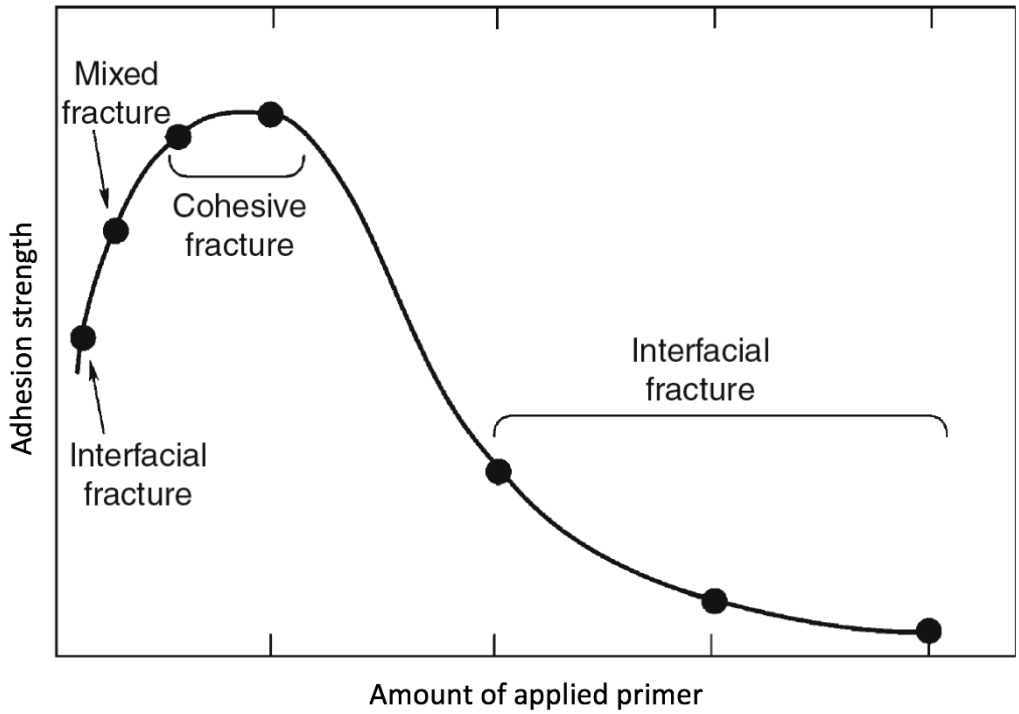

Figure 4-2: The adhesion strength and mechanism of fracture varies with the amount of primer applied for adherence of two substrates. Reprinted from [27].

4.1.2 Primer application testing

The Dow Corning product information for the liner material additionally provides two methods for applying the primer: using a clean, lint-free cloth or a clean brush [24]. The manufacturer describes the cloth application method as preferable, however TRW reports having applied the primer with a brush for rocket propulsion applications with good success [29]. This subsection describes a brief evaluation of both primer application methods to evaluate their performance for the propellant-to-liner interface.

Experimental setup

An experiment was designed and implemented to evaluate the adhesion strength of the propellant-to-liner bond.[3] Cylindrical propellant grain samples were prepared with primer and liner. A total of 9 samples were prepared: 5 samples using a lint-free

[3]The author would like to acknowledge Jakob Coray of the MIT Department of Aeronautics and Astronautics for his contributions in designing and running these experiments.

cloth for primer application, and 4 samples using a brush.

A peel testing apparatus, shown in Figure 4-3, was designed and built in order to measure the peel strength of each of the prepared samples. Each test sample was attached to a mount which could slide along a linear track. A clamp held the liner in place for each test. The liner sample was fed through a pair of rollers to ensure the delaminating liner peeled roughly horizontally off of each sample. A hook allowed the clamp to connect to a load cell which measured the force required to peel the liner away from each sample.

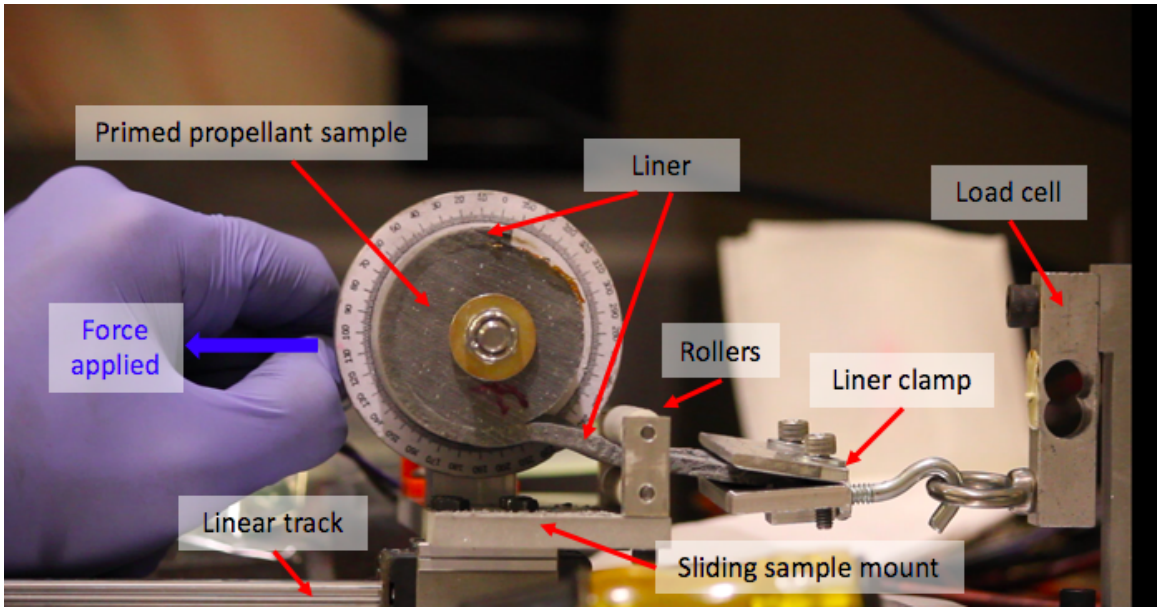

Figure 4-3: A peel testing apparatus was used to measure the peel strength of the liner for different primer application methods.

The following steps were used to prepare the test samples for the experiment:

1. A single Titanium Candle propellant grain was manufactured similarly to Steps 1 - 8 of the propellant casting procedures described in Section 3.1.3.

2. The completed propellant grain was cleaned with acetone according to manufacturer recommendations and prepared with primer. The forward section of the grain was prepared by applying the primer with a cloth, and the aft section of the grain was prepared by applying the primer with a brush.

3. The liner was injected and cured around the prepared propellant grain according to Steps 12 - 17 in Section 3.1.3.

4. The cast propellant and liner were cut into 38mm long segments. The exterior surface of the liner was measured and the 38mm intervals were marked to provide a cutting guide. The measured sections were additionally marked with numerical labels. The sections were cut using a saw and a miter box. Before each segment was cut, the grain was secured to the miter box with cable ties to prevent it from shifting while cutting. The liner surface, miter box, and saw blade were cleaned with isopropanol before and after the segment cuttings to prevent contamination.

5. 1/4" holes were drilled into each sample to enable subsequent sample mounting. The samples were drilled with a lathe at a speed of 1200 rpm. The lathe was carefully cleaned afterwards to remove all propellant dust and scraps. An example of a prepared sample can be seen in Figure 4-4.

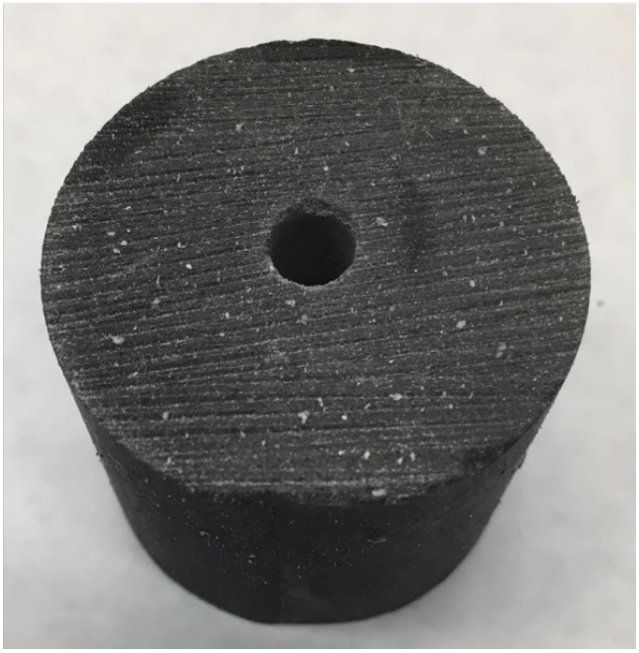

Figure 4-4: Propellant samples were drilled with 1/4" holes for mounting to the sliding sample mount. Note: This image was taken after the peel tests, so the liner has already been removed.

Each sample was then tested in the following manner:

1. A 1/4" bolt was pushed through the central hole of the sample and the sample was affixed to the sliding sample mount with a washer and nut. The sample was free to rotate on this bolt.

2. A portion of liner was peeled away form the propellant surface, fed through the rollers, and inserted into the clamp. The screws on the clamp were tightened to keep the liner in place. The clamp was then attached to the load cell with a hook.

3. The sliding sample mount was pulled on slowly, and the liner was peeled away from the sample. The force required to peel the liner was recorded by the load cell.

4. The spent sample was removed from the peel testing apparatus so that the next sample could be tested.

Results

Each sample was tested and the load cell data was recorded for each. Samples 2 and 8 had voids in the liner which caused the liner to crack and break instead of peel away from the propellant. The data from these two samples were omitted.

The relative magnitudes of the mean peel strength over time, for each sample pull are visualized in Figure 4-5. Error bars depicting one standard deviation within the time series data for each pull are shown for each sample. Although the mean peel strength performance for the cloth application method is slightly higher than for the brush method, there is no statistically significant difference between the performance for two methods. Since no statistical significance exists, the manufacturer preferred cloth application method was chosen for applying the primer.

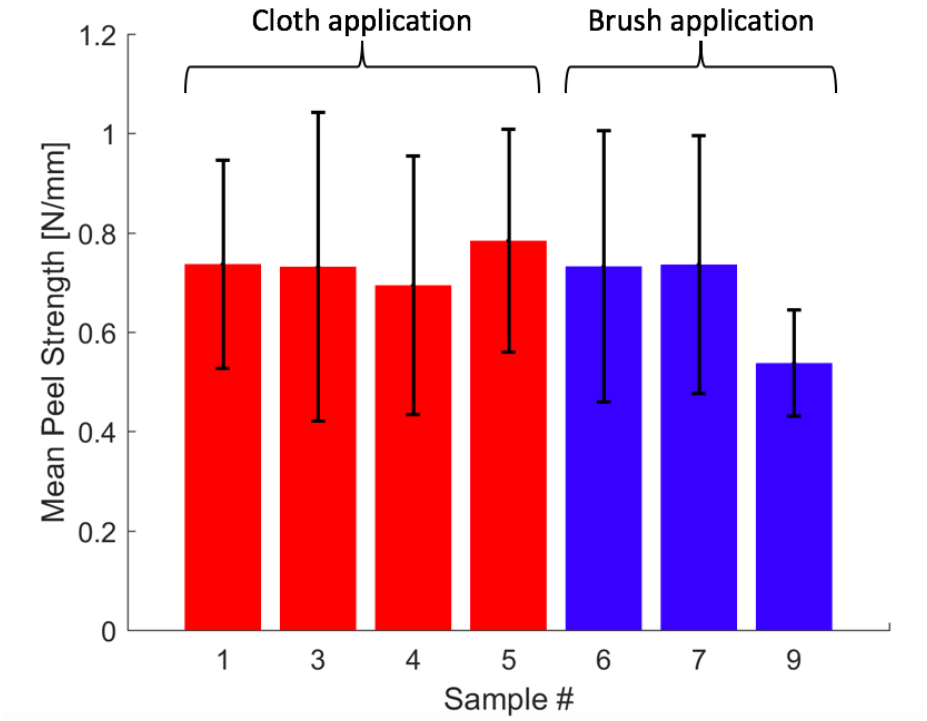

Figure 4-5: The mean peel strength for propellant and liner samples prepared with different surface application methods show no statistical significance. Note: Data from samples 2 and 8 were omitted due to voids in their liners.

4.2 Propellant voids

Dense, void-free propellant grains are needed for maximizing endurance and ensuring predictable burning area, chamber pressures, and thrust for small, fast aircraft, as discussed in Section 2.5. Voids have formed in Titanium Candle propellant grains before, such as the instance described in Section 1.4.1. The development of strategies for preventing the formation of voids in propellant grains are discussed in this section.

4.2.1 Vacuum processing and mixing

The ammonium perchlorate (AP) oxidizer and hydroxyl-terminated polybutadiene (HTPB) binder materials used in the production of propellant grains for most composite propellants, including the propellant for the Firefly motor, are hygroscopic, and therefore very sensitive to the humidity in the mixing environment [18]. If water is absorbed by these propellant precursors, it will react with the diisocyante curative

to form carbon dioxide gas [18] [30]. This can lead to small voids forming throughout the propellant as the grain cures.

This is expected to be the cause of the numerous small voids found in the propellant grain mentioned in Section 1.4.1. The propellant precursors, which were mixed in an open-air mixer in a humid casting environment[4], likely absorbed water from the air. This absorbed water started reacting with the curative once it was added, and produced carbon dioxide gas throughout the cure, resulting in voids.

One source recommends mixing all components, except for the curative, for up to several hours under vacuum to first remove all volatiles from the mixture, and then adding the curative in the last tens of minutes [14]. This strategy allows plenty of time for volatiles to be removed from the propellant, and also leaves sufficient time for packing the propellant within the relatively short pot life of the curative. Mixing under vacuum is also advantageous because it prevents air from being worked into the propellant during the mixing process itself.

In order to prevent the formation of voids in future propellant grains, a vacuum mixer was built, and is described in Section 3.1.1. The oxidizer is pre-dried in a vacuum chamber prior to mixing to further aid in the removal of water and other volatiles from the mixture. Additionally, after the propellant is packed in the molds, it is sealed in a container with desiccant to prevent any water from being absorbed while the propellant cures.

4.2.2 Mixing speed and time

The mixing speed and mixing time chosen for manufacturing propellant can have a significant effect on the rheological properties of the uncured propellant [31] [32]. These rheological properties can effect how the propellant flows within the mold during casting and curing of the propellant grain, which can be important for producing void-free propellant [31] [33] [34].

The rheological properties of the uncured propellant mixture can be modeled as

[4]The recorded relative humidity in the mixing environment was 51% during this motor mixing attempt. For all previous motor mixings, relative humidity had been between 11 and 12%.

a non-Newtonian fluid using

$$\tau = \tau_0 + \eta_0(\dot{\gamma})^n \tag{4.1}$$

where τ is the shear stress, τ_0 is the yield stress, η_0 is the viscosity at unit shear rate, $\dot{\gamma}$ is the shear rate, and n is the pseudoplasticity index [31] [34]. Equation 4.1 becomes representative of a Newtonian fluid if the yield stress τ_0 is 0 and the pseudoplasticity index n is 1. Selecting manufacturing parameters such as mixing speed and mixing time to produce an uncured propellant mixture with properties most similar to a Newtonian fluid typically results in the best flow properties and reduced presence of voids [31].

Muthiah *et al.* conducted a study which evaluated how the viscosity at unit shear rate, pseudoplasticity index, and yield stress for an HTPB propellant varied with mixing time and mixing speed [31]. The study found that mixing times greater than 180 minutes yield a pseudoplasticity index closest to 1, while having only a weak effect on the viscosity and yield stress of the propellant. This suggests that mixing times on this order will likely yield the best flow properties for the propellant during casting.

The study also found that choosing the optimal mixing speed requires trading off multiple factors. As shown in Figure 4-6, the pseudoplasticity index is nearest 1 for higher mixing speeds beginning two hours after curative addition, which supports a higher mixing speed. However, the yield stress is smallest for lower mixing speeds, as shown in Figure 4-7. This result supports a lower mixing speed. Muthiah *et al.* recommend an intermediate mixing speed of approximately 25 rpm for best results.

In order to further prevent the formation of any voids in the propellant grains, the propellant mixing time should be increased from the 60 minutes used in the procedures given in Step 3 in Section 3.1.3 to 180 minutes. Additionally, current propellant manufacturing procedures described in Section 3.1.3 include no provision for controlling mixer speed. In the manufacturing of future propellant grains, the chosen mixing speed should be recorded for each propellant mixing, and correlations

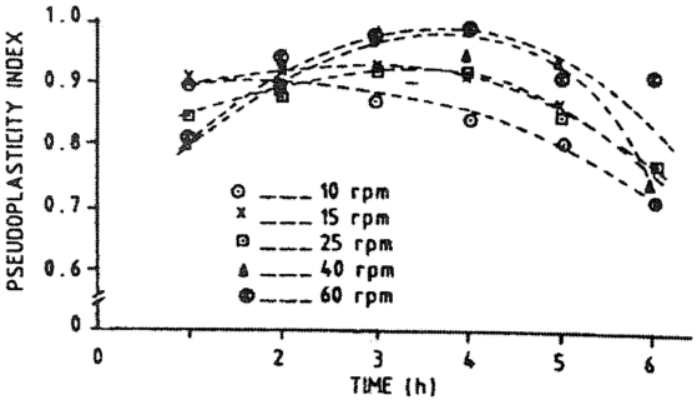

Figure 4-6: Propellant pseudoplasticity vs. time after curative addition for different mixing speeds. The pseudoplasticity index for uncured propellant is largest for higher mixing speeds starting two hours after curative addition. Reprinted from [31].

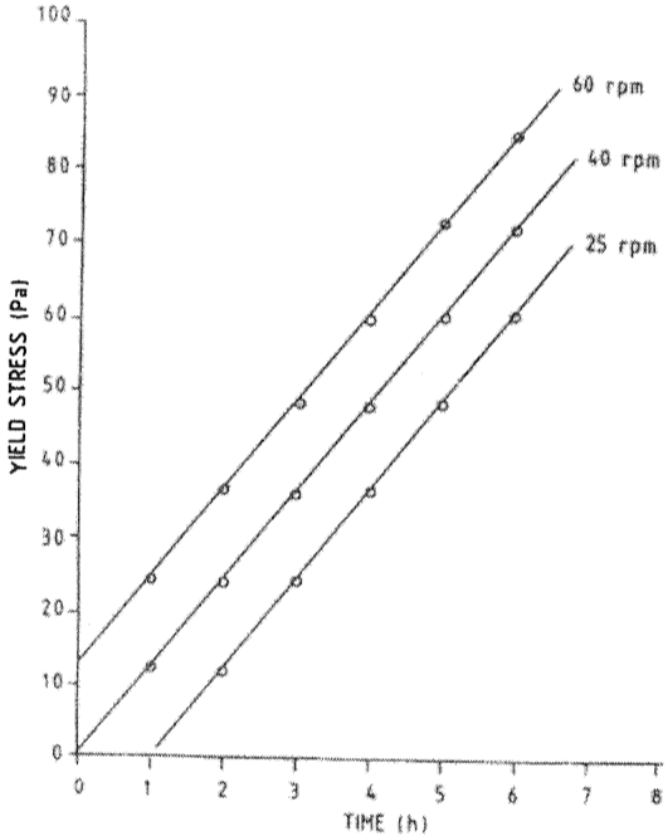

Figure 4-7: Propellant yield stress vs. time after curative addition for different mixing speeds. Propellant yield stress is smallest for lower mixing speeds at any time after curative addition. Reprinted from [31].

between propellant mixing speed and formation of voids should be noted if present. An intermediate mixing speed is likely appropriate. However, differences between the mixers used in the Muthiah *et al.* study and the procedures described in Section 3.1.3 might result in an optimal mixing speed that is different than the recommended 25 rpm.

4.3 Liner voids

The liner is cast using a vacuum injection process described in Section 3.1.3. This process often leaves large voids in the liner after curing, as shown in Figure 4-8. These large voids are fortunately easy to identify and can be reliably repaired if present. However, eliminating the voids would be desirable for simplifying the manufacturing process and creating better repeatability for production.

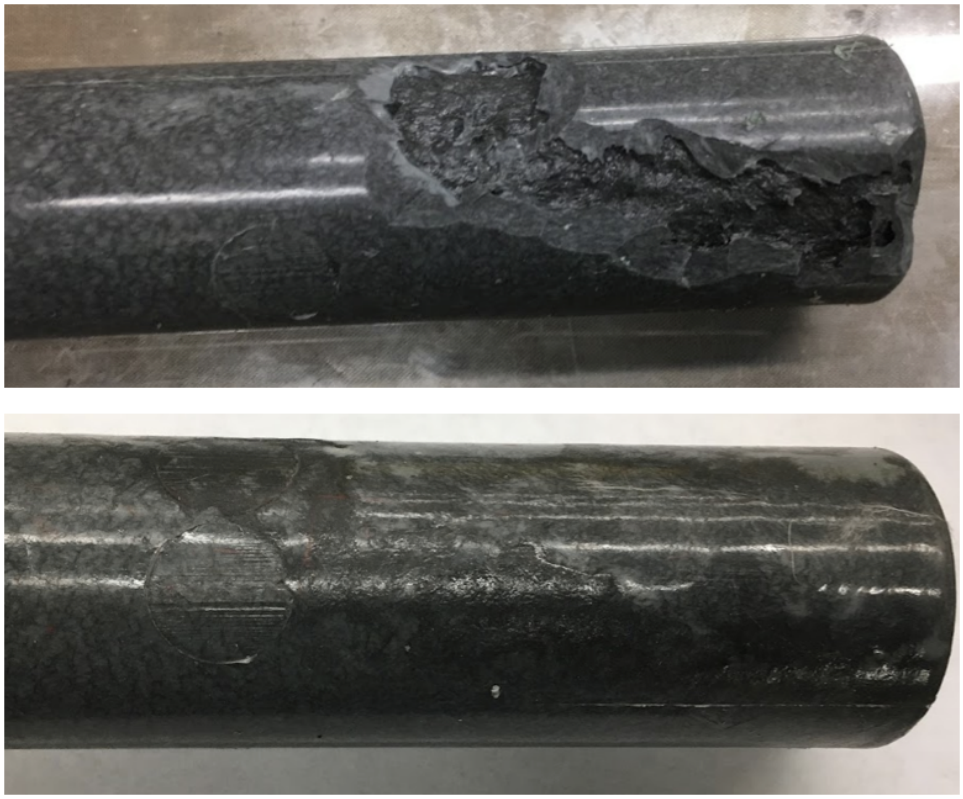

Figure 4-8: Large voids can form during the casting process for the liner in Titanium Candle motors (top). These voids can fortunately be reliably repaired (bottom).

A study by Sandén describes the preparation and characterization of silicone ablative materials for jet engines [35]. In the study, the possibility of diluting the Dow Corning 93-104 silicone ablative material – the same material used for the Firefly liner – with a lower viscosity room temperature vulcanizing (RTV) silicone is explored. Samples of different mixture ratios were tested in front of an oxygen-acetylene torch, and showed no decrease in burn-through time with the addition of the RTV silicone. It should be noted however that the diluted samples may not perform as well in the erosive environment of a solid rocket motor due to the reduction in density of the fibers.

Reducing the viscosity of the 93-104 material could improve the rheological properties of the material to help it flow more uniformly into the thin gap surrounding the propellant. A strategy such as this might prevent the formation of voids in the liner and the subsequent need for repair.

Chapter 5

Motor testing and measurements

Static fire tests of the Titanium Candle motor are used to collect pressure and thrust data and evaluate the performance of the motor. The motor performance data can be used to determine the effectiveness of the developed manufacturing strategies detailed in Chapter 3, both by validating effective manufacturing strategies and also revealing aspects to be improved in the manufacturing of subsequent motors. This chapter will describe the testing setup, procedures, and recorded data for several static firings of the Titanium Candle motor.

5.1 Testing setup

Static fire tests are conducted in a ventilated blast chamber. Within the blast chamber, a thrust stand setup enables the testing of the motor and collection of pressure and thrust data, as shown in Figure 5-1.

The motor and thrust stand setup has the following components:

- The *Titanium Candle motor* consists of the integrated propellant grain and liner installed in its cylindrical motor case.
- The *thrust stand* has clamps for mounting the Titanium Candle motor. Flexure bearings on the thrust stand allow the motor to translate in the axial direction for thrust data collection.

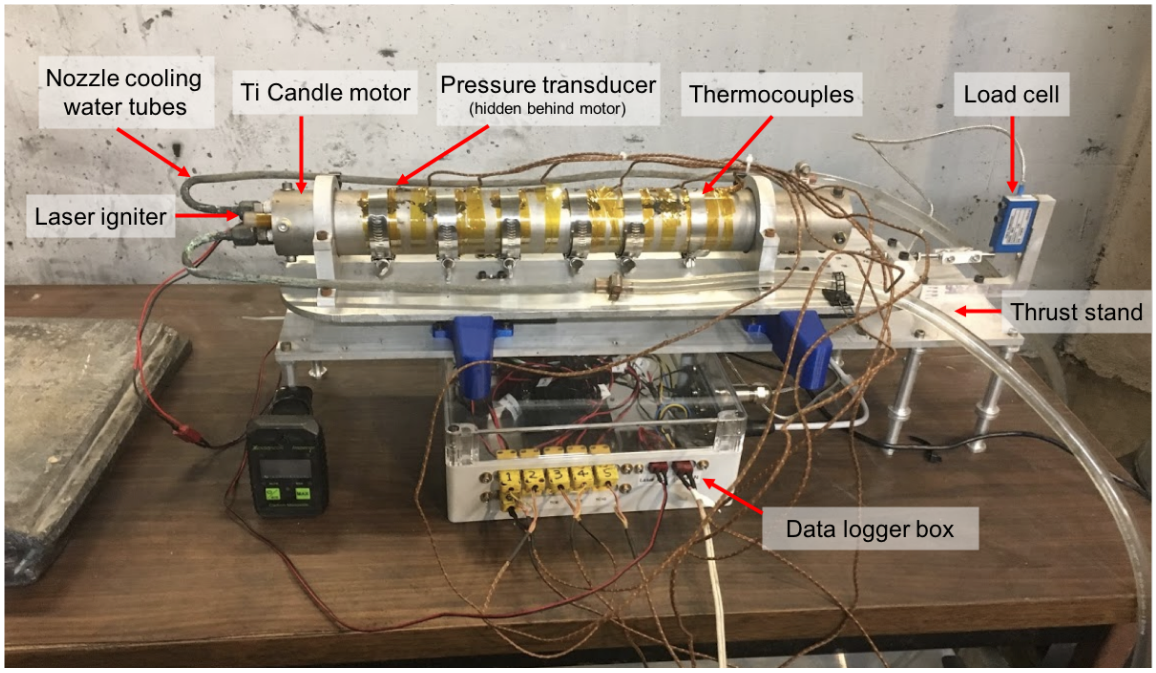

Figure 5-1: A thrust stand is used for collection of motor data during Titanium Candle static fire tests.

- A *load cell* is used for the collection of thrust data for the motor. A linkage between the thrust stand and load cell enables the collection of this data.
- A *pressure transducer* is fit to the aft closure of the Titanium Candle motor, and collects chamber pressure data for the duration of the motor burn.
- *Thermocouples* mounted to the surface of the motor case collect thermal data for the motor case during the static fire.
- A *data logger box* interfaces with the load cell, pressure transducer, and thermocouples in order to record and stream the collected data.
- The *laser igniter* is installed in front of the motor's nozzle and ignites the propellant.
- *Nozzle cooling water tubes* provide water to the aft closure to cool the nozzle during motor firings.

The setup of the thrust stand and motor within the larger blast chamber is shown

in Figure 5-2. Descriptions of some of the additional components in the setup are given below:

- An exhaust collection system consists of an *exhaust duct* and *water spray nozzles* with a *pump*, *filter*, and *water tank*. The exhaust duct directs the smoke from the motor to a vent on the ceiling of the blast chamber.

- Multiple *cameras* record video of the motor during static firings.

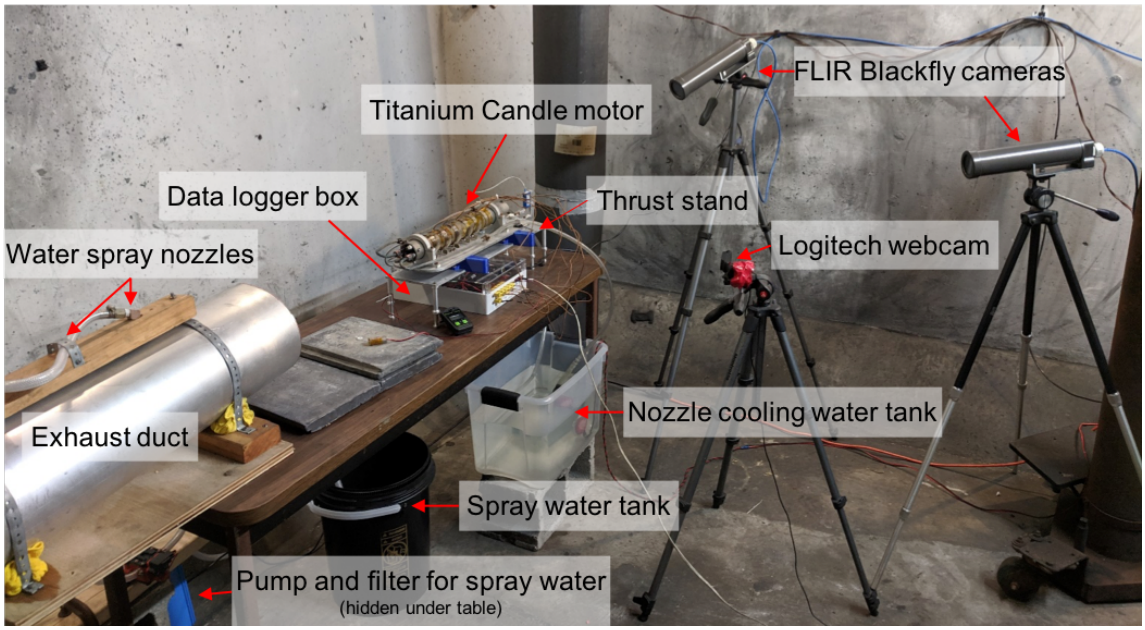

Figure 5-2: A blast chamber with cameras and an exhaust collection system is used for static fire tests.

The exhaust collection system clears the blast chamber of smoke and soot during static firings. This helps in the collection of higher quality video of the motor that is unobstructed by smoke.

5.2 Testing procedures

When conducting a static fire, the following procedures are used for preparing the motor and sensors, igniting the motor, and collecting data:

1. *Motor integration* - The completed motor is wrapped in two layers of insulating fiberglass before being inserted into the motor case. A starter grain is inserted into the starter pocket on the aft end of the propellant grain. The forward and aft closures are then installed onto the propellant grain. Thermocouples are attached to the exterior of the motor case using hose clamps.

2. *Motor mounting* - The motor is mounted onto the test stand using clamping brackets and screws. The nozzle cooling water tubes and pressure transducer are attached to the aft closure of the motor. The laser igniter is installed into the aft closure as well. The laser, pressure transducer, thermocouples, and load cell are connected to the data logger box.

3. *Sensor setup* - The power supply for the pressure transducer is turned on. The data logger user interface is checked to ensure reasonable values are streaming from the sensors.

4. *Camera setup* - The cameras are positioned in the blast chamber in the desired locations. The camera software is opened and recording capabilities for each camera are verified.

5. *Blast chamber setup* - The water levels in the tanks for the nozzle cooling and exhaust collection system are verified and the pump for the exhaust collection system is primed. The ventilation system for the blast chamber, which evacuates smoke from the chamber during the static fire, is turned on. A carbon monoxide detector is placed in the blast chamber in the field of view of a camera, such that it can be monitored from outside the chamber. The blast chamber is then cleared of personnel and the blast chamber door is closed and sealed.

6. *Motor firing* - All sensors and cameras are activated and set to record. The laser is activated and current is delivered until the propellant ignites. Once the motor is burning, data streams are reviewed for nominal values. After the motor burns out, data from the sensors are uploaded to a storage server. The

blast chamber door remains sealed until the camera feed of the carbon monoxide detector shows safe readings inside the chamber.

7. *Cleanup* - After the smoke and carbon monoxide are vented, the blast chamber can be entered. The motor and test equipment are inspected for damage and sensor power supplies are turned off.

5.3 Thrust and pressure data

Thrust and pressure data collected during static fire tests are used to evaluate motor performance and validate motor design choices. In addition, these data can also reveal information about the effectiveness of the manufacturing processes for the propellant and liner. This section will present static fire data from Titanium Candle test motors manufactured with the hardware and procedures given in Chapter 3.

5.3.1 Repeatable, long-endurance, half-length test motor data

Two half-length Titanium Candle test motor propellant grains were prepared and fired in series. For these tests, a single, full-length propellant grain with 13% oxamide mass fraction was manufactured. This grain was then cut in half, and one grain half was used per test. An inert spacer occupied the remaining volume of each motor.

These tests were conducted to further characterize the Titanium Candle propellant formulation, verify the liner thickness, and validate the liner manufacturing methods described in Section 3.1.3. Using propellant manufactured in the same mixing for each static fire eliminates differences between the data sets that might have otherwise been present due to slight inherent differences between batches. Therefore, this pair of static fire tests is especially suited for evaluating the repeatability of the liner manufacturing methods.

The thrust and pressure data for this pair of test motor static fires can be seen in Figures 5-3 and 5-4. The thrust profiles between the two tests are particularly similar: there is an initial peak in thrust due to the larger surface area of the star-

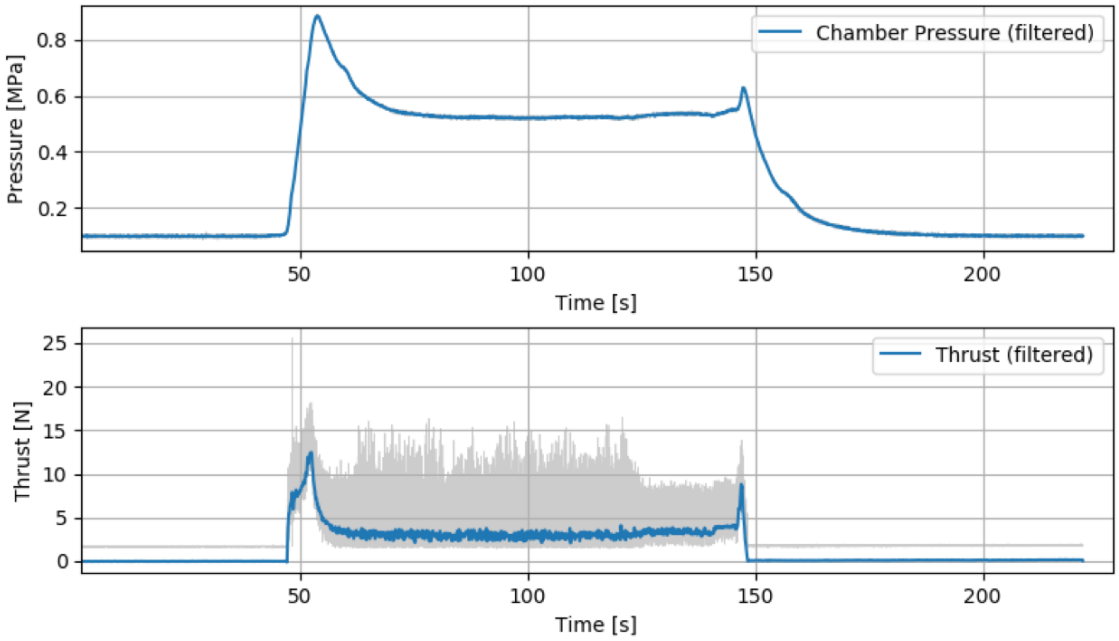

Figure 5-3: Pressure and thrust data from a half-length Titanium Candle test motor static fire using the first half of a propellant grain. Steady-state values for chamber pressure and thrust are reasonable, and no edge burning is present.

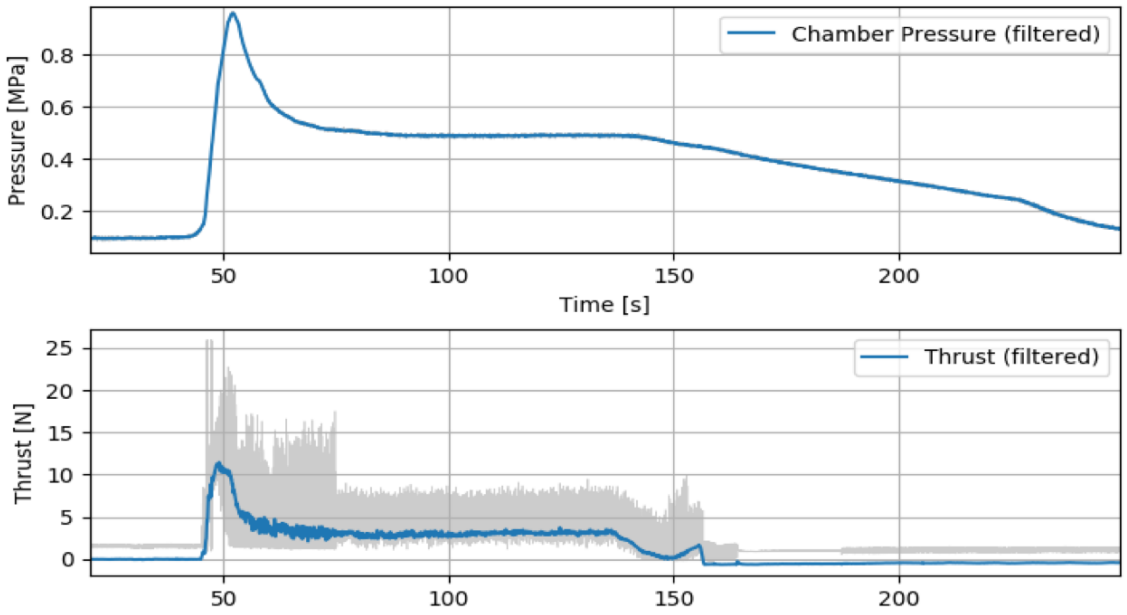

Figure 5-4: Pressure and thrust data from a half-length Titanium Candle test motor static fire using the second half of a propellant grain. These trends are similar to the first half-grain, demonstrating repeatability in the liner manufacturing methods.

shaped starter pocket on each grain, which then settles out to ~3 N of thrust in steady state.

The initial parts of the pressure profiles also look similar. There is an initial peak in pressure, which settles out to ~0.5 MPa in the steady state for each. However, a snubber installed on the pressure transducer for the static fire of the second half-grain caused measured chamber pressure data to fall off unrealistically slowly.

Selected data for this pair of test motor static fires is summarized in Table 5.1. The two tests demonstrate very similar performance, which supports the repeatability of the motor manufacturing processes. The low thrust and long burn times for each motor suggests good adhesion between the propellant and liner and that no edge burning was present. Additionally, the smooth pressure and thrust profiles after start up suggest an absence of voids in the propellant as well.

Table 5.1: Comparison of half-length Titanium Candle test motor static fire data.

	First half-grain	**Second half-grain**
Steady-state average thrust [N]	2.7	3.0
Steady-state average chamber pressure [MPa]	0.52	0.53
Burn time [s]	100.4	91.1
Total impulse [Ns]	359	333

5.3.2 Multi-segment, full-length test motor data

A multi-segment Titanium Candle propellant grain was also manufactured and tested in order to validate the multi-segment propellant manufacturing process and characterize the transition between the propellant formulations. This motor contained only two segments of propellant, with each occupying half of the volume of the motor. The propellant in the aft half of the motor had a fast-burning propellant with 0% oxamide in its formulation, and the propellant in the forward half had a slower-burning

propellant with 10% oxamide mass fraction. The thrust and pressure profiles for the static fire of this motor can be seen in Figure 5-5.

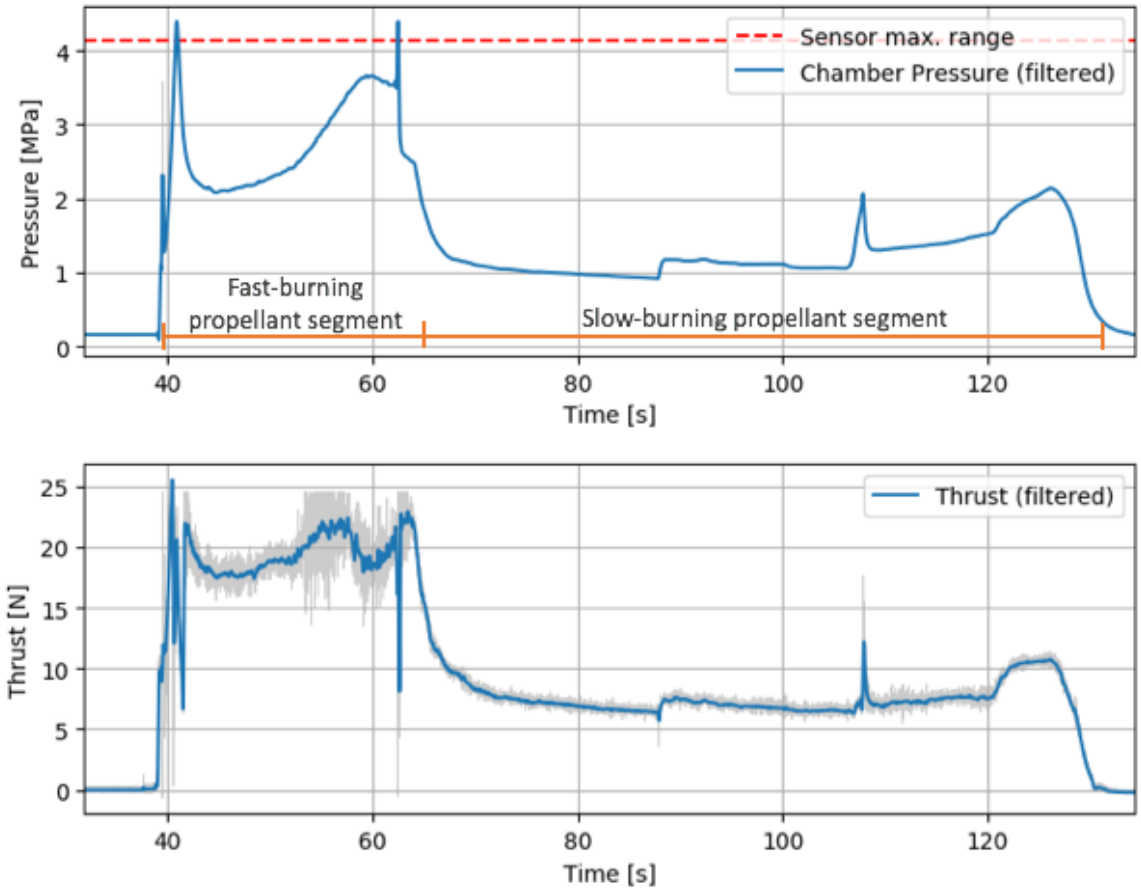

Figure 5-5: Pressure and thrust data from a full-length, multi-segment Titanium Candle test motor static fire.

The transition between the two propellant segments at approximately 25s into the burn (corresponding to $t \approx 65$s on the axes in Figure 5-5) is very apparent due to the sudden decrease in chamber pressure and thrust. There is a stable transition between the two propellant formulations, with a time constant of ~ 3s.

The transition between the two propellant segments during the static fire could also be seen in the visible plume of the propellant. As shown in Figure 5-6, the fast burning propellant created a much larger plume than the slower burning propellant.

A spike in pressure and thrust can be seen approximately 67s into the burn (corresponding to $t \approx 108$s on the axes in Figure 5-5). This is likely due to some sudden increase in the burning area. The magnitude of the pressure spike corresponds to a

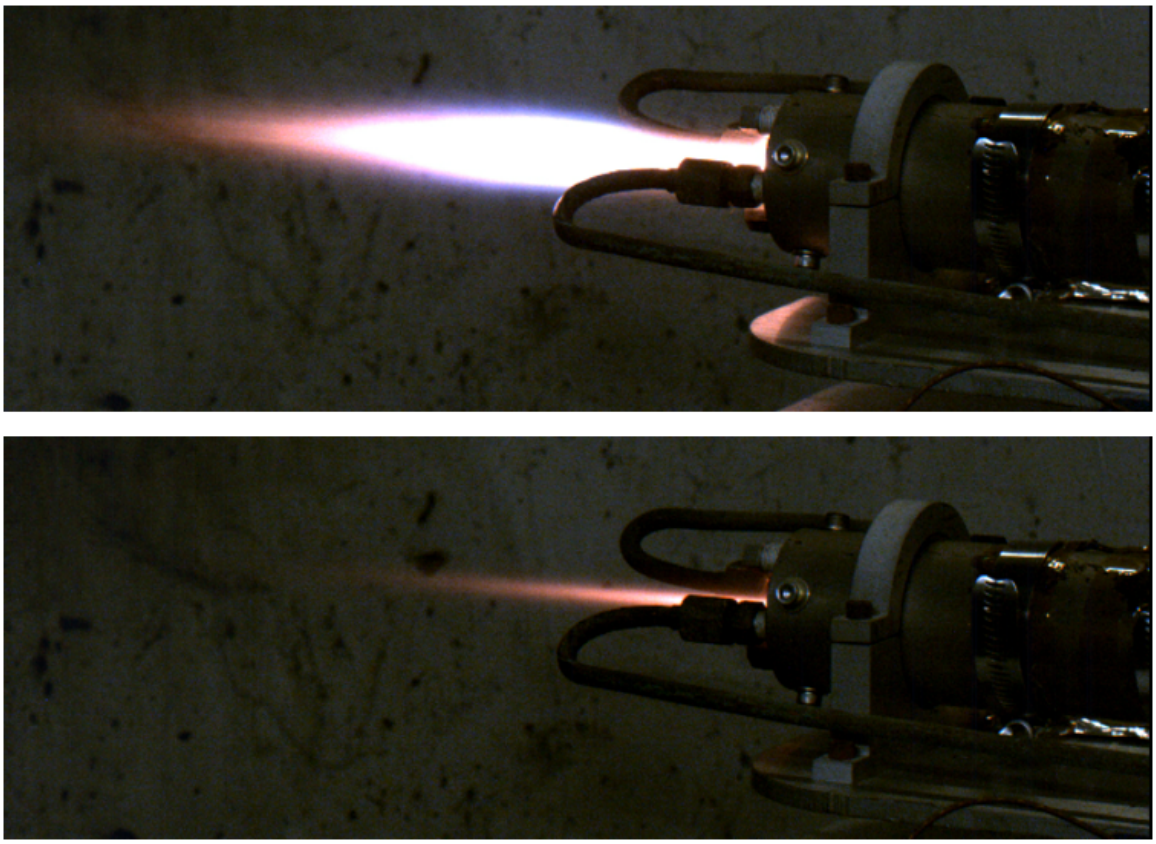

Figure 5-6: The segment of faster burning propellant created a larger visible plume (top) than the slower burning propellant (bottom).

$\sim$ 35% or $\sim$ 600 mm^2 increase in the burning area of the propellant. A spherical void with this surface area would have a diameter of $\sim$ 14 mm, which is much larger than the $\sim$ 1-3 mm voids seen in a previous Titanium Candle propellant grain (see Figure 1-8), so a spherical void of this size seems unlikely. Other possible explanations include:

- an oblong shaped void,
- a crack in the propellant grain,
- a small area of delamination between the propellant grain and liner, or
- a small void in the liner such that the liner in that location never adhered to the propellant grain.

Selected data from the static fire of this multi-segment motor is summarized in Table 5.2. The fast-burn segment shows larger values for average thrust, chamber pressure, and burn rate as expected when compared to the slow-burn data. The total impulse for each segment is also quite similar, which is reasonable since the total energy stored in each segment should be similar. However, it should be noted that a slightly higher value of specific impulse would be expected for the faster burning propellant since its characteristic velocity and thrust coefficient are higher, in contrast to what Table 5.2 shows.

Table 5.2: Summary of test data for two-segment Titanium Candle static fire test.

	Fast-burn segment	**Slow-burn segment**	**Full motor**
Steady-state average thrust [N]	~ 19	~ 8	-
Steady-state average chamber pressure [MPa]	~ 2.6	~ 1.2	-
Burn time [s]	~ 25	~ 65	90.3
Average burn rate [mm/s]	~ 8	~ 3	-
Total impulse [Ns]	~ 470	~ 510	980.4

Chapter 6

Conclusion

This thesis presents methods for manufacturing solid rocket motors for small, fast flight vehicles. These methods were developed using Firefly – a vehicle designed to explore the capabilities and challenges for small, fast aircraft.

Firefly is built around a compact, low-thrust, long-endurance solid rocket motor which powers the vehicle during flight. An end-burning motor configuration for the vehicle provides a small propellant burning area, helping to reduce thrust and extend propellant burn time. In addition to configuration choices, chemical modification of the propellant using a burn rate suppressant is also used to reduce the burn rate further and control propellant thrust and chamber pressure in a motor with changing burn area.

Manufacturing motors for small, fast vehicles presents many challenges. In order to achieve desired motor performance, a dense, void-free propellant grain with a high energy-density is required. A high-performance thermal liner is also needed to protect the motor case from the hot combustion products for the entire duration of the motor burn. In addition, this liner must have a strong propellant-to-liner bond that inhibits the edges of the propellant in order to prevent propellant edge-burning.

Many manufacturing methods were developed to aid in the production of the Firefly motor. Innovative tooling and procedures enable the production of simplified test motors with dense propellant grains and strong propellant-to-liner bonds. Additional hardware and procedures have also been developed to manufacture multi-segment

propellant grains as well as motors in the actual flight-like geometry for the Firefly flight vehicle. Successful static fires of test motors have demonstrated the effectiveness of the implemented manufacturing methods.

These manufacturing methods should be continually updated in order to incorporate insights gained through process iteration and additional motor static fire tests. Their continued improvement will lead to the production of consistent, high-quality motors than can enable the success of Firefly and other small, fast flight vehicles.

Bibliography

[1] Jane's all the world's aircraft: In service, 2016.

[2] Jane's all the world's aircraft: Unmanned, 2016.

[3] Aerovironment inc. | unmanned aircraft systems. https://www.avinc.com/, 2019.

[4] Precision weapons. https://www.raytheon.com/capabilities/precision/, 2019.

[5] Wikipedia, the free encyclopedia. en.wikipedia.org, 2019.

[6] Matthew T. Vernacchia. Development, modeling and testing of a slow-burning solid rocket propulsion system. Master's thesis, Massachusetts Institute of Technology, 2017.

[7] Jonathan R. Spirnak. Development, modeling and testing of thermal protection systems in small, slow-burning solid rocket motors. Master's thesis, Massachusetts Institute of Technology, 2018.

[8] Northrop Grumman. https://www.northropgrumman.com/Capabilities/PropulsionSystemsControls/Documents/AIM-9M_Factsheet.pdf, 2018. [Accessed: 2019-05-05].

[9] Jing Wang, Weijuan Xia, Kun Liu, and Xinlin Tuo. Improved adhesion of silicone rubber to polyurethane by surface grafting. *Journal of Applied Polymer Sciences*, 121:1245 – 1253, March 2011.

[10] Paul P. Chang, Nancy A. Hansen, Rodney D. Phoenix, and Thomas R. Schneid. The effects of primers and surface bonding characteristics on the adhesion of polyurethane to two commonly used silicone elastomers. *Journal of Prosthodontics*, 18:23 – 31, 2009.

[11] Ariyadasa Udagama. Urethane-lined silicone facial prostheses. *Journal of Prosthetic Dentistry*, 58:351 – 354, September 1987.

[12] James C. Lemon, Jack W. Martin, and Gordon E. King. Modified technique for preparing a polyurethane lining for facial prostheses. *Journal of Prosthetic Dentistry*, 67:228 – 229, February 1992.

[13] Eung-Soo Kim, Hun-Sik Kim, Seong-Hun Jung, and Jin-San Yoon. Adhesion properties and thermal degraation of silicone rubber. *Journal of Applied Polymer Science*, August 2006.

[14] Alain Davenas, editor. *Solid Rocket Propulsion Technology.* Pergamon Press, Tarytown, New York, 1993.

[15] The engine types: solid, liquid and hybrid... and a fourth. `https://www.narom.no/undervisningsressurser/sarepta/rocket-theory/rocket-engines/the-engine-types-solid-liquid-and-hybrid-and-a-fourth/`, 2018. [Accessed: 2019-05-17].

[16] George P. Sutton and Oscar Biblarz. *Rocket Propulsion Elements.* John Wiley and Sons, Inc., Hoboken, New Jersey, eighth edition, 2010.

[17] Phillip Hill and Carl Peterson. *Mechanics and Thermodynamics of Propulsion.* Pearson Education, Inc., Reading, Massachusetts, second edition, 2010.

[18] Terry McCreary. *Experimental Composite Propellant.* Murray, Kentucky, 2014.

[19] Vishwas Govindrao Ghorpade, Abhijit Dey, Lalita Sudhir Jawale, Amarnath Madiwal Kotbagi, Arind Kumar, and Manoj Gupta. Study of burn rate

supressants in ap-based composite propellants. *Propellants, Explosives, and Pyrotechnics*, 35:53 – 56, October 2008.

[20] L. H. Caveny. Solid propellant flammability including ignitability and combustion limits. Technical report, National Technical Information Service, U.S. Department of Commerce, Springfield, Virginia, March 1974.

[21] Djalal Trache, Filippo Maggi, Ilaria Palmucci, Luigi T. DeLuca, Kamel Khimeche, Marco Fassina, Stefano Dossi, and Giovanni Colombo. Effect of amide-based compounds on the combustion characteristics of composite solid rocket propellants. *Arabian Journal of Chemistry*, November 2015.

[22] Bosch universal plus mixer. `https://pleasanthillgrain.com/bosch-mixer-universal-plus`, 2019.

[23] RCS Rocket Motor Components. `https://www.rocketmotorparts.com/`, 2019. [Accessed: 2019-04-24].

[24] Dow Corning Americas. *Technical Manual*, 2017.

[25] Dow Corning. *Dow Corning 1200 OS Primer Product Information*, 2015.

[26] Dow Corning. *Dow Corning 93-104 Ablative material Product Information.*

[27] Lucas F. M. da Silva, Andreas Ochsner, and Robert D. Adams. *Handbook of Adhesion Technology*, chapter 41. Springer, 2011.

[28] Qizhou Yao and Jianmin Qu. Interfacial versus cohesive failure on polymer-metal interfaces in electronic packaging - effects of interface roughness. *Journal of Electronic Packaging*, 124:127 – 134, June 2002.

[29] Jr. G. A. VoorHees and B. G. Morton. Injector/chamber scaling feasibility program. `https://apps.dtic.mil/dtic/tr/fulltext/u2/513619.pdf`, 1970. [Accessed: 2019-05-11].

[30] Product data modified mdi isocyanate curative. https://d11fdyfhxcs9cr.cloudfront.net/templates/170652/myimages/modified_mdi_tds.pdf, 2016. [Accessed: 2019-05-13].

[31] Rm. Muthiah, R. Manjari, and V.N. Krishnamurthy. Rheology of htpb propellant: Effect of mixing speed and mixing time. *Defence Science Journal*, 43(2):167 – 172, April 1993.

[32] A. A. Osgood. Rheological characterization of non-newtonian propellants for casting optimization. In *AIAA 5th Propulsion Joint Specialist Conference*, pages 133–139, U. S. Air Force Academy, 1969. Thiokol chemical Corporation.

[33] RM. Muthiah, V. N. Krishnamurthy, and B. R. Gupta. Rheology of htpb propellant. i. effect of solid loading, oxidizer particle size, and aluminum content. *Journal of Applied Polymer Science*, 44:2043 – 2052, 1992.

[34] A. Restasari, R S Budi, and K Hartaya. Pseudoplastiity of propellant slurry with varied aluminum content for castability development. *5th International Seminar of Aerospace Science and Technology*, April 2018.

[35] Roland Sandén. Castable silicone based heat insulations for jet engines. *Polymer Testing*, 21:61 – 64, April 2001.

Appendix A

Calculations of pressure and thrust fluctuations

The equilibrium pressure and thrust expressions derived in Section 2.5 can be used to evaluate the magnitude of pressure and thrust fluctuations for a single burning propellant formulation with changing burning area.

The contoured geometry of the Firefly flight-like motor results in changing propellant burning area as the flame front progresses along the length of the motor. A plot of the propellant burning area as the burn distance progresses from the aft end of the motor is shown in Figure A-1.

The minimum burn area is ~ 320 mm^2 and the maximum is ~ 1700 mm^2, giving a ratio of maximum to minimum burning area of ~ 5.3. With this area ratio, the ratio of maximum to minimum equilibrium chamber pressure can be calculated. The expression for equilibrium chamber pressure as given in Equation 2.18 is

$$p_{c,eq.} = \left(K_n \rho_p c^* a\right)^{\frac{1}{1-n}} \tag{A.1}$$

where

$$K_n \equiv \frac{A_b}{A_t}. \tag{A.2}$$

Calculating the ratio of maximum to minimum equilibrium chamber pressure

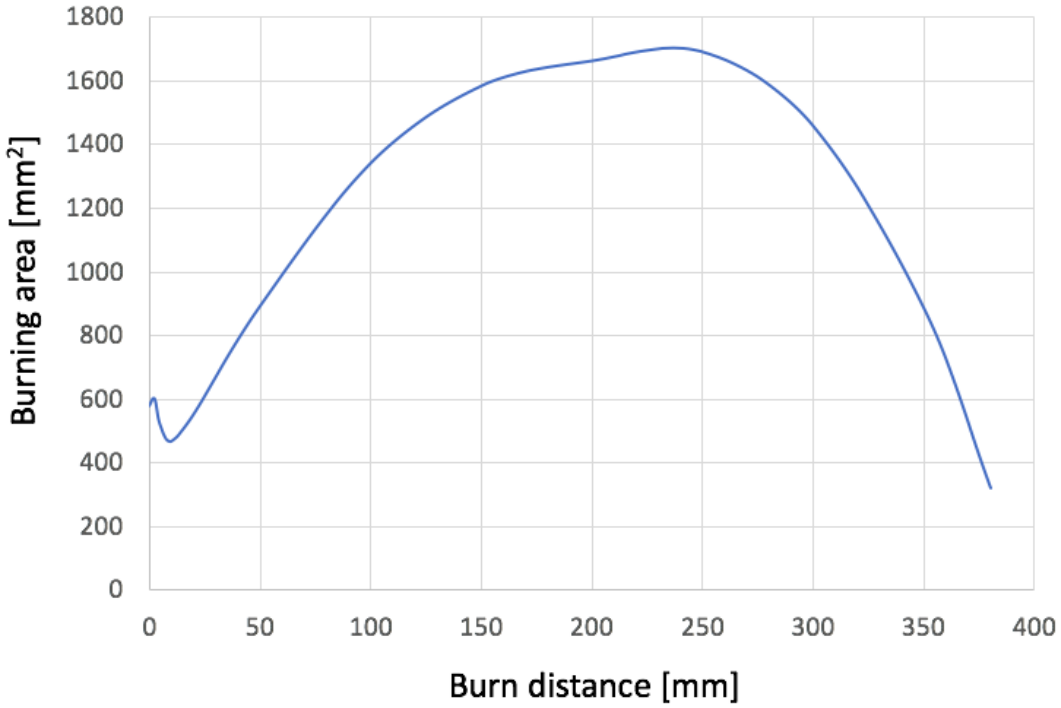

Figure A-1: The propellant burning area for the Firefly motor changes throughout the duration of the burn.

yields

$$\frac{p_{c,eq.,max}}{p_{c,eq.,min}} = \frac{\left(\frac{A_{b,max}}{A_t}\rho_p c^* a\right)^{\frac{1}{1-n}}}{\left(\frac{A_{b,min}}{A_t}\rho_p c^* a\right)^{\frac{1}{1-n}}} \tag{A.3}$$

If the motor used a single propellant, the values for ρ_p, c^*, a, and A_t would be the same at both the minimum and maximum burn areas, and subsequently these terms would cancel. The ratio of maximum to minimum equilibrium chamber pressure would then be expressed as

$$\frac{p_{c,eq.,max}}{p_{c,eq.,min}} = \left(\frac{A_{b,max}}{A_{b,min}}\right)^{\frac{1}{1-n}} \tag{A.4}$$

Burn rate experiments conducted for oxamide-doped propellant formulations suggest that the burn rate exponent n is ~ 0.5. This is in line with typical values of the burn rate exponent for APCPs [16]. With this value for the burn rate exponent n,

and with a ratio of maximum to minimum burning area, the ratio of maximum to minimum equilibrium chamber pressures for the Firefly motor would be ~ 27. This is an unacceptably large variation, thus motivating the development of a multi-segment propellant grain.

A similar analysis can be done to find the ratio of maximum to minimum thrust using the equilibrium thrust expression given in Equation 2.20:

$$F_{eq.} = C_F \left(p_{c,eq.}, p_e, \gamma \right) A_t p_{c,eq.} \tag{A.5}$$

Taking the ratio of thrust forces and canceling identical terms yields

$$\frac{F_{eq.,max}}{F_{eq.,min}} = \sqrt{\frac{1 - \left(\frac{p_{c,eq.max}}{p_e} \right)^{\frac{1-\gamma}{\gamma}}}{1 - \left(\frac{p_{c,eq.min}}{p_e} \right)^{\frac{1-\gamma}{\gamma}}}} \left(\frac{p_{c,eq.,max}}{p_{c,eq.,min}} \right) \tag{A.6}$$

To calculate the ratio of maximum to minimum thrust force, values for the equilibrium pressures are required instead of just a simple ratio. This requires values for several parameters to be defined. Representative values for an undoped propellant for the Firefly motor have been determined through measurements, burn rate tests, and thermochemical analysis using the Rocket Propulsion Analysis software, and are given in Table A.1.

Plugging these values into Equation A.6 and assuming $p_e = p_a$ yields a ratio of maximum to minimum thrust of ~ 31. These massive scalings in pressure and thrust for the changing burn area of the Firefly motor motivate the use of multi-segment propellant grains which can help to maintain more regular vehicle chamber pressure and thrust.

The method described in this appendix can also be used for calculating pressure and thrust fluctuations for changes in burning surface area due to void exposure or liner delamination. For these scenarios, the burning areas in Equation A.4 simply need to be updated with the relevant values before carrying out the rest of the calculations.

Table A.1: Representative parameters for a Firefly motor made with an undoped propellant.

Parameter	**Value at maximum burn area**	**Value at minimum burn area**
n [-]	0.5	0.5
a [mm/s $\mathrm{MPa}^{-\mathrm{n}}$]	8	8
ρ_p [kg/m^3]	1550	1550
c^* [m/s]	1300	1300
γ [-]	1.24	1.24
A_t [mm^2]	7	7
A_b [mm^2]	1700	320
K_n [-]	240	46

Appendix B

Propellant formulations for different oxamide mass fractions

The propellant formulations used for the different segments of the Firefly motor are created by diluting a baseline propellant with some mass fraction of the oxamide burn rate suppressant. This baseline propellant formulation is given in Table B.1.

To create a new formulation for an oxamide-doped propellant, the desired oxamide mass fraction w_{om} must be chosen. The mass fraction for the baseline components are then scaled by a factor of $1 - w_{om}$. With this scaling, the relative mass fractions of the baseline components remain the same, and their total mass fraction sums to $1 - w_{om}$. This scaling can be seen in the propellant formulation presented in Table 3.1, where $w_{om} = 0.13$.

Table B.1: Baseline propellant formulation for Firefly motor production.

Component	**Chemical name**	**Manufacturer**	**Mass fraction**
Binder	Hydroxyl Terminated Polybutadiene (HTPB) Resin with HX-752 and CAO-5	RCS Rocket Motor Components	0.114
Plasticizer	Isodecyl Pelargonate (IDP)	RCS Rocket Motor Components	0.047
Opacifier	Graphite powder	Cretacolor	0.022
Oxidizer	Ammonium Perchlorate 200/400 Micron Blend	RCS Rocket Motor Components	0.800
Curative	Modified MDI Isocyanate	RCS Rocket Motor Components	0.017
Burn rate suppressant	Oxamide	Sigma-Aldrich	0